Aus der Klinik für Psychiatrie, Psychotherapie und Psychosomatik
(Direktor Univ.-Prof. Dr. med. Dr. rer. soc. Frank Schneider)

Structure-Function Relationships in elderly Resting-State-Networks: Influence of Age and Cognitive Performance

Von der Medizinischen Fakultät
der Rheinisch-Westfälischen Technischen Hochschule Aachen
zur Erlangung des akademischen Grades einer Doktorin der Theoretischen Medizin
genehmigte Dissertation

vorgelegt von

Master of Science in Cognitive and Clinical Neuroscience
Christiane Jockwitz

aus Köln

Berichter: Universitätsprofessor Dr. med. Dr. h.c. Karl Zilles
Universitätsprofessor Dr. med. Dr. rer. soc. Frank Schneider

Tag der mündlichen Prüfung: 7. Juli 2016

Diese Dissertation ist auf den Internetseiten der Hochschulbibliothek online verfügbar.

Meinen Eltern gewidmet:
Volker und Petra Jockwitz

Teile dieser Dissertation wurden bereits veröffentlicht in:

Jockwitz, C., Caspers, S., Lux, S., Jütten, K., Schleicher, A., Eickhoff, S.B., Amunts, K., & Zilles, K. *Age- and function-related regional changes in cortical folding of the Default Mode Network in older adults, Brain Struct Funct,* in press. doi:10.1007/s00429-016-1202-4.

Table of Content

TABLE OF CONTENT VII

LIST OF FIGURES X

LIST OF TABLES X

ABBREVIATIONS XII

1. INTRODUCTION 1

1.1 Cognitive aging from early to late adulthood 1

1.2 Functional brain mechanisms behind cognitive performance decline from early to late adulthood 3

1.2.2 Task-based functional mechanisms 3

1.2.3 Resting state functional mechanisms 4

1.3 Structural correlates of functional reorganization in the aging brain 7

2 AIM OF THE STUDY 10

3 MATERIAL UND METHODS 11

3.1 Study population 11

3.2 MRI acquisition 12

3.3 Neuropsychological assessment 12

3.4 Anatomical identification of brain areas 12

3.5 Study 1: Characterization of "elderly" RS networks 14

3.5.1 Sample 14

3.5.2 Preprocessing of functional MR images 14

3.5.3 Extraction of RS networks 14

3.5.4 Neuropsychological variables and principal component analysis 15
3.5.5 Statistical analysis 19

3.6 Study 2: Gyrification changes in the "elderly" DMN 20
3.6.1 Sample 20
3.6.2 RS analysis 20
3.6.3 Structural MR images 22
3.6.4 Surface reconstruction and calculation of LGI 22
3.6.5 Neuropsychological assessment 24
3.6.6 Statistics 24

4. RESULTS 27

4.1 Study 1: Characterization of "elderly" RS networks 27
4.1.1 Effects of age on RSFC 27
4.1.2 Effects of gender on RSFC 29
4.1.3 Effects of cognitive performance on RSFC 33

4.2 Study 2: Gyrification changes in the "elderly" DMN 40
4.2.1 Effects of age on LGI 41
4.2.2 Effects of cognitive performance on LGI 45

5. DISCUSSION 51

5.1 Characterization of "elderly" RS networks 51
5.1.1 Effects of age on RSFC 51
5.1.2 Effects of gender on RSFC 54
5.1.3 Effects of cognitive performance on RSFC 57

5.2 Gyrification changes in the "elderly" DMN 59
5.2.1 Effects of age on LGI 59
5.2.2 Effects of cognitive performance on LGI 61

5.3 Structure – function relationship within the "elderly" DMN 63

5.4 Limitations and implications for future research **66**

6. SUMMARY **68**

7. LITERATURE **69**

AUFLISTUNGEN DER EIGENEN PUBLIKATIONEN **91**

DANKSAGUNG **92**

LEBENSLAUF **96**

List of Figures

FIGURE 1:	RS networks and the relation between parameter estimates and age in the elderly sample	16
FIGURE 2:	Overview of gyrification analysis in the “elderly” DMN	21
FIGURE 3:	Age effects in the elderly cognitive RS networks	28
FIGURE 4:	Gender effects in the elderly cognitive RS networks	30
FIGURE 5:	Screeplot of principal component analysis	34
FIGURE 6:	Cognitive functions and their involvement in the extracted components by principal components analysis	35
FIGURE 7:	Relation between cognitive performance and RSFC with respect to “WM” within the left frontoparietal RS network	39
FIGURE 8:	Description of brain areas involved in the DMN	40
FIGURE 9:	Scatterplots of relation between LGI values and age	42
FIGURE 10:	Scatterplots of relation between LGI values of DMN-ROIs and age	43
FIGURE 11:	Group comparison between youngest and oldest 25% of the participants	45
FIGURE 12:	Scatterplots of relation between LGI values of DMN-ROIs and cognitive performance	48
FIGURE 13:	Group comparison between highest and lowest 25% of the performers	49

List of Tables

TABLE 1:	Neuropsychological tests included in the current studies	13
TABLE 2:	Overview of cognitive tests included in the RS analysis	17
TABLE 3:	Overview of cognitive tests included in the gyrification analysis	25
TABLE 4:	Age-related changes in RSFC in the task-active RS networks	29
TABLE 5:	Gender differences in RSFC in the respective RS networks	32
TABLE 6:	Correlation coefficients between all cognitive functions included in the principal component analysis.	36
TABLE 7:	Eigenvalues and explained variance from the principal component analysis	37
TABLE 8:	Description of brain areas involved in the DMN	41
TABLE 9:	Mean LGI values in parts of the DMN	46
TABLE 10:	Mean test scores and mean LGI values of DMN-ROIs	50

Abbreviations

ACC	Anterior cingulate cortex
AG	Angular gyrus
aDMN	Anterior Default Mode Network
AKT	Alters-Konzentrations-Test
ANCOVA	Analysis of CoVariance
BET	Brain Extraction Tool
BOLD	Blood-oxygen-level-dependence
BTT	Block Tapping Test
cIPL	Caudal inferior parietal lobule
CRUNCH	Compensation-Related Utilization of Neural Circuits Hypothesis
dACC	Dorsal anterior cingulate cortex
DMN	Default Mode Network
EPI	Echo planar imaging
FDR	False discovery rate
FIX	FMRIB's ICA-based Xnoiseifier
FLIRT	FMRIB's Linear Image Registration Tool
fMRI	Functional magnetic resonance imaging
FMRIB	(The Oxford Centre of) functional MRI of the brain
FNIRT	FMRIB's Non-linear Image Registration Tool
FWHM	Full width half maximum
Fo	Orbitofrontal cortex
FoV	Field of view
FP	Frontal Pole
FPT	Fünf Punkte Test
FSL	FMRIB (functional MRI of the brain) Software library
FWIT	Farb-Wort-Interferenz-Test

GI	Gyrification Index
GLM	General linear model
HAROLD	Hemispheric asymmetry reduction in older adults
ICA	Independent components analysis
IFG	Inferior frontal gyrus
IPL	Inferior parietal lobule
IPS	Intraparietal sulcus
KMO	Kaiser–Meyer–Olkin
LGI	Local gyrification index
LPS	Leistungsprüfungssystsem
MCFLIRT	Motion Correction FMRIB's Linear Image Registration Tool
MCI	Mild cognitive impairment
MELODIC	Multivariate Exploratory Linear Optimized Decomposition into Independent Components
mSFG	Medial superior frontal gyrus
MFG	Middle frontal gyrus
MNI	Montreal neurological Institute
MOG	Middle occipital gyrus
mPFC	Medial prefrontal cortex
MP-RAGE	Magnetization-prepared rapid acquisition gradient-echo
MR	Magnetic resonance
MTG	Middle temporal gyrus
MSA	Measure of sampling adequacy
mSFG	Medial superior frontal gyrus
NAI	Nürnberger-Alters-Inventar
PASA	Posterior to anterior shift in aging
PCC	Posterior cingulate cortex
pgACC	Pregenual Default Mode Network
PE	Parameter estimate
PFC	Prefrontal cortex

pMTL	Posterior middle temporal lobe
rIPL	Rostral inferior parietal lobule
ROI	Region of interest
RS	Resting state
RSFC	Resting state functional connectivity
RWT	Regensburger Wortflüssigkeitstest
SD	Standard Deviation
SFG	Superior frontal gyrus
SPL	Superior parietal lobule
SPSS	Statistical Package for the Social Sciences
TC	Temporal cortex
TE	Echo time
TFCE	Threshold free cluster enhancement
TMT	Trail Making test
TR	Repetition time
VC	Visual cortex
VGT	Verbaler Gedächtnis Test
WM	Working Memory
WST	Wortschatztest
ZNS	Zahlennachsprechen

1. Introduction

At this time, the baby – boom generation is close to retirement, thus population aging takes its course. Within the next few years 23 percent of the German population will be aged 65 years and older. At one and the same time, the elderly will account for a greater part of the population than young children will do, which has never been reported before (http://epp.eurostat.ec.europa.eu/cache/ITY_OFFPUB/KS-SF-11-023/EN/KS-SF-11-023-EN.PDF). This shift in the age distribution brings along a tremendous impact on health and economic aspects of the society (Hampel et al., 2011; Prince et al., 2013). “Age” is the highest risk factor for neurodegenerative diseases, such as dementia and Parkinson’s disease, which highlights the urgent need for a better understanding of the brain in relation to healthy and pathological aging (de Lau & Breteler, 2006; Reitz, Brayne, & Mayeux, 2011). Most research until now has focused on age-related brain changes and related cognitive deficits by comparing young and older adults. However, especially within the elderly population there is a wide inter-individual variability in cognitive performance on the one hand and in brain function and structure on the other hand. This can only partially be understood from lifespan trajectories.

1.1 Cognitive aging from early to late adulthood

Changes in cognitive abilities and performance are part of the regular course of aging from early to late adulthood. Yet, the amount of cognitive decline varies between cognitive domains. While several cognitive domains seem to decline from early adulthood on, other functions remain stable until old age. (Hedden & Gabrieli, 2004; Park et al., 2002; Park & Reuter-Lorenz, 2009). For example, vocabulary and semantic knowledge were shown to remain relatively stable across the lifespan. In contrast, a significant performance decline during adulthood was reported in the domains of executive functions, processing speed and working

memory (WM) (Hedden & Gabrieli, 2004; Ikram et al., 2010; Park, et al., 2002; Salthouse, 2004). For a recent review see (Salthouse, 2010)

Remarkably, Hedden and Gabrieli (2004) found out that cognitive decline across most domains does not start until the age of 55 years (data from Seattle longitudinal study: (Schaie, 1993; Schaie & Willis, 2010)). Within the elderly subjects research has demonstrated wide inter-individual variation in cognitive performance (Christensen et al., 1999; Hedden & Gabrieli, 2004; Hultsch, MacDonald, & Dixon, 2002; Ylikoski et al., 1999). While some elderly show high performance until late adulthood, other elderly seem to show accelerated cognitive decline. Rowe and Kahn (1997) looked into the topic of inter-individual variability in the elderly population. They started to classify elderly subjects to “successful” and “usual” agers. “Sucessful” agers were defined as (a) having a low probability of disease and disease-related disability; (b) being highly cognitive and physical functioning and (c) being actively engaged in life, while “usual” agers are still non-pathologic but at high-risk. Though, an early observation by Katzman (1993) showed that explaining this inter-individual variability of cognitive functioning is more complex than just “freedom of disease”. In his observations, Katzman (1993) found that elderly women, who showed no signs of accelerated cognitive decline, were discovered to have Alzheimer’s pathology at the time of death. He concluded that the brain must have some sort of brain reserve capacity (e.g. larger brains or more synapses) that impedes the progress of cognitive decline. This in turn, was thought to explain the variability in cognitive decline within the elderly population. Thus, there is a high consensus about age-related decline of cognitive functions from early to late adulthood. Within the elderly, a high inter-individual variability of cognitive functioning has been reported that might be explained by different reserve capacities of the brain to maintain cognitive performance as stable as possible.

1.2 Functional brain mechanisms behind cognitive performance decline from early to late adulthood

1.2.2 Task-based functional mechanisms

In contrast to the hypothesis of Katzman (1993) that larger brains or more synapses will protect the subject against cognitive impairments (brain reserve capacity), newer theories focus on the functional architecture of the brain, the so-called cognitive reserve capacity (Stern, 2009). One important contributing factor to this is neuroplasticity, a property which allows the brain to re-organize itself on the functional level (Goh & Park, 2009; Raz & Rodrigue, 2006; Reuter-Lorenz et al., 2000). In studies involving task-based functional magnetic resonance imaging (fMRI), older and younger subjects were compared with respect to task performance and respective brain activation. While performing a cognitive task, such as working and episodic memory, an overactivation of brain areas has been found for elderly compared to their younger counterparts (Cabeza, 2002; Cabeza, Anderson, Locantore, & McIntosh, 2002; Cabeza et al., 2004; Davis, Dennis, Daselaar, Fleck, & Cabeza, 2008). Several theories have been postulated, that try to explain the brain activation changes with respect to cognitive performance. For example, a shift of neural resources from posterior to anterior brain regions (PASA), or a reduction in hemispheric asymmetry (HAROLD) might be a hallmark of the aging brain (Cabeza, et al., 2004; Davis, et al., 2008; Grady et al., 1994). Cabeza et al. (2002) reported the effect of HAROLD during a memory task. During this task, younger subjects and older low-performing subjects recruited the right dorsolateral prefrontal cortex (PFC). In contrast, a bilateral recruitment of the dorsolateral PFC was found for the high-performing elderly. The additional recruitment of the contralateral brain region that was recruited by older adults was interpreted as a compensatory mechanism to maintain cognitive performance as stable as possible.

Nevertheless, brain reorganization in terms of additional compensatory brain recruitment is not always related to successful cognitive performance but also to

non-compensatory effects, as stated by the Scaffolding Theory of Aging and Cognition (Goh & Park, 2009; Park & Reuter-Lorenz, 2009; Reuter-Lorenz & Park, 2014). This so-called dedifferentiation of brain function (non-task-specific recruitment of brain regions) might also be due to a loss in specificity of the elderly to recruit appropriate brain networks (Goh, 2011; Roski et al., 2013). Further, according to the compensation-related utilization of neural circuits hypothesis (CRUNCH) there is a limit in the amount of compensation a subject can raise (Reuter-Lorenz & Cappell, 2008; Reuter-Lorenz & Lustig, 2005). With increasing task demands, subjects will reach their limits to compensate for, e.g. age-related atrophy. Consequently, an under-recruitment of brain areas was reported in response to the task that in turn leads to a decline in performance. Thus, during specific task performance, older compared to younger subjects might show some cognitive reserve capacity, expressed by compensatory mechanisms of the brain. However, whether these task-related results are generalizable to the general functional architecture of the brain, in absent of a specific task, remains unanswered.

1.2.3 Resting state functional mechanisms

Functional mechanisms of the brain, in response to task performance have been an important step in explaining functional plasticity during aging and its relation to cognitive abilities. However, in recent years, spontaneous low frequency oscillations (< 0.1 Hertz) during the resting state (RS) have become of special interest. It has been discovered that during the RS, when the subject is relaxed and the eyes are closed, several, spatially separated brain regions show high correlations in their RS-blood oxygen level dependent (BOLD) time series (B. Biswal, Yetkin, Haughton, & Hyde, 1995; Raichle et al., 2001); for a review on RS functional connectivity (RSFC) see (Van den Heuvel, Mandl, Kahn, & Hulshoff Pol, 2009). For instance, Biswal et al. (1995) reported a high functional connection between brain areas involved in motor performance during rest, forming the so-called motor network. Raichle et al. (2001) extended the first observations of functionally connected brain regions in the RS, by the exploration of the default

mode network (DMN). The DMN is also called the task-negative network, and is characterized by its activation during phases of rest, while it is deactivated (or suppressed) during externally focused attentional states. Furthermore, the DMN has often been associated with episodic memory performance (Mevel, Chetelat, Eustache, & Desgranges, 2011; Westlye, Lundervold, Rootwelt, Lundervold, & Westlye, 2011). Beckmann and Smith (2004) and Smith et al. (2009) identified several perceptual and cognitive RS networks (using independent components analysis (ICA)) that resemble brain networks associated with performance of specific cognitive functions, the so-called task-related or task-positive cognitive networks. In detail, while the executive RS network is associated with executive control functions and attention, the left frontoparietal RS network seems to be associated with language and working and episodic memory functions. On the other hand, the right frontoparietal RS network is supposed to be involved in executive control functions and WM functions (Laird et al., 2011; Smith, et al., 2009).

From early to late adulthood, RS networks seem to be sensitive to age-related changes in their RSFC (Andrews-Hanna et al., 2007; Batouli et al., 2009; Damoiseaux et al., 2008; Mowinckel, Espeseth, & Westlye, 2012; Wu et al., 2011). In particular, Damoiseaux et al. (2008) reported decreases in RSFC for the DMN in older compared to younger adults, which was associated with decreases in attention in the elderly. Andrews-Hanna et al. (2007) reported a decrease of the functional coupling between the anterior and posterior parts of the DMN in older compared to younger adults, making the two parts more independent from each other. According to the latter observation, age-related increases in RSFC were reported within the anterior DMN (aDMN) but not the posterior DMN (pDMN) in elderly subjects (Jones et al., 2011). Thus, age-related shifts in the allocation of neural resources, such as PASA found in task-based functional imaging, might be also present in the elderly during the RS (Davis, et al., 2008; Grady, et al., 1994).

With respect to task-active RS networks previous studies reported general increases in RSFC from early to late adulthood that is similarly pronounced in men and women (Mowinckel et al.(2012); for a recent review see: Ferreira & Busatto

(2013)). Analogous to PASA observed in the DMN, Filippini et al. (2012) reported task-related increases within the PFC that are also present during the RS in older compared to younger subjects. Consequently, age-related shifts in brain activations seen during cognitive performance seem to be present even during the RS. Thus, in line with the model of cognitive reserve capacity, a general functional reorganization during rest seems to protect the elderly against cognitive impairments.

While RSFC changes have been reported from early to late adulthood, RS networks within the elderly have mostly been characterized with respect to pathological conditions. Several studies compared RS networks between healthy older subjects and patients suffering from neurodegenerative diseases, such as mild cognitive impairment (MCI), dementia and Parkinson's disease (Bai et al., 2009; Bai et al., 2008; Binnewijzend et al., 2012; De Vogelaere, Santens, Achten, Boon, & Vingerhoets, 2012; A. Hafkemeijer, J. van der Grond, & S. A. Rombouts, 2012a; Mevel, et al., 2011; Rombouts, Barkhof, Goekoop, Stam, & Scheltens, 2005; Szewczyk-Krolikowski et al., 2014). For instance, abnormalities in posterior cingulate cortex (PCC)-RSFC were reported within patients suffering from Alzheimer's disease and MCI (Bai, et al., 2008; Binnewijzend, et al., 2012). However, with respect to normal aging, not much research has been investigated to characterize RSFC within the elderly population. In the study of Mowinckel et al. (2012) increases in RSFC were reported for the task-active RS networks from early to late adulthood. Likewise, decreases in RSFC were reported for the DMN. Remarkably, around the age of 50 to 55 years, one might assume that the linear relationship between age and RSFC alleviates. At the same time, RSFC variability in these RS networks increases. Thus, the RS networks of the elderly might not be as homogeneous across subjects as those of younger subjects, suggesting a higher variability in functional reorganization in the RS.

1.3 Structural correlates of functional reorganization in the aging brain

So far, it is well established that the brain is functionally composed of brain networks that are sensitive to age-related changes, as well as to neurodegenerative diseases. Moreover, these brain networks are subject to functional reorganization, even in the RS. However, although it is well known that the brain undergoes structural atrophy during adulthood, whether there is a structural correlate for the age-related changes in RS networks is still unknown.

Previous studies investigating structural alterations of the brain mainly focused on whole brain approaches or on the primary gyri and sulci of the brain with the focus on age-related changes from early to late adulthood. Total brain volume decreases have been reported with increasing age, together with an enlargement of the ventricles (Hedman, van Haren, Schnack, Kahn, & Hulshoff Pol, 2012; Scahill et al., 2003). Additionally, regional differences in the rates of atrophy (e.g. brain volume, gray and white matter) have been reported previously. Thereby, association cortices seem to be more affected than, e.g. the primary visual cortex. (Good et al., 2001; Lemaitre et al., 2012; O'Sullivan et al., 2001; Salat et al., 2005; Sowell et al., 2003). Remarkably, the above mentioned atrophy estimates use methods, such as voxel based morphometry, that are based on the grey / white matter contrast of the brain. With increasing age, however, the contrast between grey and white matter decreases in anatomical magnetic resonance (MR) images, making it difficult to reliably segment the grey and white matter. In contrast, surface-based morphometric assessments make use of the contrast between grey matter and cerebrospinal fluid that remains stable until older ages (Kochunov et al., 2005). In terms of atrophy assessment, surface-based morphometric measurements focus on changes of the cortical folding patterns, such as sulcal widening.

Cortical folding is an inevitable developmental process within the human brain. The underlying mechanisms of the cortical folding, however, are still not exactly known. Older theories state that different neuronal growth rates determine the gyral and

sulcal pattern of the brain, together with the spatial limits caused by the skull (Clark & Le Gros, 1945; Richman, Stewart, Hutchinson, & Cavincss Jr, 1975; Welker, 1990). By this time, two main theories of gyrification exist: the “grey matter hypothesis” and the “tension based hypothesis” (Zilles & Palomero-Gallagher, 2015; Zilles, Palomero-Gallagher, & Amunts, 2013). The grey matter hypothesis supposes that cell proliferation and migration determine the gyrification of the cortex (Kriegstein, Noctor, & Martinez-Cerdeno, 2006). According to the tension based hypothesis, cortico-cortical connections between fiber tracts result in an outward folding of the cortex (gyrus), and cortico-subcortical connections result in an inwarding of the cortex (sulcus) (Van Essen, 1997).

During adulthood, the brain is becoming more atrophic, probably due to underlying grey and white matter reductions (Hogstrom, Westlye, Walhovd, & Fjell, 2013; Kochunov, et al., 2005; Kochunov et al., 2008; Liu et al., 2010; Magnotta et al., 1999; Rettmann, Kraut, Prince, & Resnick, 2006; Zilles, Armstrong, Schleicher, & Kretschmann, 1988). Hogstrom et al. (2013) investigated local gyrification indices (LGI) and showed age-related regional decreases in gyrification within, e.g. the postcentral gyrus and inferior parietal lobules (IPL). Liu et al. (2010) found a global decrease in gyrification, with a more pronounced atrophy in the frontal lobe within a group of elderly subject. Interestingly, global gyrification and local atrophy within the primary sulci was also positively related to cognitive performance in an elderly cohort (Liu et al., 2011).

Thus, brain atrophy from early to late adulthood was shown with regional heterogeneities across the cortex. However, none of the above mentioned studies investigated atrophy measurements to examine the structural correlates of RS functional reorganization with increasing age. Gyrification might be an interesting measurement as it is supposed to reflect the underlying structural connectivity and complexity as well as the atrophy of the brain in later decades of life (Kochunov, et al., 2005; Magnotta, et al., 1999; Van Essen, 1997; Welker, 1990; Zilles, et al., 1988). Since increases and decreases in brain activation are supposed to be the response to structural alterations of the brain, it would be extremely helpful to establish a structure-function relationship in elderly RS networks. Particularly the

DMN is the hot topic in terms of age-related changes in RSFC. For instance, while the DMN was shown to exhibit the functionally established PASA in older compared to younger adults, whether structural changes in terms of atrophy correlate to this functional reorganization is questionable.

2 Aim of the Study

From early to late adulthood, cognitive performance declines, and functional as well as structural brain changes are present. However, while most studies focused on the comparison between young and older subjects, it became apparent that especially within later decades of life, the inter-individual variability increases with respect to cognitive performance on the one hand and functional and structural brain aging on the other hand. While it is established that pathological conditions, such as Alzheimer's disease, exhibit differences in the functional as well as structural architecture of the brain, it is still questionable what normal aging is comprised of. Therefore, it is essential to investigate and to understand the inter-individual variability of normal aging, to be able to reliably separate normal from pathological brain aging.

RS networks seem to build the functional architecture of the brain that is responsible for cognitive performance. Changes in the functional organization of the elderly brain might serve as a compensatory mechanism to maintain cognitive performance as stable as possible. While this phenomenon has been reported from early to late adulthood, RS networks within the normal elderly population are not well characterized. Thus, the first aim of this work is to characterize elderly RS networks with respect to age, gender and cognitive performance.

Further, age-related changes in structural brain aging have been reported with regional differences in the rate of atrophy. However, the whole brain approaches used by previous studies did not take into account the composition of the brain into functional networks, responsible for various cognitive functions. Functionally, the DMN was shown to exhibit the functionally established PASA in older compared to younger adults. Whether structural changes in terms of atrophy correlate to this functional reorganization is questionable. Therefore, the second aim of this work is to assess the structural correlates, measured by gyrification metrics, of the functional age-related changes in the DMN.

3 Material und Methods

3.1 Study population

The present cohort was drawn from the ongoing 1000BRAINS project (Caspers et al., 2014). 1000BRAINS is a population-based study that assesses variability in brain structure and function during aging, in relation to neuropsychological functioning, motor performance and age-dependent and age-independent self-ratings and genetic and laboratory data. The 1000BRAINS sample is drawn from the 10 year follow-up cohort of the Heinz Nixdorf Recall Study and the affiliated MultiGeneration study, an epidemiological population-based study of risk factors for atherosclerosis, cardiovascular disease, cardiac infarction, and death (Schmermund et al., 2002). The inclusion criteria for the 1000BRAINS-study as a population-based cohort study were based on the participation on the Heinz Nixdorf Recall Study. Thus, the presence of neurological or psychiatric disease was not an exclusion criterion for the present study. However, exclusion from the study was dependent on the eligibility requirements for the MR acquisition based on the MR safety guidelines. In detail: coronary artery stents, cardiac pacemakers, surgical implants or prosthesis in head or trunk, history of neurosurgery and tattoos or permanent make-up on the head (Caspers, et al., 2014). Further, MR scanning was discontinued if the participant experienced claustrophobia, or if dental implants led to artefacts in the brain images. All subjects provided written informed consent prior to inclusion. The study protocol was approved by the Ethics Committee of the University of Essen, Germany.

The final sample of the current studies was drawn on January 9th 2015. At this time, 989 participants took part in the 1000BRAINS study. 844 of the 990 participants were aged above 55 years of age, and therefore being included in the current experiments. Further, two subjects had to be excluded due to considerable brain damage post stroke. Thus, the sample for the current studies consisted of 842 subjects.

3.2 MRI acquisition

Brain imaging was conducted according to the 1000BRAINS imaging protocol including structural and functional sequences (Caspers, et al., 2014). All imaging data were acquired on a 3T Siemens Tim-TRIO MR scanner (Erlangen, Germany), using a 32-channel head coil for signal reception. For the current purpose, a structural 3D anatomical scan and a functional RS scan was acquired. The structural 3D high-resolution T1-weighted magnetization-prepared rapid acquisition gradient-echo (MP-RAGE) anatomical scan consisted of 176 slices, with a slice thickness of 1 mm (repetition time (TR) = 2250 ms, echo time (TE) 3.03 ms, field of view (FoV) = 256 x 256 mm^2, flip angle = 9°, voxel resolution 1 x 1 x 1 mm^3). The RS scan consisted of 300 functional images acquired using a gradient-echo echo planar imaging (EPI) sequence (36 slices, slice thickness 3.1 mm, TR = 2200 ms, TE = 30 ms, FoV = 200 x 200 mm^2, voxel resolution 3.1 x 3.1 x 3.1 mm^3). During image acquisition, subjects were instructed to keep their eyes closed and to relax and let their mind wander, but not to fall asleep. Adherence to these instructions was confirmed during post-scan debriefing.

3.3 Neuropsychological assessment

All subjects included in the study of 1000BRAINS underwent extensive neuropsychological assessment including the cognitive domains of attention, executive functions, episodic and WM as well as language functions (Caspers, et al., 2014). An overview of cognitive functions and neuropsychological tests used in the current studies is presented in Table 1.

3.4 Anatomical identification of brain areas

The anatomical locations of brain areas involved in RS networks as well as brain areas of relevance to age- and cognitive performance-related changes in RSFC were identified using the JuBrain Cytoarchitectonic Atlas (http://jubrain.fz-juelich.de) (Zilles & Amunts, 2010), as implemented in the SPM Anatomy Toolbox

(Eickhoff et al., 2005). Cytoarchitectonic areas were denoted in accordance with the respective publications.

Table 1: Neuropsychological tests included in the current studies: Neuropsychological tests, cognitive domains measured and corresponding references.

Neuropsychological Test		Cognitive Domain	Reference
Alters-Konzentrations-Test	**(AKT)**	Attention	Gatterer, Fischer, Simanyi, & Danielczyk (1989)
Trail Making Test	**(TMT)**	Attention / Executive functions	Morris et al. (1989) (taken from CERAD-Plus)
Farb-Wort-Interferenz-Test	**(FWIT)**	Attention / Executive functions	Similar to: Bäumler & Stroop (1985) and Stroop (1935) (Jülich version)
Fünf-Punkte-Test	**(FPT)**	Executive functions	Similar to: Regard, Strauss & Knapp (1982)
Leistungsprüfungs-system 50+, Subtest 3	**(LPS)**	Executive functions	Sturm, Willmes & Horn (1993)
Wortschatztest	**(WST)**	Language	Schmidt & Metzler (1992)
Regensburger Wortflüssigkeitstest	**(RWT)**	Language	Aschenbrenner (2000)
Benton-Test		Episodic memory	Benton, Sivan, Spreen, & Steck (2009)
Verbaler Gedächtnistest	**(VGT)**	Episodic memory	Lux, Hartje, Reich, & Nagel (2012)
Block-Tapping-Test	**(BTT)**	WM	Schelling (1997)
Visual Pattern Test	**(VPT)**	WM	Similar to: Della Sala (1997) (Jülich version)
Zahlennachsprechen	**(ZNS)**	WM	Oswald & Fleischmann (1997) (taken from Nürnberger Alters-Inventar)

3.5 Study 1: Characterization of “elderly” RS networks

3.5.1 Sample

From the initial sample of 842 subjects (aged 55 to 85 years) complete MRI datasets were available for n= 767. Of these 767 subjects, 56 were excluded from further analysis due to the presence of: (i) methodological problems in the preprocessing, e.g. motion, registration (n= 45); or (ii) more than three missing values in the neuropsychological assessment (n= 11). Thus, 711 subjects (mean age: 67.32 years, SD: 6.74; 394 males, 317 females) were included in the present RS analysis.

3.5.2 Preprocessing of functional MR images

Image analysis was performed using FSL (FMRIB Software Library: http://www.fmrib.ox.ac.uk/fsl; (Jenkinson, Beckmann, Behrens, Woolrich, & Smith, 2012)). For every subject, preprocessing included brain extraction (BET; (Smith, 2002)), motion correction (MCFLIRT; (Jenkinson, Bannister, Brady, & Smith, 2002)), and high pass temporal filtering (100ms). FMRIB's Linear and Nonlinear Image Registration tool (FLIRT and FNIRT; (Jenkinson, et al., 2002; Jenkinson & Smith, 2001)) were used to register the participant's RS-fMRI volumes to the individual structural scan, that in turn was registered to the standard space template (MNI 152). Finally, images were smoothed by a 5-mm full width half maximum (FWHM) Gaussian kernel and resampled at 3 mm isotropic voxel size. For every subject EPI images were denoised using FMRIB's ICA-based Xnoiseifier and additionally corrected for motion artefacts (FIX; (Griffanti et al., 2014; Salimi-Khorshidi et al., 2014)).

3.5.3 Extraction of RS networks

After preprocessing, MELODIC multi-session temporal concatenation (Beckmann, DeLuca, Devlin, & Smith, 2005) was used to identify common spatial patterns

within the RS data across subjects. This involved probabilistic ICA decomposition of the RS signals (Beckmann & Smith, 2004). Of the resulting 35 components, the following four RS networks of interest were selected: the DMN; executive RS network; left and right frontoparietal networks (Figure 1). Visual inspection was performed to ensure a spatial match with the respective RS networks described by Beckmann and Smith (2005) and Smith et al. (2009) (available at: http://fsl.fmrib.ox.ac.uk/analysis/brainmap+rsns/). Subsequently, dual-regression analysis was applied using spatial regression (linear model fit) to delineate subject-specific temporal dynamics for each component. Next, a temporal regression (linear model fit) was performed to identify subject-specific spatial maps for each component. Finally, a single 4D file containing the components of all subjects (one file per component with the fourth dimension being “subject”) was created for further analysis.

3.5.4 Neuropsychological variables and principal component analysis

The included neuropsychological tests, variables used as well as group mean and standard deviation (SD) are presented in Table 2. For subjects having single missing values in the neuropsychological assessment (> 3 missing values led to exclusion, see above), the missing values were replaced by the median (matched for gender and age decades: 55 - 64 years, 65 - 74 years, 75 – 85 years). To meaningfully reduce and classify the neuropsychological data, principal component analysis was used. First, all variables were transformed into z-scores. Second, data was proven on suitability for principal component analysis. The Kaiser–Meyer–Olkin (KMO) index measures the degree of common variability. KMO index reached a value of 0.883, thus ranked as “great” and therefore suitable for principal component analysis. Additionally, Bartlett's test of sphericity tests whether the variables of interest correlate with each other, which is

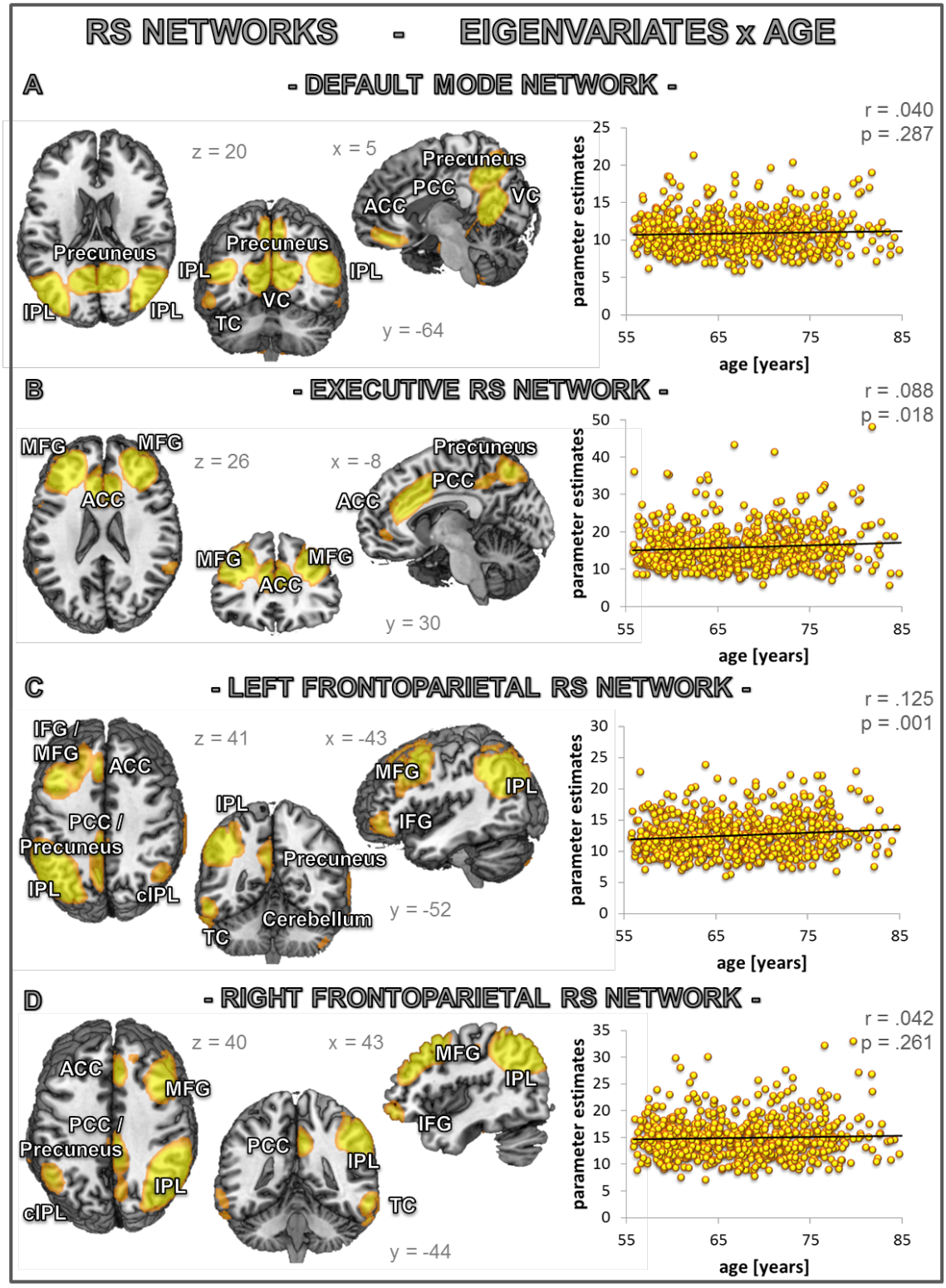

Figure 1: RS networks and the relation between parameter estimates and age in the elderly sample (as revealed by ICA): RS networks are displayed in yellow (thresholded at z > 2); (A) DMN; (B) executive RS network; (C) left frontoparietal RS network ; (D) right RS frontoparietal network: ACC: anterior cingulate cortex, IFG: inferior frontal gyrus, (c)IPL: (caudal) inferior parietal lobule, MFG: middle frontal gyrus, PCC: posterior cingulate cortex, TC: temporal cortex, VC: visual cortex.

essential for data reduction tools, such as principal component analysis. An approximate X^2 of 4270.141 (df= 105; p < .001) was revealed; thus the variables are sufficiently correlated for using principal component analysis. A measure of sampling adequacy (MSA) index was additionally obtained for each variable, to verify that every variable contributed to the component definition. MSA-indices ranged from 0.697 to 0.946, indicating that every variable included in the analysis contributed to the component definition (cut-off score >= 0.5). Principal component analysis was used to extract the neuropsychological components. Afterwards, Varimax rotation was applied to the component loadings; an orthogonal rotation to enhance interpretability of the extracted components. All steps were executed using IBM SPSS Statistics 20 (http://www-01.ibm.com/software/de/analytics/spss/).

Table 2: Overview of cognitive tests included in the RS analysis: Cognitive domains measured, corresponding cognitive functions, tests and selected variables included in the RS analysis, together with mean test scores and standard deviations (SD).

Cognitive Domain	Cognitive Function	Test	Variables	Mean of raw scores (± SD)
Attention	Selective Attention	AKT	Time (sec.) to find and cross out target items	34.85 (±11.29)
	Processing speed	TMT	Time (sec.) to connect randomly arranged digits in ascending order	39.92 (±13.63)
Executive Functions	Susceptibility to interference	FWIT	Time difference (sec.) between naming the ink that color words were printed in (part 3) and naming the ink of colored squares (part 2)	44.29 (±25.10)
	Figural fluency	FPT	Total number of unique patterns designed by connecting 5 dots within 3 min.	26.38 (±7.89)
	Problem solving	LPS	Total number of correctly identified irregularities in rows of geometric figures within 5 min.	20.50 (±5.10)

	Concept shifting	TMT	Time difference (sec.) between connecting alternately numbers and letters in ascending order (part B) and randomly arranged digits in ascending order (part A)	56.23 (±42.92)
Language	Vocabulary	WST	Total number of correctly identified real words within rows of 5 pseudowords	30.82 (±4.93)
	Phonemic verbal fluency	RWT	Total number of produced words beginning with the letter “B” in 2 min.	18.64 (±6.56)
	Semantic verbal fluency	RWT	Total number of produced words belonging to the category “Berufe (job)” in 2 min.	23.87 (±6.80)
Episodic Memory	Figural Memory	Benton-Test	Total number of errors made during the free recall of 20 previously presented figures	16.73 (±8.23)
	Verbal episodic memory (free recall)	VGT	Total number of free recalled words in 5 trials from a list containing 15 words	41.49 (±10.53)
	Verbal episodic memory (free/total recall)	VGT	Percentage of free recalled words measured against total recalled words (free recall and cued recall) within 5 trials	64.34 (±11.89)
WM	Visual spatial WM	BTT	Total number of blocks given in a sequence which were correctly) repeated (sum score forward and backward)	11.39 (±2.97)
	Visual WM	VPT	Total number of memorized patterns given as a matrix of black and white squares with increasing complexity	7.70 (± 1.77)
	Verbal WM	ZNS	Total number of digits given in a sequence which were correctly repeated (sum scores forward and backward)	14.61 (±3.30)

3.5.5 Statistical analysis

In the first step, the effects of age on RSFC in the four RS networks of interest were tested. In the second step, analyses were performed to identify the relation between RSFC and gender differences. Third, the relation between RSFC and cognitive performance (as revealed by principal component analysis) was explored.

All effects were tested using between-subject voxel-wise permutation testing (RANDOMISE) within the framework of a General Linear Model (GLM). The threshold was set at 0.05 TFCE (Threshold-free Cluster Enhancement). For each group comparison, 5,000 permutations were applied to compute the null-distribution of the critical TFCE threshold. To correct for differences in local brain volume secondary to atrophy, gray matter density maps were calculated using the T1-weighted anatomical image and the feat_gm_prepare script implemented in FSL (Smith et al., 2004). The concatenated gray matter density maps were then included as a voxel-wise covariate in all analyses. Additionally, for the analysis of age effects, gender was included as covariate of no interest in the GLM. In turn, for the analysis of gender effects, age was included as covariate of no interest. For the analysis of cognitive performance effects, both age and gender were included as covariates of no interest in the GLM. Before being entered into the GLM, all covariates were demeaned.

3.6 Study 2: Gyrification changes in the “elderly” DMN

3.6.1 Sample

From the initial sample of 842 subjects aged between 55 and 85 years, complete T1-weighted MRI data sets were available for 793. 25 subjects had to be excluded due to postprocessing failure within FreeSurfer (see below) and another 16 subjects had more than 3 missing values in the neuropsychological assessment and therefore were excluded as well. Finally, 749 subjects (mean age: 67.24, SD: 6.78, 413 males, 336 females) were eligible for the structural analysis of the gyrification index.

3.6.2 RS analysis

Preprocessing and group MELODIC were executed as explained above (see section 3.5.2 and 3.5.3). Subjects for this study were selected based on availability of structural MRI data to increase sample size. Since not all subjects also completed the RS scan, a bootstrapping approach was used to reliably define the DMN across the whole sample: From all available RS datasets (n=692), 200 datasets were randomly selected and MELODIC was performed. Out of the resulting RS networks, the DMN was selected via visual inspection to identify the best spatial match to the DMN as published by Beckmann and Smith (2004) and Smith et al. (2009). This procedure was repeated 100 times (Figure 2A), giving 100 DMNs, each based on a random sample of 200 subjects. All 100 DMNs were superimposed onto each other in standard MNI space, providing a DMN probability map (ranging from 0-100%) (Figure 2B). This probability map was thresholded at 95% (using fslmaths, FSL) to include only those areas into the final definition of the DMN, which were most consistent across subjects (Figure 2C). Each region of interest (ROI) was finally represented by a 6mm sphere around its center of gravity (Figure 2D). These final ROIs as defined in MNI-152 space were transformed into each subject’s individual space (using FNIRT / as implemented in FSL) to allow

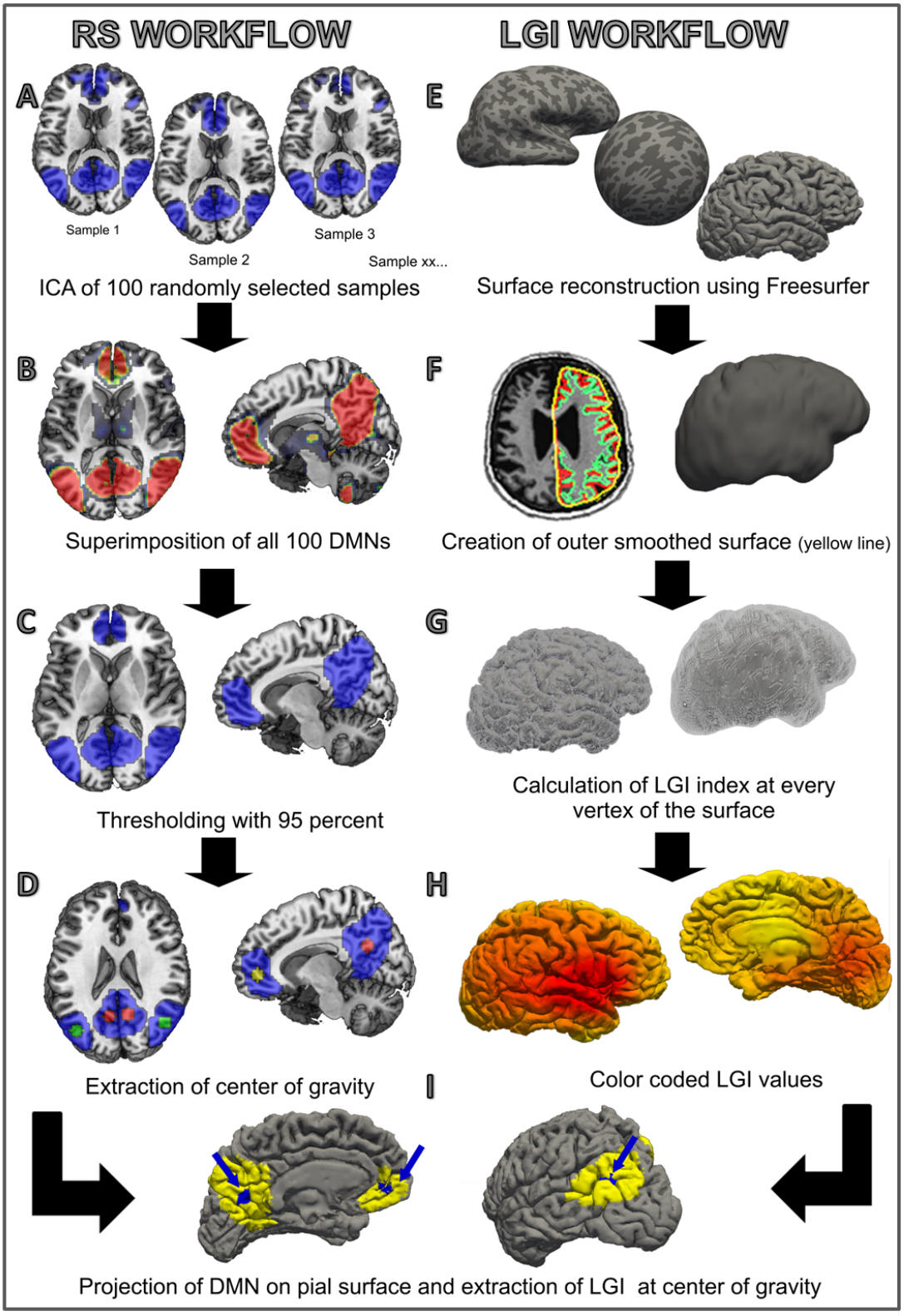

Figure 2: Overview of Gyrification analysis in the "elderly" DMN: Left panel: RS workflow. Extraction of DMN, superimposing of all extracted DMNs, thresholding and projection on pial surface. Right panel: Freesurfer pipeline and calculation of LGI (of every vertex on the pial surface and ROI; used from Jockwitz et al., in press. Brain Struct Funct, with permission of Springer).

for subsequent surface-based extraction of the local GI by means of FreeSurfer (Figure 2I).

3.6.3 Structural MR images

Anatomical images were preprocessed using SPM8 (Statistical Parametric Modeling: www.fil.ion.ucl.ac.uk/spm). All anatomical images were segmented into grey matter, white matter and cerebrospinal fluid. Afterwards, the grey and white matter images were combined to generate a reliable brain mask for subsequent processing within the FreeSurfer pipeline. Afterwards, all skull stripped images were processed using the cortical reconstruction pipeline implemented in FreeSurfer 5.1.0 (http://freesurfer.net/, (Dale, Fischl, & Sereno, 1999; Fischl, Sereno, & Dale, 1999)). This included motion and intensity correction, transformation to Talairach space, and segmentation of grey and white matter tissue, tessellation of grey/white matter boundary and correction of topological defects. The grey/white matter interface was expanded to create the pial surface, followed by spherical morphing and registration (Figure 2E).

3.6.4 Surface reconstruction and calculation of LGI

LGI was calculated according to Schaer et al. (2012; 2008) as implemented in FreeSurfer. The LGI as a measure of the cortical folding is a three-dimensional extension of the contour-based measure of the gyrification index (GI), that was introduced by Zilles et al. (1988). The original GI is measured as the ratio (of the sum of the number N of coronal slices i with slice thickness t) between the perimeter of the superficially exposed part of the pial surface without the buried sulci (outer contour; P_p^j) and the perimeter of the total pial surface (inner contour, including sulci; P_O^j) (formula taken from: (Schaer, et al., 2008)).

$$\mathrm{GI_{2D}} = \frac{\sum_{i=1}^{N} P_p^j .t}{\sum_{i=1}^{N} P_O^j .t}$$

The GI can be interpreted as the higher the GI, the higher the degree of cortical folding. The three-dimensional (3D) extension of the GI uses the reconstructed surface from *in vivo* T1-weigthed brain images (Schaer, et al., 2008). Thereby, the so-called local gyrification index (LGI) is calculated by the ratio between the outer hull surface and the pial surface over thousands of vertices. While the pial surface was already generated in the standard processing pipeline of FreeSurfer, the outer hull had to be created for calculation of the local GI. This was achieved by tightly warping the pial surface by means of a morphological closing operation that uses a 15mm sphere to close every sulcus (Figure 2F). For each vertex of the pial surface, an LGI value is assigned, calculated as the ratio of the pial surface area (defined as a sphere with the vertex as center and a 25mm radius) to the outer hull (Figure 2G,H; (Schaer, et al., 2008)). The formula is thus extended as the perimeter P_p^j and P_O^j are replaced by the area A_p^j and A_O^j and the number of slices N are replaced by the number of vertices within the cortical mesh of the pial M_p and outer M_o surface respectively (Schaer, et al., 2008):

$$\mathrm{GI}_{3D} = \frac{\sum_{j=1}^{M_p} A_p^j}{\sum_{j=1}^{M_o} PA_O^j}$$

The vertex-wise LGI values were averaged across each hemisphere for quality control purposes, i.e. to demonstrate similar age-related LGI decreases in the present sample as reported previously (Hogstrom, et al., 2013).

With regard to the present ROI-based analysis of the gyrification, this approach poses a challenge. As already stressed by Schaer et al. (2012), this LGI calculation approach is optimal for subsequent vertex-wise whole-brain analyses. For the present analysis, however, it would have been necessary to average over the LGI values of all vertices included in each ROI of the DMN. This would introduce a bias for those vertices which were at the periphery of the ROI: Due to the procedure of how the LGI is calculated for each vertex, the peripheric vertices of a ROI inevitably contain information about the gyrification of the surrounding cortex. To alleviate this problem, the ROIs of the present analysis were represented as small

spheres around their centers (see above). Finally, LGI was extracted for the vertices at the position of the center of gravity that best represented the gyrification over the whole extent of the ROI (Figure 2G, H).

3.6.5 Neuropsychological assessment

All subjects underwent extensive neuropsychological assessment as explained in section 3.3. Detailed description of cognitive functions measured, included tests, variables chosen and group means (± SD) are provided in Table 3.

3.6.6 Statistics

The overall relation between age and LGI in parts of the DMN was analyzed using multivariate ANCOVA (Anlysis of CoVariance) with gender as covariate. Afterwards, post hoc partial correlation analyses were carried out to assess the influence of age on every single part of the DMN after correcting for gender. Reported results were significant at $p < 0.05$, corrected for multiple comparisons using the false discovery rate (FDR; (Benjamini & Hochberg, 1995)). For the relation between cognitive performance and LGI in parts of the DMN, the following steps were executed: First, all neuropsychological variables were rank-transformed as they were not normally distributed. Afterwards, the ranks were transformed into standard scores (using mean centering and scaling). Then partial correlations between cognitive function scores and LGI while correcting for gender and age were calculated. All of the reported correlation results were significant at $p < 0.05$, FDR-corrected for multiple comparisons across the number of neuropsychological variables and brain regions.

Table 3: Overview of cognitive tests included in the gyrification analysis: Cognitive domains measured, corresponding cognitive functions, tests and selected variables included in the gyrification analysis, together with mean test scores and standard deviations (SD).

Cognitive Domain	Cognitive Function	Test	Variables	Mean of raw scores (± SD)
Attention	Selective Attention	AKT	Time (sec.) to find and cross out target items	34.86 (±12.19)
	Processing speed	TMT	Time (sec.) to connect randomly arranged digits in ascending order	40.37 (±18.33)
Executive Functions	Susceptibility to interference	FWIT	Time difference (sec.) between naming the ink that color words were printed in (part 3) and naming the ink of colored squares (part 2)	57.74 (±23.76)
	Figural fluency	FPT	Total number of unique patterns designed by connecting 5 dots within 3 min.	26.29 (±7.76)
	Problem solving	LPS	Total number of correctly identified irregularities in rows of geometric figures within 5 min.	20.28 (±5.15)
	Concept shifting	TMT	Time difference (sec.) between connecting alternately numbers and letters in ascending order (part B) and randomly arranged digits in ascending order (part A)	56.51 (±44.89)
Language	Vocabulary	WST	Total number of correctly identified real words within rows of 5 pseudowords	30.87 (±5.06)
	Phonemic verbal fluency	RWT	Total number of produced words beginning with the letter “B” in 2 min.	18.90 (±6.61)
	Semantic verbal fluency	RWT	Total number of produced words belonging to the category “Berufe (job)” in 2 min.	24.07 (±6.87)
Episodic Memory	Figural Memory	Benton-Test	Total number of errors made during the free recall of 20 previously presented figures	16.87 (±8.56)
	Verbal episodic memory (free recall)	VGT	Total number of free recalled words in 5 trials from a list containing 15 words	41.57 (±10.76)

WM	Visual spatial WM	BTT	Total number of blocks given in a sequence which were correctly) repeated (sum score forward and backward)	11.37 (±2.96)
	Visual WM	VPT	Total number of memorized patterns given as a matrix of black and white squares with increasing complexity	7.63 (±1.78)
	Verbal WM	ZNS	Total number of digits given in a sequence which were correctly repeated (sum scores forward and backward)	14.48 (±3.26)

4. Results

4.1 Study 1: Characterization of "elderly" RS networks

Reliable identification of the four cognitive RS networks of interest (DMN, executive RS network, left and right frontoparietal RS networks) was achieved in the present cohort (Figure 1).

4.1.1 Effects of age on RSFC

The parameter estimates (PE) of the timeseries of the thresholded RS networks were plotted against age, to illustrate the effect size of age-related changes in RSFC within the respective RS networks. PE x age plots for the four RS networks of interest are shown in Figure 1. Significant age-related increases in PE were present for the executive RS network ($r = .088$, $p = .018$) and the left frontoparietal RS network ($r = .125$, $p = .001$). For the DMN ($r = .040$, $p = .287$) and right frontoparietal RS network ($r = .042$, $p = .261$) increasing age was not significantly associated with increasing PE. Though, for all four RS networks of interest, considerable variance in the pattern of PE was observed across the cohort.

For the executive, left and right frontoparietal RS networks, small age-dependent increases in RSFC were found ($p < 0.05$, two-tailed), with comparable patterns of increase (Fig. 3). In contrast, the DMN did not show significant age-related increases or decreases in RSFC. For the executive RS network (Fig. 3A), age-related increases in RSFC were observed with the caudate nucleus of the left and right hemisphere. For the left frontoparietal RS network (Fig. 3B), age-related increases in RSFC were observed with the left caudal inferior parietal lobule (IPL) (PGa, PGp;(Caspers et al., 2008; Caspers et al., 2006)) and the left medial superior frontal gyrus (mSFG) / anterior cingulate cortex (ACC) (area 32'; (Palomero-Gallagher, Mohlberg, Zilles, & Vogt, 2008; Palomero-Gallagher, Vogt, Schleicher, Mayberg, & Zilles, 2009)). For the right frontoparietal RS network (Fig.

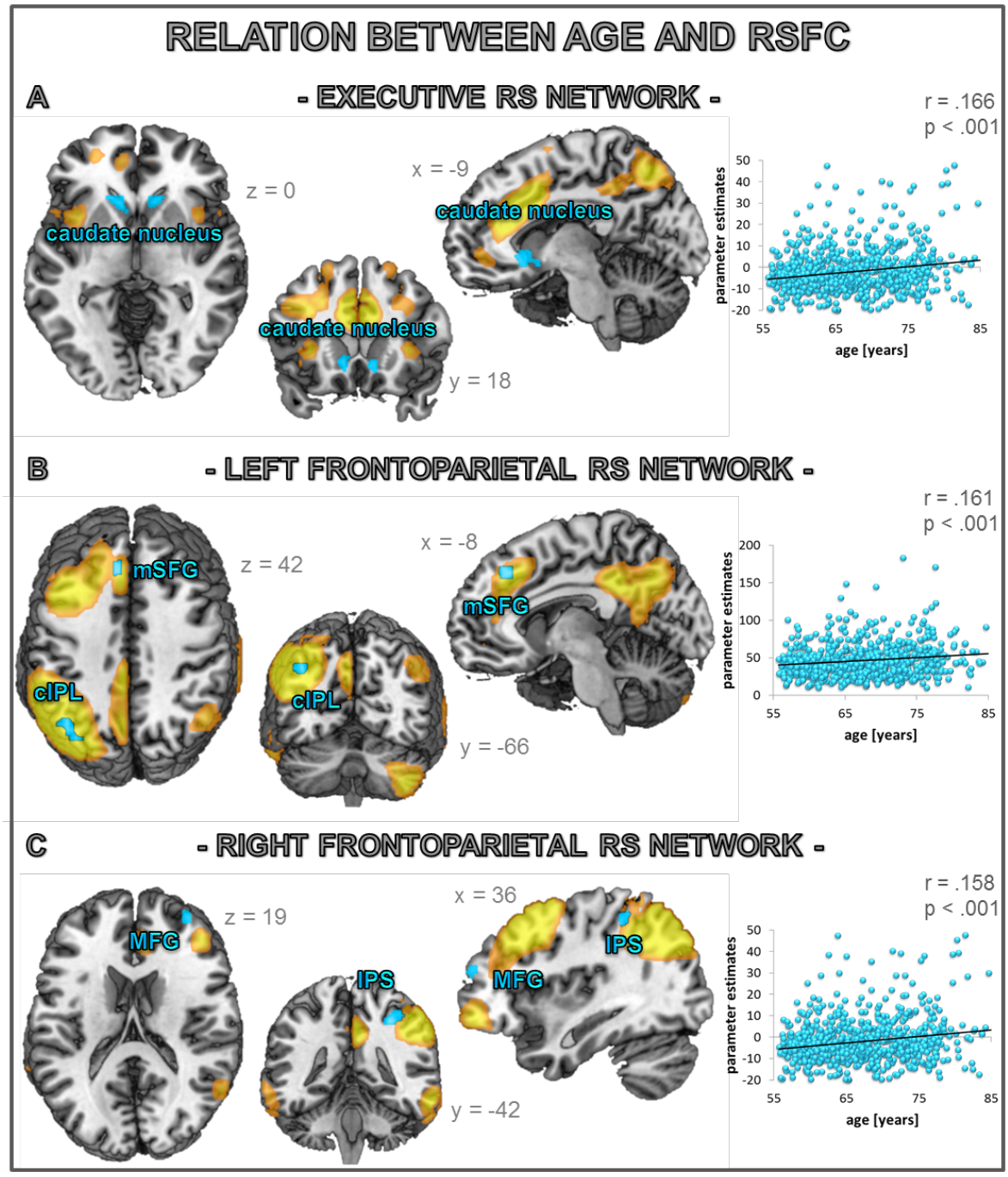

Figure 3: Age effects in the elderly cognitive RS networks: (A) executive RS network, (B) left frontoparietal RS network, and (C) right frontoparietal RS network. RS networks are displayed in yellow (thresholded at z > 2), age-dependent increases in RSFC are displayed in blue ($p < 0.05$, two-tailed). The corresponding plots (right) display the relation between age and parameter estimates of the largest cluster in the respective RS network. (c)IPL: (caudal) inferior parietal lobule, IPS: intraparietal sulcus, MFG: middle frontal gyrus, (m)SFG: (medial) superior frontal gyrus.

3C), age-related increases in RSFC were observed with the right intraparietal sulcus (IPS; hIP3; (Scheperjans et al., 2008)) and the right middle frontal gyrus (MFG) (anterior part). Since the effects of age were relatively small, results

presented were not corrected for multiple comparisons across networks. However, even after Bonferroni correction across the four RS networks of interest ($p < 0.05 / (2$ [two-tailed] x 4 [RS networks of interest] = $p= 0.00625$), age-related increases in RSFC with most of the aforementioned brain areas remain significant (see table 4 for number of voxels before and after Bonferroni correction across networks).

Table 4: Age-related changes in RSFC in the task-active RS networks: RS networks, macro- and cytoanatomical labels, MNI coordinates, number of voxels (thresholded at $p < .05$, two-tailed and thresholded at $p < .05$, two-tailed, corrected for multiple comparisons).

RS network	Macro. label	Cyto. label	Hemi	MNI			# vox. (two-tailed)	# vox. (mult. comparisons)
Executive RS network	caudate nucleus		L	-15	20	2	33	11
			R	12	17	-1	23	9
Left fronto-parietal RS network	IPL	PGa, PGp	L	-42	-70	44	27	1
	mSFG		L	-6	29	47	14	10
Right fronto-parietal RS network	IPS	hIP3	R	30	-46	53	23	6
	MFG		R	36	50	23	10	0

4.1.2 Effects of gender on RSFC

For all RS networks of interest gender-dependent differences in RSFC were found ($p < 0.05$, two-tailed, Bonferroni-corrected for RS networks (Fig. 4)). For the DMN (Fig. 4A) women showed a higher RSFC with the right caudal IPL (PGp; (Caspers, et al., 2008; Caspers, et al., 2006)) ranging into the middle occipital gyrus (MOG), left and right precuneus, left MFG (posterior division), and left extrastriate cortex (VC; hOc4lp; (Malikovic et al., 2015)). Men, in comparison to women showed a higher RSFC with the PCC (bilaterally), right middle temporal gyrus (MTG, posterior division), left MOG, left and right precuneus and the left SFG (anterior division).

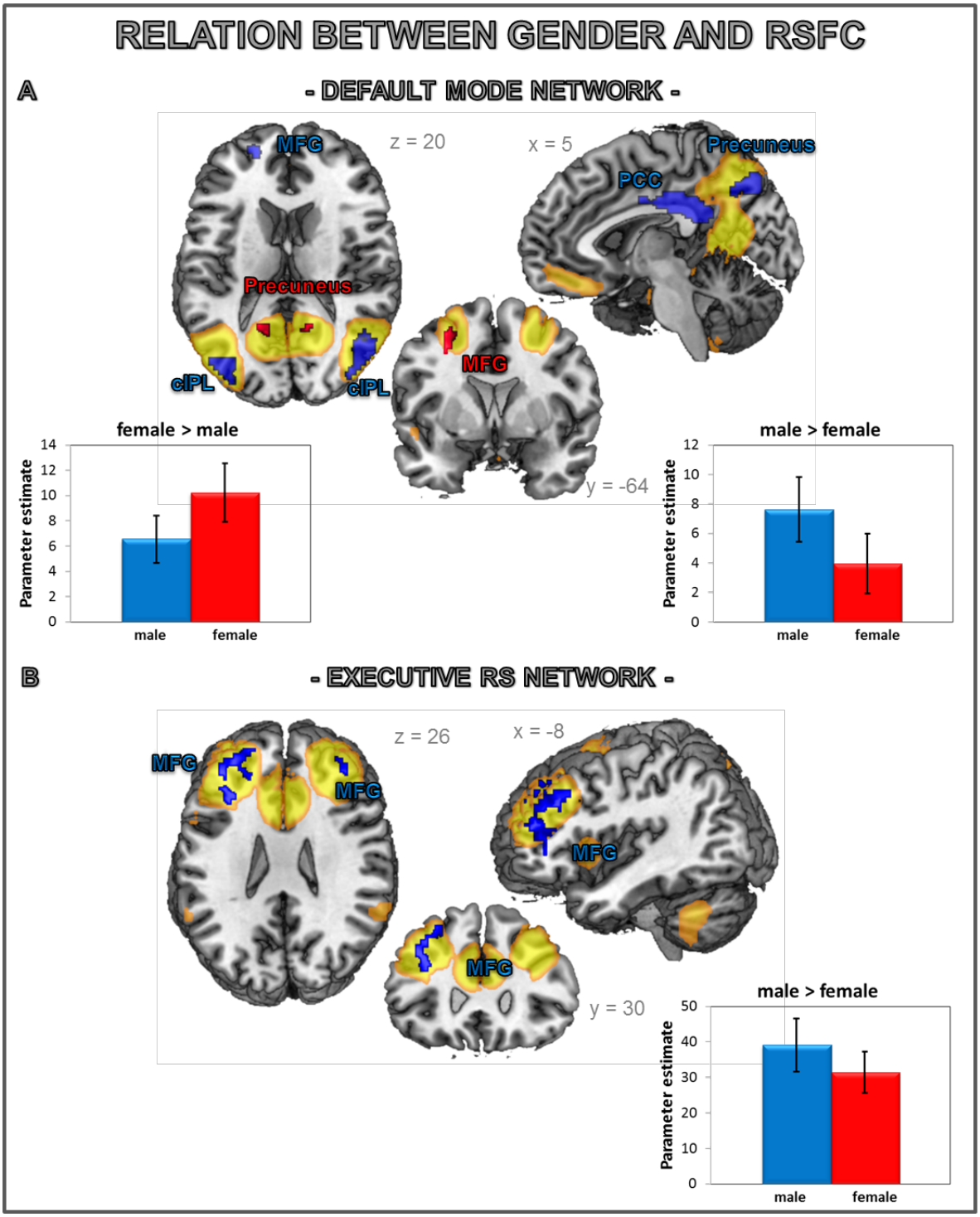

Figure 4: Gender effects in the elderly cognitive RS networks: (A) the DMN, (B) the executive RS network. RS networks are displayed in yellow (thresholded at z > 2). Female > male RSFC is displayed in red ($p < 0.05$, TFCE, corrected for multiple comparisons). Male > female RSFC is displayed in blue ($p < 0.05$, TFCE, corrected for multiple comparisons). The corresponding bar graphs (right) display the relation between gender and parameter estimates of the significant voxels in the respective RS network. (c)IPL: (caudal) inferior parietal lobule, MFG: middle frontal gyrus, PCC: posterior cingulate cortex.

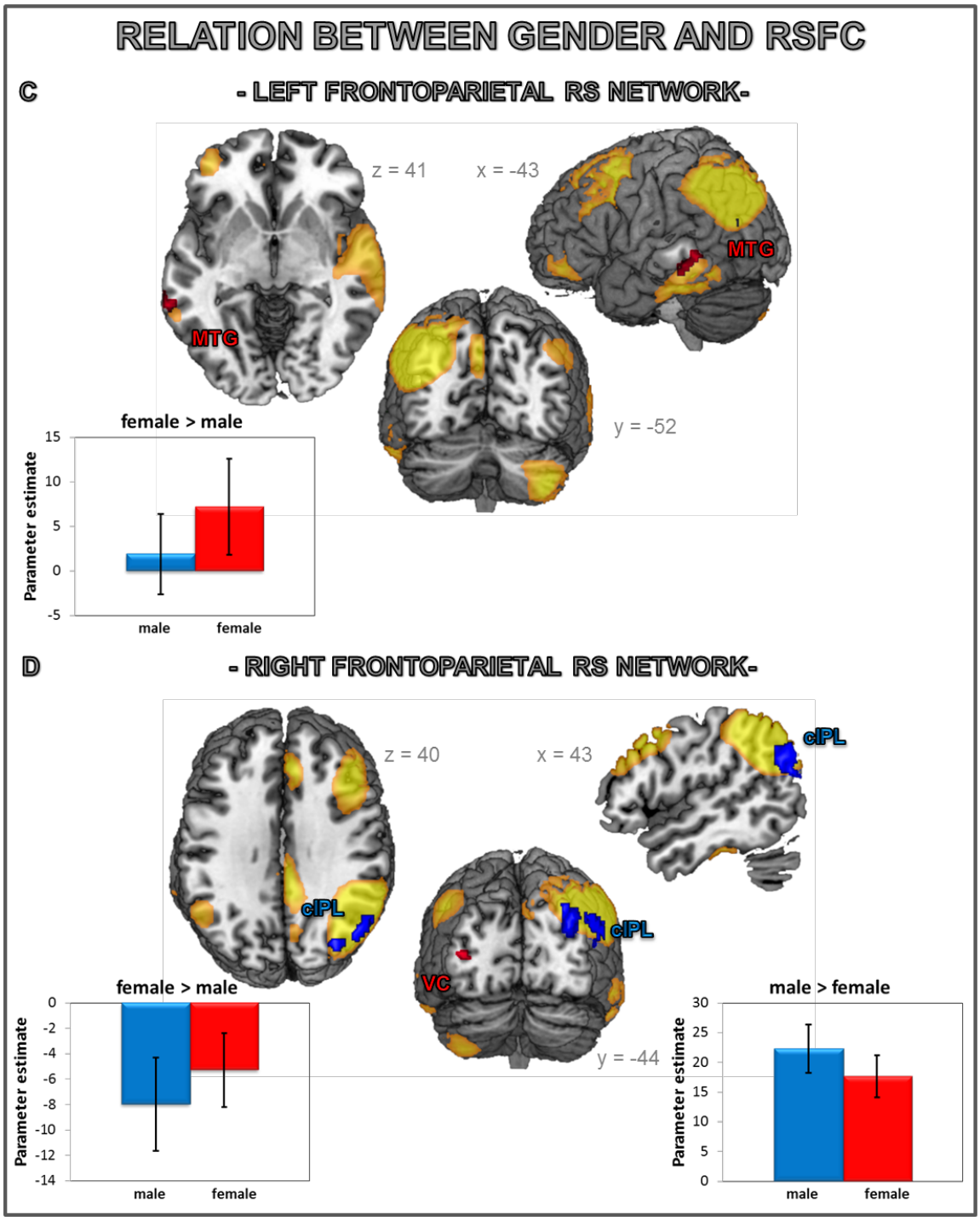

Figure 4: Gender effects in the elderly cognitive RS networks: (C) the left frontoparietal RS network, and (D) the right frontoparietal RS network. RS networks are displayed in yellow (thresholded at z > 2). Female > male RSFC is displayed in red ($p < 0.05$, TFCE, corrected for multiple comparisons). Male > female RSFC is displayed in blue ($p < 0.05$, TFCE, corrected for multiple comparisons). The corresponding bar graphs (right) display the relation between gender and parameter estimates (PE) of the significant voxels in the respective RS network. (c)IPL: (caudal) inferior parietal lobule, MFG: middle frontal gyrus, MTG: middle temporal gyrus, VC: visual cortex.

For the executive RS network (Fig. 4B), men showed higher RSFC with the MFG (bilaterally) and left inferior frontal gyrus (IFG) and junction (IFJ1; (Amunts et al., 2010)). For the left frontoparietal RS network (Fig. 4C), women showed higher RSFC with the left MTG (posterior division). For the right frontoparietal RS network (Fig. 4D), women showed increases in RSFC with the left extrastriate cortex (VC; hOc4lp; (Malikovic, et al., 2015)). On the contrary men showed a higher RSFC with the right caudal IPL (Angular gyrus (AG); PGp; (Caspers, et al., 2008; Caspers, et al., 2006), and the right MOG (Table 5).

Table 5: Gender differences in RSFC in the respective RS networks: RS networks, macro- and cytoanatomical labels, MNI coordinates, number of voxels (thresholded at $p < .05$, two-tailed, corrected for multiple comparisons).

RS network	Macro. label	Cyto. label	Hemi	# vox.	MNI		
Men > women							
DMN	PCC		R	208	3	-45	24
	MTG		R	133	45	-66	6
	MOG (VC)	hOc4la	L	79	-42	-81	12
	Precuneus		L	61	-6	78	42
	Precuneus		R	57	12	-63	39
	SFG		L	27	-21	54	9
Executive RS network	MFG		L	272	-36	45	27
	MFG		R	18	39	48	21
right frontoparietal RS network	AG	PGp	R	81	51	-69	24
	AG	PGp	R	48	36	-78	27
Women > men							
DMN	AG	PGp	R	115	42	-69	30

	Calcarine Gyrus		R	95	18	-60	18
	Precuneus		L	79	-12	-57	15
	Precentral Gyrus		L	43	-30	0	45
	Fusiform Gyrus		R	17	24	-36	-15
Left frontoparietal RS network	MTG		L	21	-69	-33	-9
Right frontoparietal RS network	MOG (VC)	hOc4lp	L	20	-36	-84	9

4.1.3 Effects of cognitive performance on RSFC

Principal component analysis was used for reduction and classification of the neuropsychological data (correlations between cognitive variables, see Table 6). Using an explorative approach, there is still no clear decision about which criterion to use to extract the optimal number of components. Based on the Screeplot criterion (Cattell, 1966), only one component would have been the preferable number of components to extract. Based on the Kaiser-Guttman criterion on eigenvalues (cut-off: eigenvalue < 1) (Guttman, 1954), three components would have been the preferable number of components (Fig. 5; Figure 6, left part). The first component was composed of performance in the following cognitive functions: visual, visual-spatial, figural and verbal (working-) memory, problem solving, processing speed, selective attention, concept shifting, figural fluency and susceptibility to interference. The first component can thus be summarized as indicator of performance in the domains of WM, attention and executive control. The second component included two measures of verbal episodic memory, i.e. free recall and the ratio between free recall and total (free + cued) recall, at this indicating episodic memory performance. The third component was driven by phonematic and sematic verbal fluency as well as vocabulary, which could be summarized as an indicator of language-related performance.

The first component of this “three component solution” summarized such diverse cognitive abilities as WM, attention and executive control functions. However, looking at the relation between RS networks and cognitive functions, it became evident that especially the left and right frontoparietal RS networks are strongly associated with WM tasks, whereas the executive RS network is more strongly involved in executive control, such as action inhibition (Laird, et al., 2011; Smith, et al., 2009). We thus aimed at further splitting this component to have distinct components representing specific cognitive domains since these are known to involve different neuronal resources in the task-based as well as the resting-state setting (Smith et al. 2009).

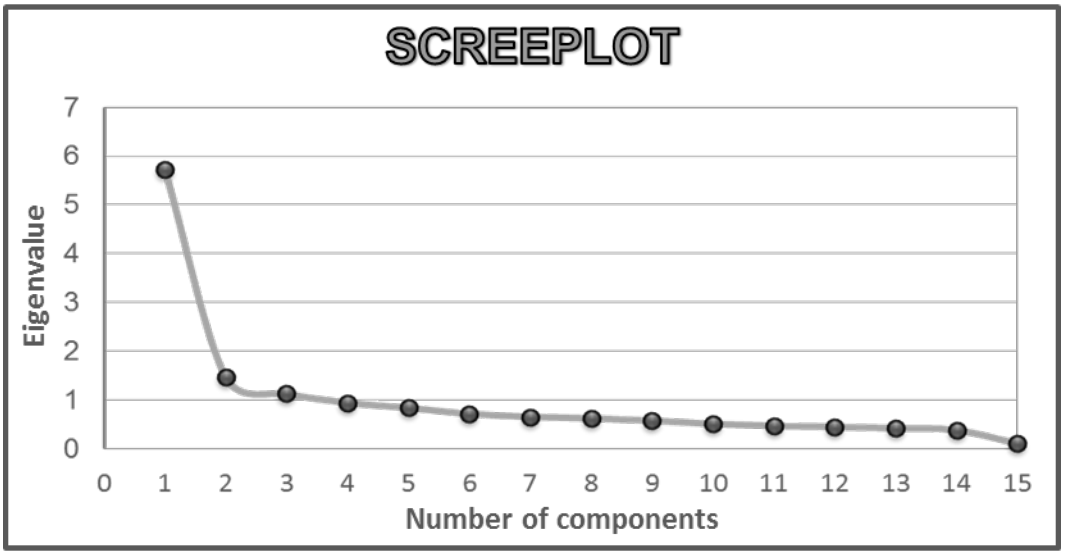

Figure 5: Screeplot of principal component analysis: x-axis represents the number of components extracted; the y-axis represents the eigenvalues for each component.

As expected, a principal component analysis with four components led to a split of the first component, while the other two components “episodic memory” and “language” remained the same (see Fig. 6, right part, and Table 7 for eigenvalues of the four component solution). The former first component (Fig. 6, left part, gray bars) split into: (i) a “WM” component (Fig. 6, right part, green bars); and (ii) an “attention – executive control component” (Fig. 6, right part, blue bars).

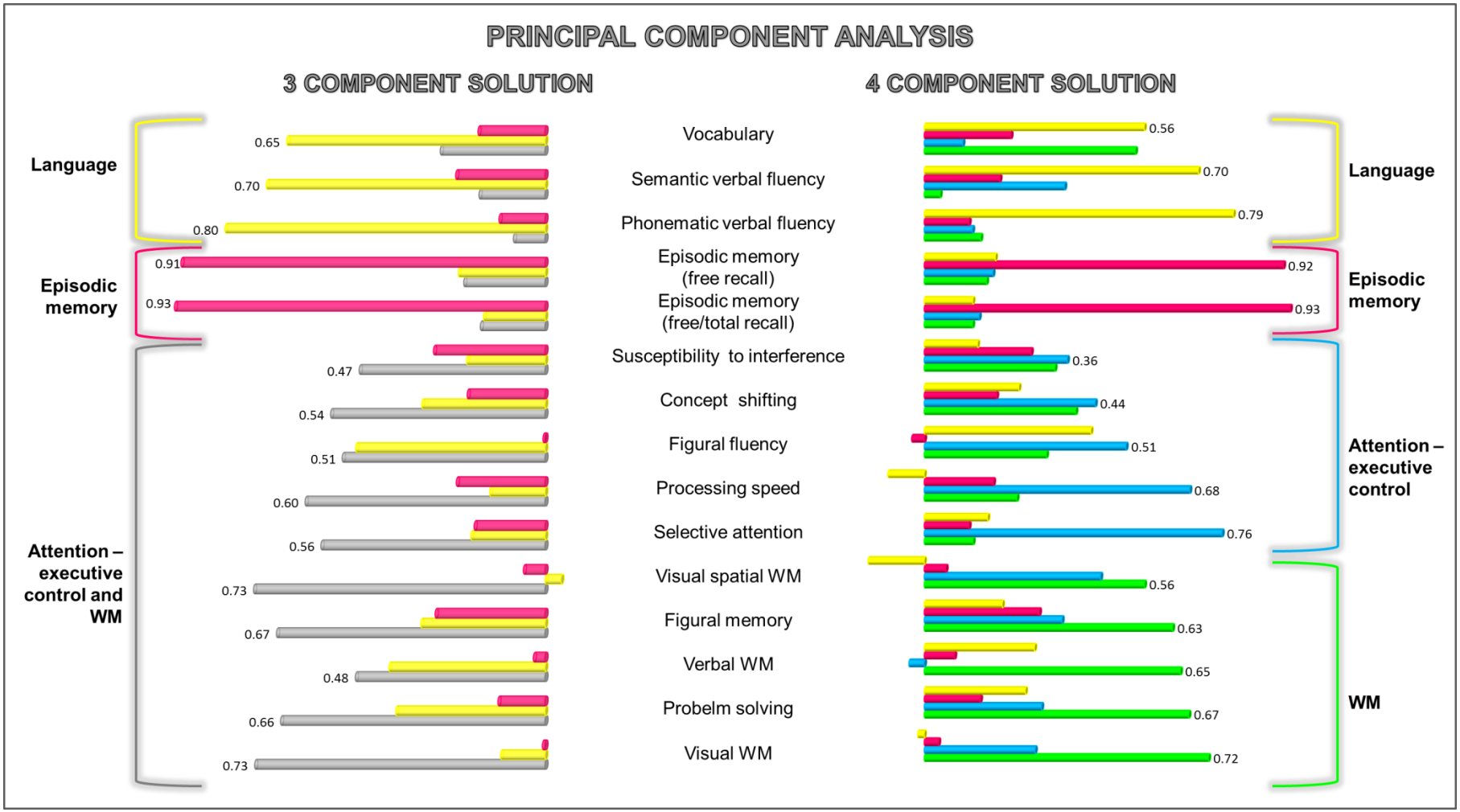

Figure 6: Cognitive functions and their involvement in the extracted components by principal components anylsis: loadings of each variable on each component extracted from principal component analysis (loading after Varimax rotation; Left: three component solution: grey = attention-executive control-WM, pink= episodic memory, yellow= language. Right: four component solution: green= WM; blue= attention-executive control, pink= episodic memory, yellow= language, eigenvalues and explained variance of each component, cf. Table 7).

Table 6: Correlation coefficients between all cognitive functions included in the principal component analysis.

	Selective Attention	Processing speed	Susceptibility to interference	Problem solving	Concept shifting	Figural fluency	Figural memory	Episodic memory (free recall)	Episodic memory (free / cued recall)	Visual spatial WM	Visual WM	Verbal WM	Vocabulary	Phonematic verbal fluency	Semantic verbal fluency
Selective Attention	1.00	0.42	0.29	0.39	0.41	0.39	0.41	0.28	0.26	0.32	0.28	0.26	0.21	0.24	0.31
Processing speed	0.42	1.00	0.35	0.40	0.34	0.37	0.43	0.31	0.28	0.35	0.35	0.28	0.23	0.26	0.29
Susceptibility to interference	0.29	0.35	1.00	0.38	0.40	0.26	0.38	0.32	0.29	0.26	0.26	0.30	0.27	0.25	0.25
Problem solving	0.39	0.40	0.38	1.00	0.44	0.46	0.56	0.34	0.29	0.40	0.50	0.45	0.46	0.33	0.32
Concept shifting	0.41	0.34	0.40	0.44	1.00	0.37	0.46	0.33	0.27	0.32	0.31	0.32	0.37	0.27	0.30
Figural fluency	0.39	0.37	0.26	0.46	0.37	1.00	0.44	0.25	0.19	0.30	0.38	0.31	0.34	0.30	0.43
Figural memory	0.41	0.43	0.38	0.56	0.46	0.44	1.00	0.45	0.38	0.44	0.54	0.40	0.47	0.31	0.37
Episodic memory (free recall)	0.28	0.31	0.32	0.34	0.33	0.25	0.45	1.00	0.89	0.21	0.21	0.24	0.35	0.29	0.37
Episodic memory (free / cued recall)	0.26	0.28	0.29	0.29	0.27	0.19	0.38	0.89	1.00	0.18	0.20	0.22	0.30	0.25	0.32
Visual spatial WM	0.32	0.35	0.26	0.40	0.32	0.30	0.44	0.21	0.18	1.00	0.45	0.32	0.17	0.15	0.21
Visual WM	0.28	0.35	0.26	0.50	0.31	0.38	0.54	0.21	0.20	0.45	1.00	0.34	0.30	0.18	0.23
Verbal WM	0.26	0.28	0.30	0.45	0.32	0.31	0.40	0.24	0.22	0.32	0.34	1.00	0.37	0.31	0.23
Vocabulary	0.21	0.23	0.27	0.46	0.37	0.34	0.47	0.35	0.30	0.17	0.30	0.37	1.00	0.40	0.34
Phonematic verbal fluency	0.24	0.26	0.25	0.33	0.27	0.30	0.31	0.29	0.25	0.15	0.18	0.31	0.40	1.00	0.49
Semantic verbal fluency	0.31	0.29	0.25	0.32	0.30	0.43	0.37	0.37	0.32	0.21	0.23	0.23	0.34	0.49	1.00

Table 7: Eigenvalues and explained variance from the principal component analysis: Initial eigenvalues, eigenvalues after extraction, and eigenvalues and percentage of explained variance after Varimax rotation (for cognitive functions and their involvement in the extracted components in four component solution, cf. Figure 6).

Component	Initial eigenvalues			Extraction sums of squared loadings			Rotation sums of squared loadings		
	Total	% of variance	Cumulative %	Total	% of variance	Cumulative %	Total	% of variance	Cumulative %
1 (WM)	5.723	38.154	38.154	5.723	38.154	38.154	2.897	19.313	19.313
2 (Attention-executive control)	1.461	9.741	47.895	1.461	9.741	47.895	2.316	15.441	34.754
3 (episodic memory)	1.127	7.515	55.410	1.127	7.515	55.410	2.074	13.826	48.580
4 (Language)	.943	6.285	61.696	.943	6.285	61.696	1.967	13.115	61.696
5	.839	5.592	67.287						
6	.715	4.765	72.052						
7	.655	4.365	76.417						
8	.623	4.155	80.573						
9	.576	3.843	84.416						
10	.510	3.398	87.813						
11	.471	3.140	90.953						
12	.450	3.002	93.955						
13	.418	2.788	96.743						
14	.381	2.538	99.282						
15	.108	.718	100.000						

The first component was composed of performance in the following cognitive functions: visual WM (.72), problem solving (.67), verbal WM (.65), figural memory (.63), visual-spatial WM (.56) and vocabulary (.54). Thus, the first component included tests of visual and visual-spatial (working-) memory, verbal WM, problem solving and vocabulary. Verbal as well as nonverbal WM performance had a great influence to this component, as most as well as highest contributing tests included WM tests. Further, two additional measurements contributed to the first extracted component from the principal component analysis: The problem solving performance (taken from LPS, component loading: .67) and vocabulary (taken from WST; loading: .54). Both tests include estimates for (verbal and non-verbal) intelligence. Thus, the first component might give information about WM performance and general intelligence in this group of elderly subjects.

The second component included selective attention (.76), processing speed (.68), figural fluency (.51), concept shifting (.44) and susceptibility to interference (.36). While the first two functions measure attention primarily, the last three functions belong to the domain of executive functions. Thus, the second component represents an attention – executive control component.

The third component included two measurements of verbal episodic memory, i.e. free recall (.93) and the ratio between free recall and cued recall (.92). Thus, the third component relies on episodic memory performance.

The fourth component was driven by phonematic (.79) and sematic (.70) verbal fluency as well as vocabulary (.56). Thus, the fourth component represented language functions.

Based on the meta-analysis of Smith et al. (2009), the following correlations between cognitive performance and RSFC were hypothesized: (i) the first component (WM) might be associated with the left and right frontoparietal RS networks (ii) the second component (attention-executive control) might be correlated to RSFC within all RS networks of interest (iii) the third component (verbal episodic memory) is related to RSFC within the left frontoparietal RS network and the DMN and (iv) the fourth component (language function) is most

likely correlated to the left frontoparietal RS network. Out of the hypothesized correlations, only one significant finding was obtained in the RSFC analyses, i.e. for the left frontoparietal RS network and WM ($p < 0.05$, corrected for multiple comparisons). Here, a better performance correlated with a decrease in RSFC of left rostral IPL (supramarginal gyrus; PF, PFt; (Caspers, et al., 2008; Caspers, et al., 2006)) with the left frontoparietal RS network (Fig. 7).

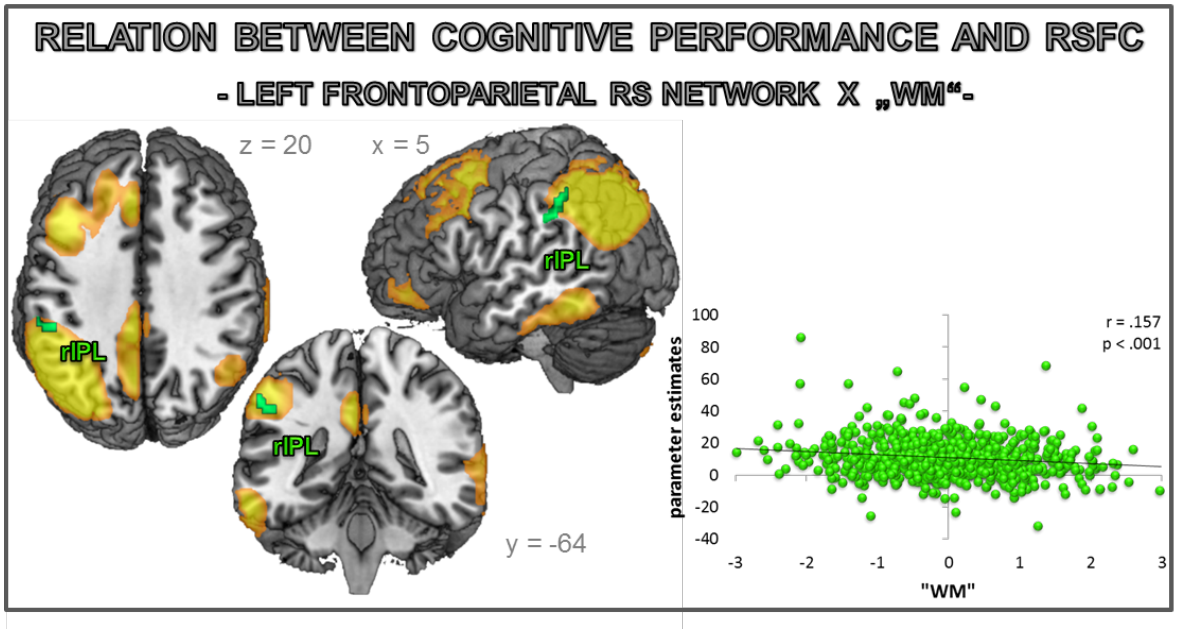

Figure 7: Relation between cognitive performance and RSFC with respect to "WM" within the left frontoparietal RS network: RS network is displayed in yellow (thresholded at $z > 2$). Increased RSFC in lower performing subjects is displayed in green ($p < 0.05$, TFCE corrected for multiple comparisons). rIPL: rostral inferior parietal lobule. The corresponding plot (right) displays the relation between cognitive performance and parameter estimates of the significant voxels.

4.2 Study 2: Gyrification changes in the “elderly” DMN

The DMN was reliably extracted in each of the 100 permutations of the bootstrapping procedure. The resulting mean DMN, averaged over all permutations and thresholded at 95%, consisted of 6 clusters: Two anterior and four posterior clusters: (i) left aDMN (left mPFC) (ii) right aDMN (right mPFC) (iii) left medial pDMN (left PCC/precuneus), (iv) right medial pDMN (right PCC/precuneus), (v) left lateral pDMN (left angular gyrus), and (vi) right lateral pDMN (right angular gyrus). Figure 8 provides an overview of these six DMN-ROIs. Table 8 represents macroanatomical and cytoarchitectonical identification of brain areas.

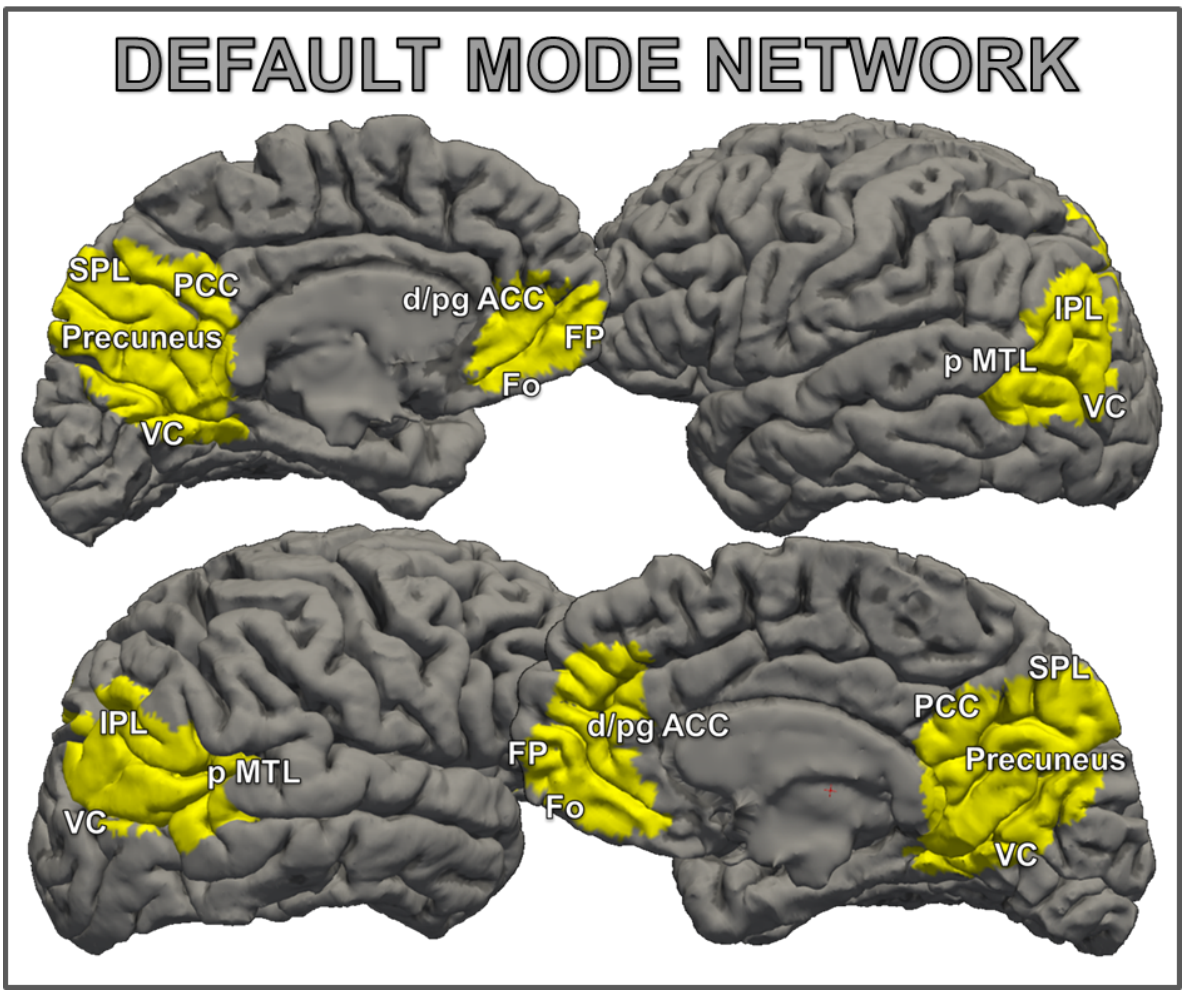

Figure 8: Description of brain areas involved in the DMN: d/pg ACC: dorsal/pregenual anterior cingulate cortex; Fo: orbitofrontal cortex; FP: frontal pole; IPL: inferior parietal lobule; pMTL: posterior middle temporal lobe; SPL: superior parietal lobule; VC: visual cortex.

Table 8: Description of brain areas involved in the DMN: including macroanatomical and cytoarchitectonical labels.

DMN-ROI	Macroanatomical label	Cytoarchitectonical label	Hemi-sphere
aDMN	dorsal/pregenual ACC (d/pg ACC)	p32, s32, p24, s24 (Palomero-Gallagher et al., 2015)	L
		p32, s32, s24	R
	Frontal pole (FP)	Fp1, Fp2 (Bludau et al., 2013)	B
	Orbitofrontal cortex (Fo)	Fo1, Fo2	B
lateral pDMN	IPL	PGa, PGp, PFm (Caspers, et al., 2008; Caspers, et al., 2006)	B
	posterior middle temporal lobe (pMTL)		B
	VC	hOc4lp [V4], hOc4la [V4] (Malikovic, et al., 2015), hOc4d [V3A] (Kujovic et al., 2013), hOc5 [V5/MT](Malikovic et al., 2007)	L
		hOc4la [V4], hOc5 [V5/MT], hOc4lp [V4]	R
medial pDMN	PCC		B
	Superior parietal lobule (SPL)	7A, 7P (Scheperjans, et al., 2008)	L
		7A, 5m, 7P, 5Ci (Scheperjans, et al., 2008)	R
	VC	hoC1 [V1], hoC2 [V2], hoC3d [V3d], hoC4d [V3A]	B

4.2.1 Effects of age on LGI

First, LGI values for both hemispheres (averaged over all vertices) were extracted (Figure 9). Mean LGI values for the left hemisphere ranged from 2.48 to 3.08, with a mean LGI of 2.75 (± 0.10). Mean LGI values for the right hemisphere did not differ significantly from the left hemisphere, ranging from 2.45 to 3.08 (mean: 2.75; ± 0.10). Further, LGI values for both hemispheres showed age- related decreases

(left: r= -.107, p= .003; right: r= -.110, p= .003), which are similarly pronounced in both hemispheres (Fisher's-Z = .06, p= .4761).

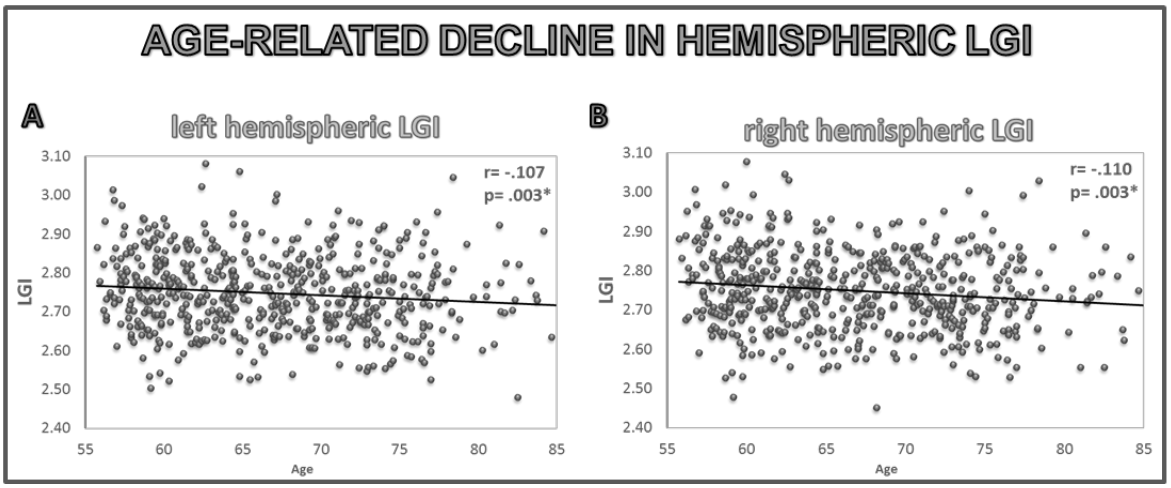

Figure 9: Scatterplots of relation between LGI values and age: raw scores, averaged over each hemisphere; with regression lines and correlation coefficients.

Afterwards, the relation between age and LGI of the DMN-ROI was investigated (raw LGI values for each DMN-ROI are shown in Table 9). ANCOVA revealed a significant interaction between age and LGI for the ROIs (F= 3.75, p= .0022, df= 5) after controlling for gender. To verify that LGI values did not show gender-specific courses with age, an additional three-way ANCOVA was applied using age, LGI and gender as factors. No significant interaction between the three factors was found (F= 0.39, p= .8593, df= 5). Thus, gender was included as covariate in subsequent analyses, but not considered separately. Post hoc partial correlation analysis (FDR-corrected for multiple comparisons) revealed heterogeneous relations between LGI and age for the DMN-ROIs.

For the aDMN, LGI of the right aDMN showed decreases with age (r = -.128; p = .0004; Figure 10D), while there was no significant effect of age on LGI in the left

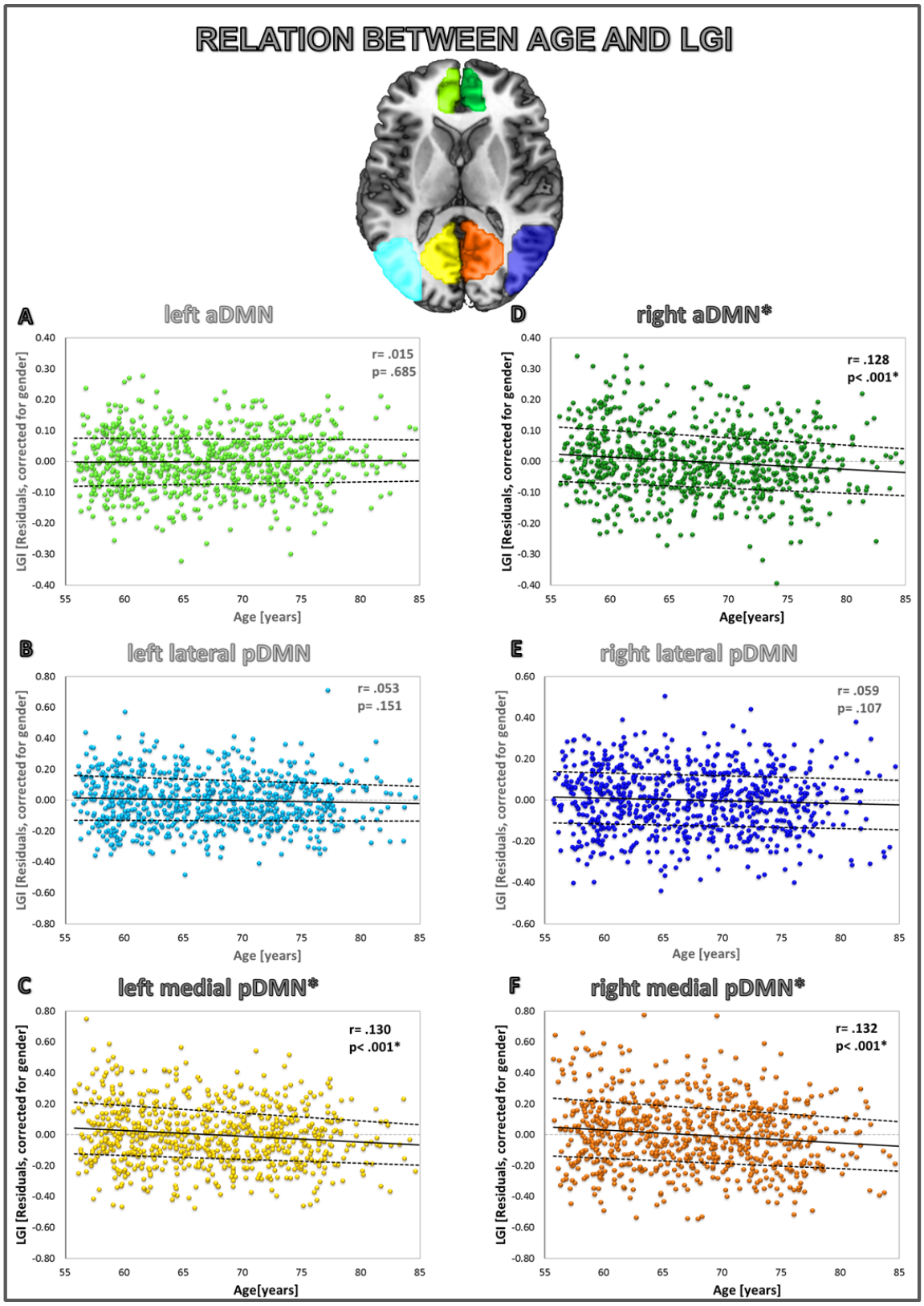

Figure 10: Scatterplots of relation between LGI values of DMN-ROIs and age: residuals, corrected for gender; with regression lines and correlation coefficients. aDMN: anterior DMN; pDMN: posterior DMN.

aDMN (r = .015; p = .6853; Figure 10A). For the pDMN, significant age-related decreases in LGI within the left (r = -.129; p = .0004; Figure 10C) and right medial pDMN (r = -.132; p = .0003; Figure 10F) were found. In contrast, left (r = -.053; p = .1512; Figure 10B) and right lateral pDMN (r = .059; p = .1052; Figure 10E) did not show significant decreases in LGI with increasing age. Figure 10 shows the relation between residual LGI values (with gender regressed out of the raw LGI values) and age.

To test whether the LGI decrease in the pDMN was more pronounced than in the aDMN and whether right hemispheric parts of the DMN showed more pronounced LGI decreases than left hemispheric parts, differences of correlation strength were assessed (using average LGI values across the respective DMN-ROIs). We found that the pDMN showed a more pronounced decrease in LGI as compared to the aDMN (Z= 1.86, p=.032, one-tailed). Furthermore, the right hemispheric DMN showed a more pronounced LGI decrease compared to the left DMN (Z=1.81; p=.035, one-tailed).

To further illustrate the size of these age effects within the raw LGI data, mean LGI values were calculated for every ROI for the 25% youngest (mean age: 58.9 years ± 1.37) as well as 25% oldest subjects (mean age: 76.2 years ± 2.93). Overview of raw scores including standard deviations and group comparisons (corrected for gender) are presented in Table 9. Group comparison between youngest and oldest 25% of the participants are presented in Figure 11.

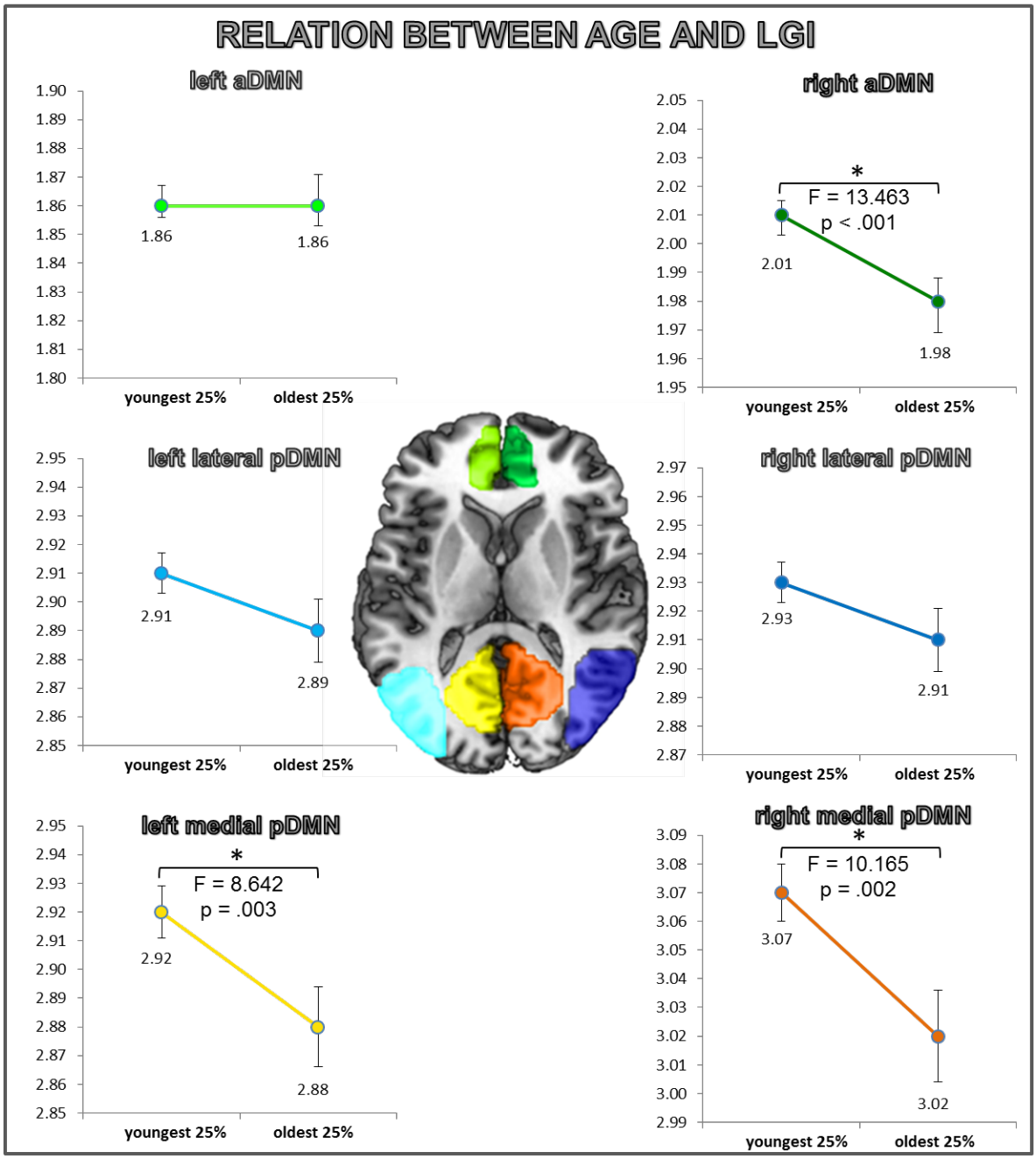

Figure 11: Group comparison between youngest and oldest 25% of the participants: with raw LGI values and statistical outcomes (cf. Table 9).

Table 9: Mean LGI values in parts of the DMN: raw scores (± standard deviation; SD) for the whole sample, youngest 25% participants and oldest 25% participants and group comparisons (cf. Fig11).

Hemi-sphere	ROI	Mean LGI value (raw score)			
		Whole sample (± SD)	Youngest 25% (± SD)	Oldest 25% (± SD)	F- value (youngest – oldest)
left	aDMN	1.86 (± .09)	1.86 (± .10)	1.86 (± .09)	.084 (p= .772)
	lateral pDMN	2.90 (± .16)	2.91 (± .17)	2.89 (± .16)	.818 (p= .366)
	medial pDMN	2.90 (± .20)	2.93 (± .22)	2.88 (± .19)	8.642 (p= .003)
right	aDMN	1.99 (± .11)	2.02 (± .11)	1.98 (± .10)	13.463 (p< .001)
	lateral pDMN	2.92 (± .15)	2.93 (± .15)	2.91 (± .15)	2.030 (p= .155)
	medial pDMN	3.05 (± .23)	3.07 (± .25)	3.02 (± .22)	10.165 (p= .002)

4.2.2 Effects of cognitive performance on LGI

Partial correlations were calculated to assess the relation between cognitive performance (domains of attention, executive functions, episodic memory, WM and language functions) and LGI within the ROIs of the DMN, using age and gender as covariates. Results were corrected for the number of correlations using FDR correction (6 ROIs x 14 neuropsychological tests). Significant correlations were found for LGI within the right aDMN, left and right medial pDMN and right lateral pDMN and the domains of attention, WM and language: Selective attention test scores were negatively correlated with LGI in the left medial pDMN (r= -.135; p= .0002; Figure 12C). Since selective attention was measured as time in seconds, a better performance (i.e. less time needed) is correlated with a higher LGI. Visual WM performance revealed a positive correlation with both the left medial pDMN (r= .115; p= .0016; Figure 12C) and the right lateral pDMN (r= .113; p= .0019; Figure 12E). Visual-spatial WM performance was positively correlated to LGI within the right medial pDMN (r= .108; p= .0031; Figure 12F). Further, semantic verbal

fluency was positively correlated with LGI of the right lateral pDMN (r= .133; p= .0003; Figure 12A) and right aDMN (r= .109; p= .0028; Figure 11D). All other correlations did not reveal significant results.

In summary, similar to the effects of age on the DMN-ROIs, the current results showed significant relations between cognitive performance and all right hemispheric DMN-ROIs. In turn, only the left medial pDMN showed significant correlations to cognitive performance. To illustrate the size of the effects of cognitive performance on LGI, mean LGI values were calculated for every ROI for the highest (best 25%) as well as lowest (worst 25%) performing subjects for every significant correlation described above (matched for age, gender and group size). Overview of raw scores of cognitive performance and LGI values including SD and group comparisons are presented in Table 10. Group comparison between highest and lowest 25% of the performers are presented in Figure 13.

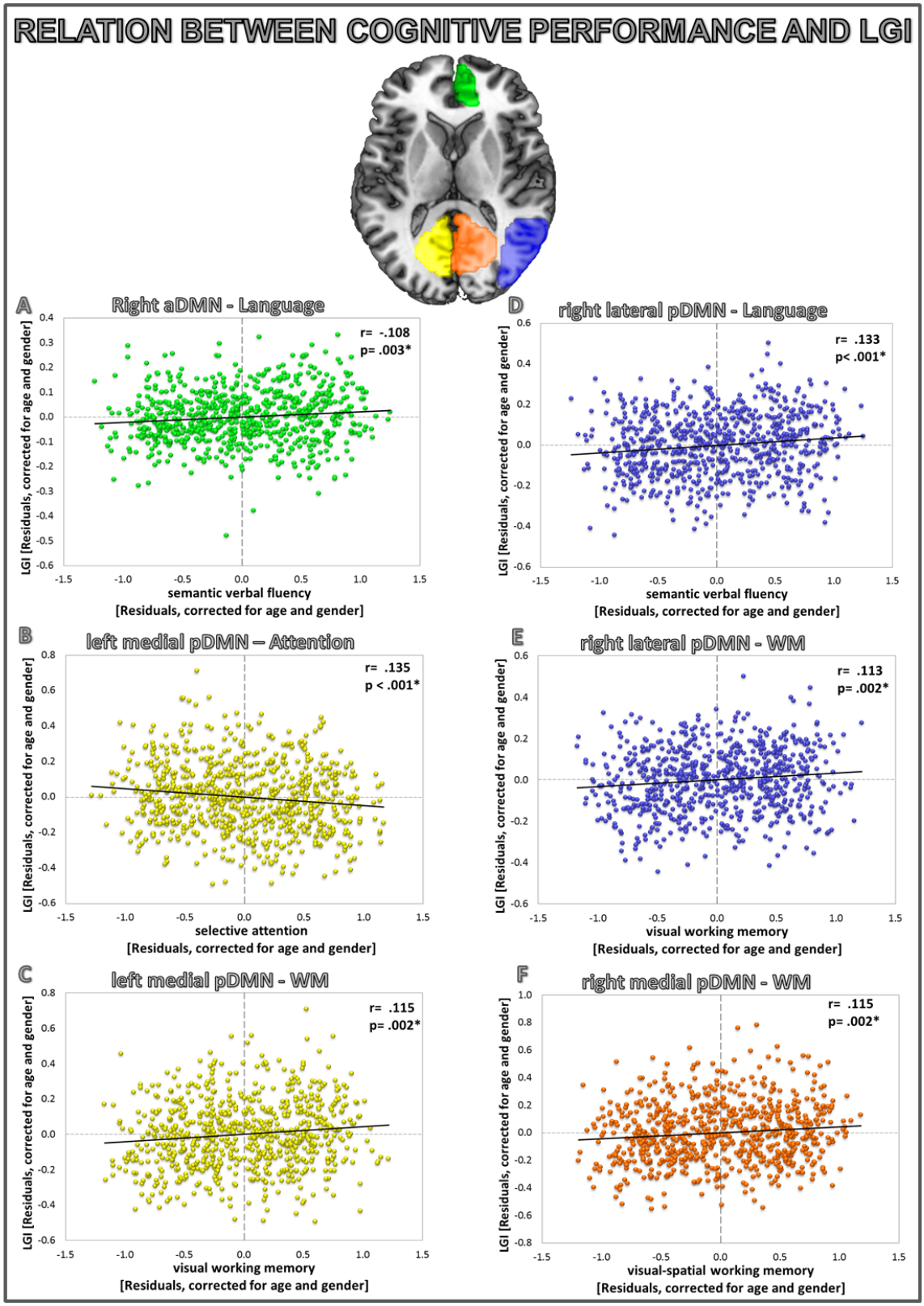

Figure 12: Scatterplots of relation between LGI values of DMN-ROIs and cognitive performance: residuals, corrected for age and gender; with regression lines and correlation coefficients. aDMN: anterior DMN; pDMN: posterior DMN; WM: working memory.

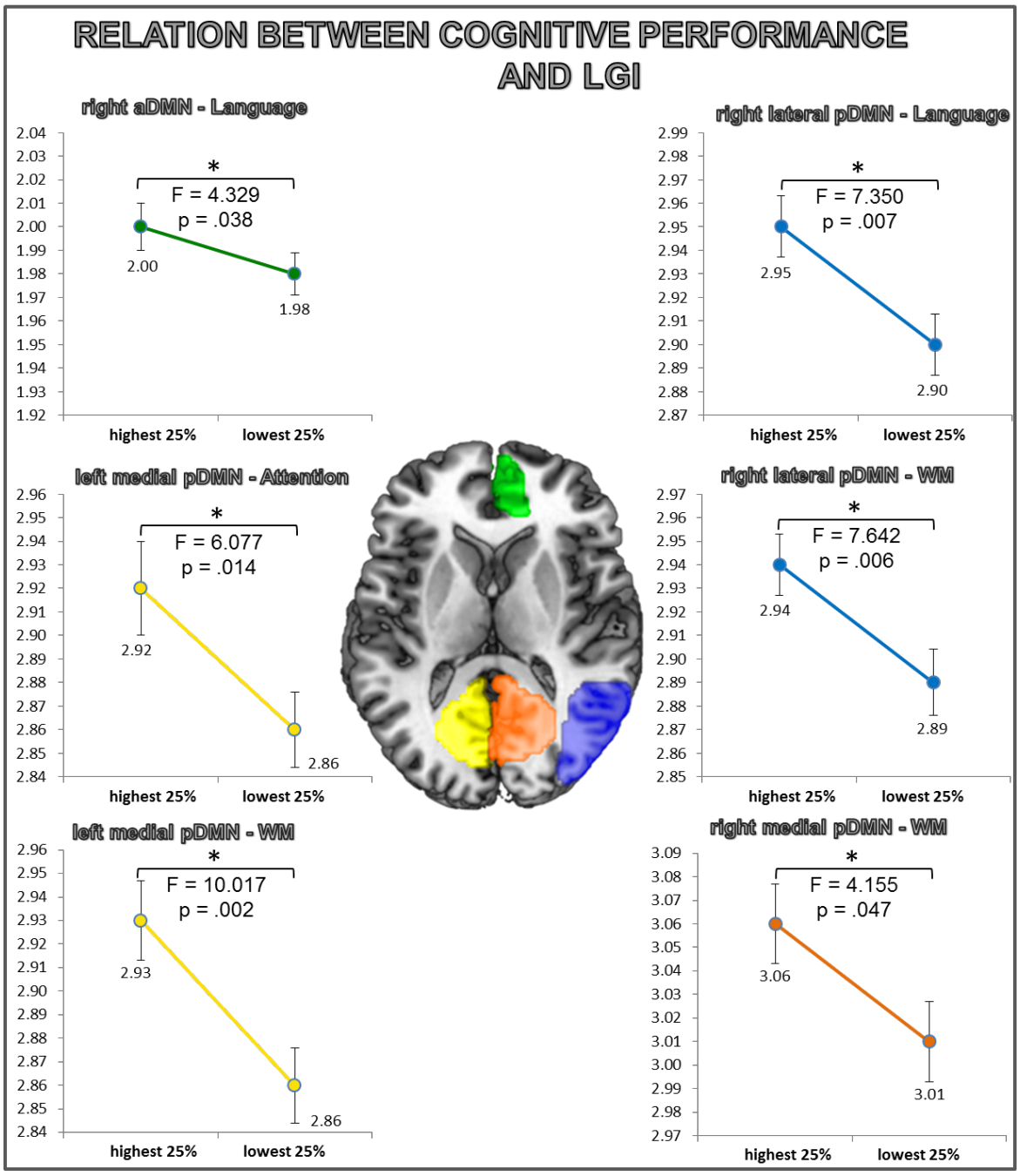

Figure 13: Group comparison between highest and lowest 25% of the performers: with raw LGI values and statistical outcomes (cf. Table 10).

Table 10: Mean test scores and mean LGI values of DMN-ROIs: raw scores (± standard deviation; SD); for the whole sample, 25% highest performers and 25% lowest performers and group comparisons (cf. Fig. 13)

Cognitive Domain / *ROI*	Function	Test score whole sample (± SD)	Mean Test score - Mean LGI value (raw scores)				
			Highest 25% Performers		Lowest 25% Performers		F-value LGI (highest 25% performers – lowest 25% performers)
			Test score (± SD)	LGI (± SD)	Test score (± SD)	LGI (± SD)	
Attention and WM/ *left medial pDMN*	Selective Attention (time in sec.)	35.95 (± 13.08)	24.74 (± 2.30)	2.92 (± .22)	47.16 (± 9.21)	2.86 (± .18)	6.077 (p= .014)
	Visual WM (# correct)	7.51 (± 2.175)	9.55 (± .829)	2.93 (± .20)	5.46 (± .630)	2.86 (± .19)	10.017 (p= .002)
Language and WM/ *right lateral pDMN*	Semantic verbal fluency (# correct)	23.9 (± 8.99)	32.16 (± 4.18)	2.95 (± .16)	15.70 (± 2.89)	2.90 (± .15)	7.350 (p= .007)
	Visual WM (# correct)	7.51 (± 2.175)	9.55 (± .829)	2.94 (± .15)	5.46 (± .630)	2.89 (± .16)	7.642 (p= .006)
WM/ *right medial pDMN*	Visual-spatial WM (# correct)	11.05 (± 3.59)	14.36 (± 1.32)	3.06 (± .22)	7.74 (± 1.42)	3.01 (± .22)	4.155 (p= .047)
Language / *right aDMN*	Semantic verbal fluency (# correct)	23.9 (± 8.99)	32.16 (± 4.18)	2.00 (± .12)	15.70 (± 2.89)	1.98 (± .10)	4.329 (p= .038)

5. Discussion

The current work addressed the relationship between the functional and structural architecture of elderly RS networks.

The first study characterized RSFC in four cognitive RS networks with respect to age, gender and cognitive performance in a large population-based elderly cohort. Small age-related increases in RSFC were observed for the task-active RS networks of interest (executive, left and right frontoparietal RS networks). The DMN did not show any age-related changes in RSFC. Further, men and women were found to differ in their RSFC across all RS networks of interest. Beyond age and gender, “WM” performance was negatively associated with RSFC within the left frontoparietal RS network. Functional reorganization within RS networks regarding age, gender, and cognitive performance differ from the functional reorganization reported from early to late adulthood.

The aim of the second study was to assess the structural correlates of age-related changes in RSFC within the DMN. Therefore, gyrification was assessed within the main parts of the elderly DMN (aDMN, medial and lateral pDMN) with respect to age and cognitive performance. Age-related decreases were found for the right aDMN and the medial pDMN bilaterally. Relations of gyrification to cognitive performance were found for the right aDMN and medial and right lateral pDMN.

5.1 Characterization of “elderly” RS networks

5.1.1 Effects of age on RSFC

Within a population-based sample of elderly subjects, small effects of age on RSFC were observed for the task-active RS networks of interest: executive, left and right frontoparietal RS networks (results reported were significant at $p < .05$, two-tailed; cf. Table 4 for significant effects of age). For the executive RS network, an age-related increase in RSFC with the caudate nucleus was present. For the

left frontoparietal RS network, age-related increases in RSFC were found for the left angular gyrus and mSFG. Lastly, age-related increases in the functional coupling between right frontoparietal RS network and right IPS and MFG were present. In contrast, there were no effects of age on RSFC within the DMN.

Increases in RSFC have been previously reported for the task-active RS networks from early to late adulthood, which is in accordance with the current results (Filippini, et al., 2012; Mowinckel, et al., 2012). For instance, Mowinckel et al. (2012) reported large increases of RSFC with the medial PFC and ACC for the executive RS network; with the left PFC and precentral gyrus for the left frontoparietal RS network; and with the anterior middle cingulate cortex for the right frontoparietal RS network from early to late adulthood. Noticeably, in contrast to studies covering the entire adulthood, the current study focused on elderly subjects only. Within this elderly population, age-related increases in RSFC are much smaller. Thus, in the elderly, other factors might become more important in terms of RSFC, such as cognitive performance, lifestyle or genetics.

The executive RS network showed increases in RSFC with the caudate nucleus bilaterally. Together with the (dorsolateral) PFC, the caudate nucleus (as part of the striatum) compose the fronto-striatal circuit (Aron et al., 2007; Middleton & Strick, 2000a, 2000b; Pugh & Lipsitz, 2002), that seems to be highly involved in tasks requiring executive functions, such as WM (Braskie et al., 2008; Klostermann, Braskie, Landau, O'Neil, & Jagust, 2012; Landau, Lal, O'Neil, Baker, & Jagust, 2009). Thereby the caudate nucleus has been reported to play an important role in the automatisation of processes, such as rule application (Muhammad, Wallis, & Miller, 2006; Stocco & Prat, 2014; Teichmann, Dupoux, Kouider, & Bachoud-Lévi, 2006). During aging, the caudate nucleus shows a consistent shrinkage and coincident dopamine loss. As a result, age-related cognitive performance decreases occur in a variety of tasks that require executive control functions, e.g. WM (Erixon-Lindroth et al., 2005); for a recent review about dopamine, aging and cognition see: (Bäckman, Nyberg, Lindenberger, Li, & Farde, 2006). Relating this to the current elderly cohort the caudate nucleus and the executive RS network showed a higher functional coupling with increasing age.

While previous studies reported increases in RSFC of the executive RS network and the PFC (Filippini, et al., 2012), elderly subjects seem to rely more heavily on the fronto-striatal circuitry. Thus, elderly might rely more heavily on automatic processes, such as previously learned rules, and knowledge. Consequently, with increasing age, elderly subjects might not be able to increase the executive control by increasing functional connectivity to the PFC. Rather; the elderly might use different strategies (i.e. more automatic processes) to solve executive control tasks expressed by the additional caudate nucleus activation to maintain cognitive performance as stable as possible.

For the left frontoparietal RS network, age-related increases in RSFC were found for the left AG and mSFG (functional: pre-supplementary motor area (SMA)). The left frontoparietal RS network has been reported to be strongly involved in language functions, attention and WM functions (Laird, et al., 2011; Smith, et al., 2009). The left AG (area PGp, PGa) has been shown to be involved in language processing, such as phonological and semantic word processing (Binder, Desai, Graves, & Conant, 2009; Seghier, 2013). The preSMA on the other hand, has been reported to be involved in cognitive control, referring e.g. to the adaption of actions in response to changing goals (Nachev, Kennard, & Husain, 2008; Rushworth, Hadland, Paus, & Sipila, 2002; Simmonds, Pekar, & Mostofsky, 2008). In older adults, reduced cognitive control was observed and found to be accompanied by reduced activation of preSMA (Coxon et al., 2014; Hu, Chao, Zhang, Ide, & Li, 2014). Thus, in terms of cognitive reserve capacity, the elderly already use compensatory brain networks during the RS. However, when task demand increases, the elderly brain functionally reaches its limit, which might then lead to performance decline during high demanding tasks according to CRUNCH.

For the right frontoparietal RS network age-related increases in the functional coupling with the right IPS and MFG were present in the current elderly population-based cohort. The right IPS has been shown to be involved in visuospatial attention (Gillebert et al., 2011; Nobre et al., 1997; Silk, Bellgrove, Wrafter, Mattingley, & Cunnington, 2010). In accordance with this, the right frontoparietal RS network is supposed to be related to attention and WM performance.

Additionally, the MFG (anterior part, BA 46), part of the dorsolateral PFC, is predominantly involved in attention and WM performance (Olesen, Westerberg, & Klingberg, 2004; Rottschy et al., 2012; Rypma & D'Esposito, 2000). Rypma and D'Esposito (2000) showed that brain activity of the dorsolateral PFC during a WM task was positively correlated to task performance in a sample of elderly subjects. Thus, similar to the effects found for the other task-active RS networks compensatory mechanisms in terms of increases in RSFC might already be present during rest, which in turn lead to decreases in task performance at higher task load.

Taken together, the task-related RS networks showed small increases in RSFC. Compared to previous research covering the entire adulthood, it has to be noted that age-related enhancements in RSFC are much smaller. As it was previously shown by Mowinckel et al. (2012), large effects of age on RSFC might be misinterpreted due to missing or only weak motion correction. In the current study all images were corrected for motion. Thus, the effects of age on RSFC found in the current study were not confounded by motion. Thus, although the task-active RS follow the trajectory seen from early to late adulthood, age and RSFC does not seem to follow a linear relationship. Increases in RSFC in the current study might serve as compensatory mechanisms in the elderly to maintain cognitive performance as stable as possible. However, according to CRUNCH, there is a limit in the capacity a subject can compensate for atrophy in the brain. Thus, it is likely that at higher task demands, the elderly will reach their limits in compensatory capacity. Consecutively, task performances will decrease.

5.1.2 Effects of gender on RSFC

In the current sample of elderly, RS networks were also characterized with respect to gender. Differences in RSFC between men and women were present within all RS networks. These effects were not attributable to one gender having a higher RSFC than the other. Instead, men and women showed higher RSFC with different parts of the respective RS network.

Differences in terms of brain structure and cognitive functions are well established between men and women. While women generally show a better performance in verbal tasks, men outperform women in tasks requiring spatial processing and mathematics (for a recent review, see: (Miller & Halpern, 2014)). Structural and neurobiological studies investigating gender effects in the aging brain revealed an earlier degeneration in women of many cortical and subcortical structures such as the SFG, hippocampus and the amygdala (Fjell et al., 2009; Yuan, Chen, Boyd-Kirkup, Khaitovich, & Somel, 2012). Important to note, research on gender differences on the four RS networks of interest is rare and results are inconclusive. For example, Mowinckel et al. (2012) and Koch et al. (2010) did not find gender effects or gender x age interactions. Other studies found women to exhibit a higher RSFC compared to men, e.g. between MFG and the right frontoparietal RS network (Hjelmervik, Hausmann, Osnes, Westerhausen, & Specht, 2014; Tomasi & Volkow, 2012; Xu et al., 2015).

The above mentioned studies either investigated young adults or subjects ranging from early to late adulthood. However, the current results correspond to a study investigating RSFC with respect to gender effects in elderly APOE4 carriers (Damoiseaux et al., 2012). With respect to the DMN the authors reported a higher RSFC with the left PCC in male APOE4 carriers (Damoiseaux, et al., 2012). This is in line with the current results as men showed higher RSFC within the PCC. Within the DMN, especially the PCC/precuneus is a hot spot of discussion with respect to healthy and pathological aging, such as MCI and Alzheimer's disease. In addition, Mann et al. (2011) found the PCC to show significant age x gender interaction between 70 and 80 years of age. Thereby men showed a smaller brain volume within BA 31. Thus, men might have to compensate for accelerated structural decline within the PCC.

For the executive RS network, men showed a higher RSFC with the MFG (anterior part). The MFG as part of the dorsolateral PFC is involved in executive control conditions (Rypma & D'Esposito, 2000). While this effect is not in accordance with the study of Hjelmervik et al. (2014), who found women to show a higher RSFC within the PFC, again, our results fit well with the results reported by Damoiseaux

et al. (2012). In their study, men exhibited a higher functional coupling between the executive RS network and the MFG. Thus, men seem to exhibit higher compensatory brain activation during the RS.

For the right frontoparietal RS networks, men showed higher RSFC with the right AG, while women showed a higher RSFC of the left frontoparietal RS network with the left MTG. The AG and the MTG are main parts of the frontoparietal RS networks. In terms of lateralization of RS networks, (Speck et al., 2000) revealed a stronger lateralization of the WM network for men in the right hemisphere and for women in the left hemisphere, that might explain different processing strategies between men and women. Thus, there might be different functional strategies men and women use to solve cognitive tests, that are also present in the elderly.

Women showed higher RSFC between the DMN and right frontoparietal RS networks and the extrastriate cortex (left area hOC4lp). This is an interesting result, since area hOC4lp is supposed to be functionally coupled with the IPL and Broca's region. It is thought to be involved in visual processing of object shapes, spatial location discrimination, mental rotation, visual attention, visual tracking and language (Malikovic, et al., 2015). To elaborate on that, the higher RSFC of women with the left extrastriate cortex relates to the observation that men outperform women in visuospatial tasks; e.g. women show slower reaction times in a spatial attention task (Bell, Willson, Wilman, Dave, & Silverstone, 2006). Thus, a higher RSFC with the left extrastriate cortex in women might serve as a compensatory mechanism for general gender differences in visual processing.

Taken together, men and women differed in all RS networks of interest. There might be hints at higher compensatory mechanisms of men within the PCC, maybe due to accelerated structural decreases. In turn, women showed a higher RSFC of the DMN and right frontoparietal RS network with the extrastriate cortex that might explain gender differences in visuospatial processing. Further, different strategies in cognitive tasks could be explained by the stronger lateralization of the right frontoparietal RS networks in men and the left frontoparietal RS network in women. Thus, differences between men and women with respect to RSFC might explain

differences in compensatory mechanisms of the elderly used to perform cognitive tasks. Further studies should investigate gender differences in RSFC in the elderly to further elucidate compensatory mechanisms in men and women.

5.1.3 Effects of cognitive performance on RSFC

In the current study the relation between cognitive performance and RSFC was examined. First, principal component analysis was carried out to reduce and classify neuropsychological data (Varimax rotation). Four components were extracted, describing the following cognitive domains: WM, attention - executive control, episodic verbal memory and language. The relation between WM and the left frontoparietal RS network revealed a significant change in RSFC with the left rostral IPL (supramarginal gyrus; areas: PF and PFt). All other cognitive components did not correlate to RSFC in any of the respective RS networks.

Functionally, the left frontoparietal RS network seems to be involved in WM performance. Using a meta-analytic approach, it was shown that the WM network consisted of the lateral premotor cortex; dorsal cingulate and medial premotor cortex; dorsolateral and ventrolateral PFC, frontal poles, and medial and lateral posterior parietal cortex (Owen, McMillan, Laird, & Bullmore, 2005). Thereby, several studies separated the WM network into a left and right lateralized network. While the left frontoparietal WM network seems to be responsible for verbal WM functions, the right frontoparietal WM network might be rather involved in spatial WM functions (Owen, et al., 2005; Reuter-Lorenz, et al., 2000). The current results showed that the lower the task performance within the factor “WM” the higher the RSFC between the rostral IPL (PF, PFt) and the left frontoparietal RS network. Noticeable, WM performance in this study included both, verbal and non-verbal WM performance, thus it seems to be unlikely that the higher RSFC between the rostral IPL and the frontoparietal RS network is caused by verbal WM performance alone. Further, it was shown that in the elderly, WM networks become more bilateral than that of younger adults (Reuter-Lorenz, et al., 2000). Ravizza et al. (2004) concluded from their task-related imaging study, that the dorsal part of the

rostral IPL is involved in the attentional part of the WM task, while the more ventral part is involved in the verbal aspect of the WM task. Further, Caspers et al. (2010) reported that area PFt within the rostral IPL is involved in action control (observation and imitation) and higher order motor functions (Caspers et al., 2011). Zhang et al. (2014) reported the middle IPL (including area PF) to be involved in the top-down attentional system. During WM, it has been shown that the IPL is involved in the planning stage, including searching for a strategic, goal-directed behavior (Koshino, Minamoto, Yaoi, Osaka, & Osaka, 2014). Thus, the IPL seems to be responsible for planning and controlling goal-directed behavior in higher cognitive tasks. Lower performing subjects in the component "WM" show increases in RSFC between the left frontoparietal RS network and the rostral IPL. Consequently, lower performing subjects might need to raise more neural resources with respect to action planning and control already in the RS as a method of compensation. When it comes to higher cognitive tasks the compensatory capacity is exhausted. Thus, comparable to the age-related effects on RSFC, the higher baseline RSFC might be an attempt for compensation. According to CRUNCH, in higher cognitive load conditions, leading to a decrease in cognitive performance.

Essentially, no effects on RSFC were found for the other investigated cognitive functions. Westlye et al. (2011) found negative correlations between memory performance and RSFC in a hippocampal cluster of the DMN in 95 APOE 4 carriers and non-carriers (63.8 ± 7.3). Damoiseaux et al. (2008) investigated RSFC within the DMN in 22 healthy elderly subjects (70.7 years ± 6.0) and found a significant negative correlation between the aDMN and the TMT part B (time in seconds) only. While these studies focused on specific regions of interest, the present study adopted a whole-brain approach to RSFC analyses in order to use all available information on the functional architecture of the brains. The present study indicates that global functional reorganization of the brain already takes place at rest for brain networks involved in WM functions, while deficits in other cognitive functions might become evident only in the specific task setting. This

argues in favor of a more global and profound alteration of WM functions in older adults as compared to other cognitive domains. (Cabeza, et al., 2002).

5.2 Gyrification changes in the “elderly” DMN

The second study assessed the relation between LGI and age as well as cognitive performance within the DMN-ROIs (left and right aDMN, medial and lateral pDMN) in an elderly population-based cohort. Remarkably, age and cognitive performance showed similar relations to LGI across the DMN-ROIs. First, LGI within the pDMN showed a stronger relation to age and cognitive performance compared to the aDMN. Second, LGI of right hemispheric DMN-ROIs was stronger affected by age and cognitive performance than that of the left hemispheric DMN-ROIs.

5.2.1 Effects of age on LGI

Age-related decreases in LGI were present for the right aDMN and medial pDMN bilaterally. According to previous studies, increasing age leads the brain to become more atrophic, with a similar progression within the left and right hemisphere. (Hogstrom, et al., 2013; Kochunov, et al., 2005; Kochunov, et al., 2008; Liu, et al., 2010; Magnotta, et al., 1999; Rettmann, et al., 2006; Zilles, et al., 1988). This is in line with the LGI decreases (averaged over the hemisphere) found in the current study. Nevertheless, the current study focused on age-related LGI decline across different multimodal brain areas encompassed in the DMN. On the one hand, the medial pDMN showed a larger age-related LGI decrease than the aDMN. One the other hand, LGI decrease of right hemispheric parts of the DMN was more pronounced than that of the left hemispheric DMN. This, in turn hints at a regional asymmetry of age-related decreases in LGI within the DMN.

Until now, there is no study exploring age-related LGI decreases within parts of the DMN in an elderly cohort. While, in the first study, there were no age-related changes in RSFC within an elderly population (cf. Study 1), several studies discovered alterations in the functional organization from early to late adulthood

within the DMN (Andrews-Hanna, et al., 2007; Damoiseaux, et al., 2008; Gould, Brown, Owen, Bullmore, & Howard, 2006; Mowinckel, et al., 2012; Sambataro et al., 2010). Interestingly, most of the aforementioned studies showed increases in RSFC within the aDMN. Additionally, age-related decreases of medial pDMN activity have been shown (Schlee, Leirer, Kolassa, Weisz, & Elbert, 2012). As proposed by Davis et al. (2008), the increase in aDMN deactivation together with a decrease in deactivations of the medial pDMN is part of the PASA theory. So, in the elderly brain the medial pDMN shows lower (de-) activations as compared to younger subjects. This observation is structurally supported, as the medial pDMN seems to be highly vulnerable to age-related gray matter decline (within area BA 31)(Mann, et al., 2011). At the same time, increases in aDMN activation might act as a compensatory mechanism to counteract the structural decline of the pDMN. Following, increases in aDMN (de-) activation might be an attempt to maintain cognitive performance as stable as possible (Ansado, Monchi, Ennabil, Faure, & Joanette, 2012; Davis, et al., 2008). Thus, the present study provides first evidence for a structural correlate of to the functionally identified effects of aging (from early to late adulthood) according to PASA: less (de-) activation of medial pDMN relates to more pronounced atrophy (as measured via decrease in LGI), while increased (de-) activation of the (left) aDMN relates to less pronounced atrophy. Consequently, the results provide evidence for a structural equivalent of the functionally proposed PASA theory.

In addition to this structural correlate of PASA, the present study revealed a potential structural correlate for another functional motivated theory of reorganization in the aging brain. The current study revealed a more pronounced LGI-decrease of the right hemispheric DMN-ROIs (right aDMN and medial pDMN vs. left medial pDMN). Previous research indicated that the right hemisphere might be more prone to show age-related decline compared to the left hemisphere, the so-called right-hemi-aging hypothesis (Grady, et al., 1994). Hemispheric asymmetries have been previously reported in structural and functional brain aging. For example, Kovalev, Kruggel, & von Cramon (2003) reported accelerated brain aging for the right ACC, using MRI texture analysis. Further, Lu et al. (2010) showed that age-related decreases in RS activity from 20 to 89 years of age were

most notably present within the right PFC. Interestingly, in addition to suggesting the PASA theory within the DMN, Davis et al. (2008) reported deactivation increases particularly for the left aDMN (left ACC). The current results revealed more pronounced age-related decreases in LGI for the right hemisphere. Indeed, an age-related LGI decrease was present for the aDMN, while LGI of the left aDMN remained constant. Thus, the left aDMN might be the main driving factor for the compensatory mechanism, as it is less affected by age-related atrophy, supporting the right hemi-aging theory.

Taken together, the current results indicate a higher decrease in LGI within the pDMN, supporting the functionally established PASA theory, together with a higher susceptibility of LGI decrease of the right hemispheric parts of the DMN, reinforcing the right-hemi-aging-model. Hence, gyrification changes within the parts of the DMN represent a structural correlate for the functionally established theories of aging.

5.2.2 Effects of cognitive performance on LGI

In the current study, significant correlations between LGI and cognitive performance were established in similar ROIs that were correlated to age. In detail, performance in the domain of attention was positively correlated to LGI of the left medial pDMN. A better WM performance correlated with a higher LGI of the medial pDMN and right lateral pDMN and a better performance in language performance positively correlated with the LGI of the right aDMN and right lateral pDMN.

Comparable with age-related decreases in LGI, the current results show a stronger relation between the pDMN and cognitive performance compared to the aDMN. In detail, LGI decreases of the pDMN (medial and right lateral pDMN) were related to deficits in selective attention, as well as visual and visual-spatial WM performance. Functionally, the DMN as such and the medial pDMN in particular, seem to be strongly involved in attentional processes. Moreover, the molecular organization (i.e. the receptor distribution) of the lateral pDMN (AG) is similar to that of the extrastriate visual brain areas (Buckner, Andrews-Hanna, & Schacter, 2008;

Buckner et al., 2009; Caspers et al., 2013). Thus, it seems likely that these functions correlate to LGI decreases within the DMN. During aging, selective attention might be disturbed at early visual processing stages, which in turn impair visual WM performance (Gazzaley et al., 2008; Gazzaley & Nobre, 2012). A lack of desynchronization of brain oscillatory activity within medial and right lateral pDMN (i.e. precuneus and right IPL) disrupted the efficient use of the fronto-parietal WM network, which in turn led to a decline in visual WM performance (Pinal, Zurron, Diaz, & Sauseng, 2015). Thus, the results of the present study illustrate that a decline in LGI within the pDMN impairs cognitive performance, supporting PASA. Further, the current results complement the age-related LGI decreases. On the one hand, the pDMN is more prone to age-related LGI decreases. On the other hand, the pDMN additionally relates to cognitive performance decline. At this point it has to be mentioned that in the analysis of cognitive performance x LGI, age was regressed out of both, cognitive parameters and LGI values. Thus, the effects of cognitive performance on LGI were not attributable to the effects of age. The functionally established PASA theory could thus also be applied to structural LGI changes in the elderly.

Remarkably, LGI of all right hemispheric DMN-ROIs was correlated to cognitive performance decline, which is in line with the right hemi-aging theory. While LGI of the right medial and lateral pDMN were associated with visual (-spatial) WM, LGI of the right aDMN and lateral pDMN were positively correlated to performance in semantic verbal fluency. Functionally, both, the aDMN (i.e. ACC) and the lateral pDMN have been associated with semantic verbal fluency (Binder, et al., 2009; Pardo et al., 2007; Shalom & Poeppel, 2008); for a recent review see (Seghier, 2013). However, contrary to the current results, previous studies showed a more prominent involvement of the left hemispheric aDMN and lateral pDMN in semantic verbal fluency tasks (Binder, et al., 2009; Wagner, Sebastian, Lieb, Tuscher, & Tadic, 2014). Even though the relation between LGI of right aDMN and lateral pDMN and cognitive performance support the right hemi-aging hypothesis, it remains questionable why only the right hemispheric DMN-ROIs relate to cognitive performance in the usually left hemispheric processed task. Most of the aforementioned studies investigated younger participants than those included in

the current study. At older ages, it is known, at least from prefrontal brain regions, that a more bilateral involvement of brain regions is necessary to perform higher cognitive tasks at the same level as younger subjects do (HAROLD-Model; Hemispheric-asymmetry-reduction-in-older-adults) (Cabeza, 2002). Thus, if this might also apply to semantic verbal fluency, then the right lateral pDMN and aDMN gain importance in the semantic verbal fluency in older adults. Consequently, a more pronounced atrophy of these brain regions (according to the right-hemi-aging theory) would lead to insufficient functional capacity and therefore result in lower performance.

Taken together, similar to the age-related LGI decreases within the DMN, LGI of the pDMN showed stronger correlation to cognitive performance decline, supporting PASA. Second, LGI of all right hemispheric parts of the DMN correlated to cognitive performance decline, strengthening the right-hemi-aging-model. Consequently, gyrification changes within the parts of the DMN represent a structural correlate for the functionally established theories of aging and cognitive performance.

5.3 Structure – function relationship within the “elderly” DMN

For the DMN, a structure-function relationship has been established in this work. Surprisingly, the DMN did not show any age-related changes in RSFC, but decreases in LGI in the present elderly cohort. In interpreting the absence of functional changes of the brain, the fact that previous studies spanned early to late adulthood must be taken into account. Previous research has demonstrated a decrease in RSFC of the DMN from early to late adulthood (Batouli, et al., 2009; Damoiseaux, et al., 2008; Mowinckel, et al., 2012). However, the issue of whether this age-related trend continues into older age remained unclear. Mowinckel et al. (2012) demonstrated that the steep decrease of RSFC within the DMN slowed down at the age of 50 to 55 years, i.e. the age regression slope plateaued. Additionally, Westlye et al. (2011) found no age-related changes in RSFC of the

posterior DMN in a small group of healthy elderly APOE E4 carriers (n = 33; mean age: 62.6years ± 7.6). In the present population-based elderly cohort there were no effects of age on RSFC within the DMN. Especially within the elderly population it was shown that both, the functional and structural architecture of the brain show a high variability (Dickie et al., 2013; Mowinckel, et al., 2012). Investigating subtle age-related changes in RSFC in such a heterogeneous population might thus require larger sample sizes. With respect to the study of Westlye et al. (2011) it could have been argued that reliable detection of subtle, but relevant, effects in RSFC requires large sample sizes (B. B. Biswal et al., 2010; Button et al., 2013). Given the large number of elderly subjects (i.e. 55 years and above) investigated, the present study did indeed have sufficient power to demonstrate age-related effects on RSFC in the elderly. Further, Mowinckel et al. (2012) reported strong influences of subject motion on RSFC in a sample from early to late adulthood. The current RS data was corrected for subject motion and for gray matter differences across subjects. Thus, the missing effects of age on RSFC were not caused by confounding effects of motion or gray matter variability in the elderly population. Hence, together with the results of previous studies, the present data indicate that the aging process for RSFC in the DMN follow a non-linear trajectory from early to late adulthood. This is characterized by a pronounced decrease of RSFC between youth and middle age, which in turn disappears in older subjects.

Interestingly, despite this missing effect of age on RSFC of the DMN, the second study revealed age-related effects on LGI within the DMN. Based on theories of functional and structural brain aging, the brain has a specific reserve capacity to prevent cognitive impairments. The brain reserve capacity (also called the passive model; (Stern, 2002)) thereby states that the brain is structurally able to resist brain damage until a certain threshold before functional, cognitive or behavioral deficits occur (Satz, 1993). This may be due to an increasing number of neurons, synapses or due to larger brain volumes. Regarding the current work, the elderly subjects might have a high brain reserve capacity. This, in turn could explain structural decreases in LGI with increasing age and the absence of age-related effects on the functional level. However, according to the brain reserve capacity, a higher brain reserve would be also protective against behavior deficits (i.e. deficits

in cognitive performance). The current elderly sample showed a correlation between cognitive performance and LGI. Thus, brain atrophy, in terms of LGI decreases, resulted in behavioral deficits. If the brain reserve capacity is able to inhibit or delay cognitive impairment, than both, cognitive as well as functional differences should be absent in the current samples.

Another possibility would be the more active model of cognitive reserve capacity from Stern (2002). In this model, the maintenance of cognitive abilities in the elderly is based on the capacity of the brain to functionally reorganize itself. By using the same networks in a more efficient way (cognitive reserve) or using alternate brain networks to perform cognitive tasks (compensation), the elderly is able to maintain cognitive performance. In the current sample of elderly age-related decreases in LGI were present. In contrast, no effects of age on RSFC were present in the current elderly sample. Thus, the DMN might not be able to work efficiently in older subjects (i.e. no age-related increase in RSFC). In line with this, a decline in LGI within the DMN-ROIs also correlated with cognitive performance. Thus, elderly subjects of the current sample might not be able to recruit alternative brain networks to compensate for the atrophy, as expressed by cognitive deficits seen in the second study.

Previous studies investigating structure-function relationships in the elderly compared healthy elderly with diseased subjects, such as MCI or Alzheimer's disease (Bai, et al., 2008; Greicius, Srivastava, Reiss, & Menon, 2004; A. Hafkemeijer, J. van der Grond, & S. A. R. B. Rombouts, 2012b; Jones, et al., 2011; Rombouts, et al., 2005). For example, Bai et al. (2008) found that elderly subjects suffering from MCI show gray matter decreases in the PCC/precuneus. At the same time (even when controlling for these gray matter decreases) these subjects showed lower RSFC of this region with the DMN. Such a finding could not been shown in the current study comprising normal elderly subjects. Hence, differences in cognitive performance in these populations are much larger than those found in the current study. Additionally, it might be that healthy elderly only exhibit age-related changes in the functional brain activation during cognitive performance. In the study of Davis et al. (2008) the effect of PASA was not only present during the

RS, but also during cognitive performance (when the DMN was deactivated). However, in their study elderly subjects were compared to young adults. Thus, the effects of aging were more pronounced than comparing elderly subjects. Therefore, it might be the case that in a normal elderly population the shift of brain activation from posterior to anterior brain regions (PASA) is only present during cognitive performance.

5.4 Limitations and implications for future research

The samples of the current studies were drawn from 1000BRAINS, a cross-sectional population-based study. This precludes inferences concerning the intra-individual course of cognitive decline: (i) during aging; or (ii) with respect to cognitive performance. Previous studies have investigated longitudinal changes in measures such as cognitive performance from early to late adulthood or during late adulthood only (Raina et al., 2009; Schaie, 1993; Schaie, Willis, & Caskie, 2004), or in health vs. disease, e.g. dementia (Mueller et al., 2005). The present findings therefore require replication in longitudinal studies.

The current results give indications for future research. First, longitudinal study designs should be used to explore effects of aging on the functional and structural architecture of RS networks in the elderly population. These investigations should explore correlations between functional brain architecture and cognitive markers of age-related decline and variability in the elderly. Furthermore, the current study draws inferences solely on the LGI of DMN regions. It remains for future studies to investigate regional patterns of age effects on LGI in other cognitive brain networks, e.g. frontoparietal RS networks. Further, research should also investigate LGI changes within RS networks for patient groups. With respect to gender, more research has to be conducted to explore the differences in the functional architecture of RS networks. Further, gender differences in RS networks should be also correlated to cognitive decline. Importantly, future research should also take into account the fact that further factors may influence RSFC in elderly subjects, such as genetics and environmental factors. On the one hand, genetic influences on RSFC should be investigated in future research. Research suggests

that RSFC is influenced by genetic predisposition, such APOE4 allele carrier status, and the deposition of amyloid protein (Hafkemeijer, et al., 2012b; Westlye, et al., 2011). On the other hand, environmental factors might also influence RSFC connectivity and related cognitive performance. These factors include physical fitness, risk factors, such as nicotine and alcohol consumption, and social conditions.

6. Summary

The aim of this work was to investigate the structure-function relationship in cognitive resting state networks in a large population-based elderly sample. The first study characterized the functional connectivity in four cognitive resting state networks with respect to age, gender and cognitive performance: Default Mode Network (DMN), executive, and left and right frontoparietal resting state networks. The second study assessed the structural correlates of the functional reorganization of the DMN during aging, using local gyrification indices.

Small age-related increases in functional connectivity were present for the executive, left and right frontoparietal resting state networks, but not for the DMN. Men and women were found to differ across all resting state networks of interest. Performance in working memory was negatively associated with functional connectivity within the left frontoparietal resting state network. Elderly seem to exhibit compensatory mechanisms as an attempt to maintain cognitive performance. However, the negative correlation between resting state functional connectivity and cognitive performance emphasizes limits in cognitive reserve in the elderly. Interestingly, men and women seem to show differences in cognitive strategies, which might be related to differences in performance of various cognitive domains. Thus, the current results provide a basis for further research with a particular focus on the functional organization of the elderly brain.

Structurally, age-related decreases in gyrification were present for the right anterior DMN and the medial posterior DMN bilaterally. Relations of gyrification to cognitive performance were found for all right hemispheric parts of the DMN and the left medial posterior DMN. The more pronounced vulnerability of the posterior DMN as well as the right hemispheric parts of the DMN in relation to age and cognitive performance provide the structural underpinning of functional theories of aging, i.e. posterior to anterior shift in aging and the right-hemi aging theory. Thus, gyrification decreases within the DMN may functionally lead to an insufficient DMN in the current elderly sample.

7. Literature

Amunts, K., Lenzen, M., Friederici, A. D., Schleicher, A., Morosan, P., Palomero-Gallagher, N., et al. (2010). Broca's region: novel organizational principles and multiple receptor mapping. *PLOS Biology, 8*(9).

Andrews-Hanna, J. R., Snyder, A. Z., Vincent, J. L., Lustig, C., Head, D., Raichle, M. E., et al. (2007) Disruption of large-scale brain systems in advanced aging. *Vol. 56. Neuron* (pp. 924-935).

Ansado, J., Monchi, O., Ennabil, N., Faure, S., & Joanette, Y. (2012). Load-dependent posterior-anterior shift in aging in complex visual selective attention situations. *Brain Research, 1454*, 14-22.

Aron, A. R., Durston, S., Eagle, D. M., Logan, G. D., Stinear, C. M., & Stuphorn, V. (2007). Converging evidence for a fronto-basal-ganglia network for inhibitory control of action and cognition. *The Journal of Neuroscience, 27*(44), 11860-11864.

Aschenbrenner, A., Tucha, O., & Lange, K. (2000). *RWT Regensburger Wortflüssigkeits-Test*. Göttingen.

Bäckman, L., Nyberg, L., Lindenberger, U., Li, S.-C., & Farde, L. (2006). The correlative triad among aging, dopamine, and cognition: current status and future prospects. *Neuroscience & Biobehavioral Reviews, 30*(6), 791-807.

Bai, F., Zhang, Z., Watson, D. R., Yu, H., Shi, Y., Yuan, Y., et al. (2009). Abnormal functional connectivity of hippocampus during episodic memory retrieval processing network in amnestic mild cognitive impairment. *Biological Psychiatry, 65*(11), 951-958.

Bai, F., Zhang, Z., Yu, H., Shi, Y., Yuan, Y., Zhu, W., et al. (2008). Default-mode network activity distinguishes amnestic type mild cognitive impairment from

healthy aging: a combined structural and resting-state functional MRI study. *Neuroscience Letters, 438*(1), 111-115.

Batouli, A. H., Boroomand, A., Fakhri, M., Sikaroodi, H., Oghabian, M. A., & Firouznia, K. (2009). The Effect of Aging on Resting-State Brain Function: An fMRI Study. *Iranian Journal of Radiology, 6*(3), 153-158.

Bäumler, G., & Stroop, J. R. (1985). *Farbe-Wort-Interferenztest nach JR Stroop (FWIT)*: Hogrefe, Verlag für Psychologie.

Beckmann, C. F., DeLuca, M., Devlin, J. T., & Smith, S. M. (2005). Investigations into resting-state connectivity using independent component analysis. *Philosophical Transactions of the Royal Society of London, 360*(1457), 1001-1013.

Beckmann, C. F., & Smith, S. M. (2004). Probabilistic independent component analysis for functional magnetic resonance imaging. *IEEE Transactions on Medical Imaging, 23*(2), 137-152.

Bell, E. C., Willson, M. C., Wilman, A. H., Dave, S., & Silverstone, P. H. (2006). Males and females differ in brain activation during cognitive tasks. *NeuroImage, 30*(2), 529-538.

Benjamini, Y., & Hochberg, Y. (1995). Controlling the false discovery rate: a practical and powerful approach to multiple testing. *Journal of the Royal Statistical Society*, 289-300.

Benton, A. L., Sivan, A. B., Spreen, O., & Steck, P. (2009). Der Benton-Test Huber, Hogrefe.

Binder, J. R., Desai, R. H., Graves, W. W., & Conant, L. L. (2009). Where is the semantic system? A critical review and meta-analysis of 120 functional neuroimaging studies. *Cerebral Cortex, 19*(12), 2767-2796.

Binnewijzend, M. A. A., Schoonheim, M. M., Sanz-Arigita, E., Wink, A. M., van der Flier, W. M., Tolboom, N., et al. (2012). Resting-state fMRI changes in

Alzheimer's disease and mild cognitive impairment. *Neurobiology of Aging, 33*(9), 2018-2028.

Biswal, B., Yetkin, F. Z., Haughton, V. M., & Hyde, J. S. (1995). Functional connectivity in the motor cortex of resting human brain using echo-planar MRI. *Magnetic Resonance in Medicine, 34*(4), 537-541.

Biswal, B. B., Mennes, M., Zuo, X. N., Gohel, S., Kelly, C., Smith, S. M., et al. (2010). Toward discovery science of human brain function. *Proceedings of the National Academy of Sciences of the United States of America, 107*(10), 4734-4739.

Bludau, S., Eickhoff, S. B., Mohlberg, H., Caspers, S., Laird, A. R., Fox, P. T., et al. (2013). Cytoarchitecture, probability maps and functions of the human frontal pole. *NeuroImage*.

Braskie, M. N., Wilcox, C. E., Landau, S. M., O'Neil, J. P., Baker, S. L., Madison, C. M., et al. (2008). Relationship of striatal dopamine synthesis capacity to age and cognition. *The Journal of Neuroscience, 28*(52), 14320-14328.

Buckner, R. L., Andrews-Hanna, J. R., & Schacter, D. L. (2008). The brain's default network: anatomy, function, and relevance to disease. *Annals of the New York Academy of Sciences, 1124*, 1-38.

Buckner, R. L., Sepulcre, J., Talukdar, T., Krienen, F. M., Liu, H., Hedden, T., et al. (2009). Cortical hubs revealed by intrinsic functional connectivity: mapping, assessment of stability, and relation to Alzheimer's disease. *The Journal of Neuroscience, 29*(6), 1860-1873.

Button, K. S., Ioannidis, J. P., Mokrysz, C., Nosek, B. A., Flint, J., Robinson, E. S., et al. (2013). Power failure: why small sample size undermines the reliability of neuroscience. *Nature Reviews Neuroscience, 14*(5), 365-376.

Cabeza, R. (2002). Hemispheric asymmetry reduction in older adults: the HAROLD model. *Psychology and Aging, 17*(1), 85-100.

Cabeza, R., Anderson, N. D., Locantore, J. K., & McIntosh, A. R. (2002). Aging gracefully: compensatory brain activity in high-performing older adults. *NeuroImage, 17*(3), 1394-1402.

Cabeza, R., Daselaar, S. M., Dolcos, F., Prince, S. E., Budde, M., & Nyberg, L. (2004). Task-independent and task-specific age effects on brain activity during working memory, visual attention and episodic retrieval. *Cerebral Cortex, 14*(4), 364-375.

Caspers, S., Eickhoff, S. B., Geyer, S., Scheperjans, F., Mohlberg, H., Zilles, K., et al. (2008). The human inferior parietal lobule in stereotaxic space. *Brain Structure & Function, 212*(6), 481-495.

Caspers, S., Eickhoff, S. B., Rick, T., von Kapri, A., Kuhlen, T., Huang, R., et al. (2011). Probabilistic fibre tract analysis of cytoarchitectonically defined human inferior parietal lobule areas reveals similarities to macaques. *NeuroImage, 58*(2), 362-380.

Caspers, S., Geyer, S., Schleicher, A., Mohlberg, H., Amunts, K., & Zilles, K. (2006). The human inferior parietal cortex: cytoarchitectonic parcellation and interindividual variability. *NeuroImage, 33*(2), 430-448.

Caspers, S., Moebus, S., Lux, S., Pundt, N., Schutz, H., Muhleisen, T. W., et al. (2014). Studying variability in human brain aging in a population-based German cohort-rationale and design of 1000BRAINS. *Frontiers in Aging Neuroscience, 6*, 149.

Caspers, S., Schleicher, A., Bacha-Trams, M., Palomero-Gallagher, N., Amunts, K., & Zilles, K. (2013). Organization of the human inferior parietal lobule based on receptor architectonics. *Cerebral Cortex, 23*(3), 615-628.

Caspers, S., Zilles, K., Laird, A. R., & Eickhoff, S. B. (2010). ALE meta-analysis of action observation and imitation in the human brain. *NeuroImage, 50*(3), 1148-1167.

Cattell, R. B. (1966). The scree test for the number of factors. *Multivariate Behavioral Research, 1*(2), 245-276.

Christensen, H., Mackinnon, A. J., Korten, A. E., Jorm, A. F., Henderson, A. S., Jacomb, P., et al. (1999). An analysis of diversity in the cognitive performance of elderly community dwellers: individual differences in change scores as a function of age. *Psychology and Aging, 14*(3), 365.

Clark, W., & Le Gros, E. (1945). *Deformation patterns in the cerebral cortex*: Printed at the Oxford University Press by John Johnson.

Coxon, J. P., Goble, D. J., Leunissen, I., Van Impe, A., Wenderoth, N., & Swinnen, S. P. (2014). Functional Brain Activation Associated with Inhibitory Control Deficits in Older Adults. *Cerebral cortex*.

Dale, A. M., Fischl, B., & Sereno, M. I. (1999). Cortical surface-based analysis. I. Segmentation and surface reconstruction. *NeuroImage, 9*(2), 179-194.

Damoiseaux, J. S., Beckmann, C. F., Arigita, E. J., Barkhof, F., Scheltens, P., Stam, C. J., et al. (2008). Reduced resting-state brain activity in the "default network" in normal aging. *Cerebral Cortex, 18*(8), 1856-1864.

Damoiseaux, J. S., Seeley, W. W., Zhou, J., Shirer, W. R., Coppola, G., Karydas, A., et al. (2012). Gender modulates the APOE epsilon4 effect in healthy older adults: convergent evidence from functional brain connectivity and spinal fluid tau levels. *The Journal of Neuroscience, 32*(24), 8254-8262.

Davis, S. W., Dennis, N. A., Daselaar, S. M., Fleck, M. S., & Cabeza, R. (2008). Que PASA? The posterior-anterior shift in aging. *Cerebral Cortex, 18*(5), 1201-1209.

de Lau, L., & Breteler, M. (2006). Epidemiology of Parkinson's disease. *The Lancet Neurology, 5*(6), 525-535.

De Vogelaere, F., Santens, P., Achten, E., Boon, P., & Vingerhoets, G. (2012). Altered default-mode network activation in mild cognitive impairment compared with healthy aging. *Neuroradiology, 54*(11), 1195-1206.

Della Sala, S., Gray, C., Baddeley, A. D., & Wilson, L. (1997). The visual patterns test: A test of short-term visual recall. *Thames Valley Test Company*.

Dickie, D. A., Job, D. E., Gonzalez, D. R., Shenkin, S. D., Ahearn, T. S., Murray, A. D., et al. (2013). Variance in brain volume with advancing age: implications for defining the limits of normality. *PloS one, 8*(12), e84093.

Eickhoff, S. B., Stephan, K. E., Mohlberg, H., Grefkes, C., Fink, G. R., Amunts, K., et al. (2005). A new SPM toolbox for combining probabilistic cytoarchitectonic maps and functional imaging data. *NeuroImage, 25*(4), 1325-1335.

Erixon-Lindroth, N., Farde, L., Wahlin, T.-B., Sovago, J., Halldin, C., & Bäckman, L. (2005). The role of the striatal dopamine transporter in cognitive aging. *Psychiatry Research: Neuroimaging, 138*(1), 1-12.

Ferreira, L. K., & Busatto, G. F. (2013). Resting-state functional connectivity in normal brain aging. *Neuroscience and Biobehavioral Reviews, 37*(3), 384-400.

Filippini, N., Nickerson, L. D., Beckmann, C. F., Ebmeier, K. P., Frisoni, G. B., Matthews, P. M., et al. (2012). Age-related adaptations of brain function during a memory task are also present at rest. *NeuroImage, 59*(4), 3821-3828.

Fischl, B., Sereno, M. I., & Dale, A. M. (1999). Cortical surface-based analysis. II: Inflation, flattening, and a surface-based coordinate system. *NeuroImage, 9*(2), 195-207.

Fjell, A. M., Westlye, L. T., Amlien, I., Espeseth, T., Reinvang, I., Raz, N., et al. (2009). Minute effects of sex on the aging brain: a multisample magnetic resonance imaging study of healthy aging and Alzheimer's disease. *The*

Journal of neuroscience : the official journal of the Society for Neuroscience, 29(27), 8774-8783.

Gatterer, G., Fischer, P., Simanyi, M., & Danielczyk, W. (1989). The A-K-T ("Alters-Konzentrations-Test") a new psychometric test for geriatric patients. *Functional Neurology, 4*(3), 273-276.

Gazzaley, A., Clapp, W., Kelley, J., McEvoy, K., Knight, R. T., & D'Esposito, M. (2008). Age-related top-down suppression deficit in the early stages of cortical visual memory processing. *Proceedings of the National Academy of Sciences of the United States of America, 105*(35), 13122-13126.

Gazzaley, A., & Nobre, A. C. (2012). Top-down modulation: bridging selective attention and working memory. *Trends in cognitive sciences, 16*(2), 129-135.

Gillebert, C. R., Mantini, D., Thijs, V., Sunaert, S., Dupont, P., & Vandenberghe, R. (2011). *Lesion evidence for the critical role of the intraparietal sulcus in spatial attention*.

Goh, J. O. (2011). Functional Dedifferentiation and Altered Connectivity in Older Adults: Neural Accounts of Cognitive Aging. *Aging and Disease, 2*(1), 30-48.

Goh, J. O., & Park, D. C. (2009). Neuroplasticity and cognitive aging: the scaffolding theory of aging and cognition. *Restorative Neurology and Neuroscience, 27*(5), 391-403.

Good, C. D., Johnsrude, I. S., Ashburner, J., Henson, R. N., Friston, K. J., & Frackowiak, R. S. (2001). A voxel-based morphometric study of ageing in 465 normal adult human brains. *NeuroImage, 14*(1 Pt 1), 21-36.

Gould, R. L., Brown, R. G., Owen, A. M., Bullmore, E. T., & Howard, R. J. (2006). Task-induced deactivations during successful paired associates learning: an effect of age but not Alzheimer's disease. *NeuroImage, 31*(2), 818-831.

Grady, C. L., Maisog, J. M., Horwitz, B., Ungerleider, L. G., Mentis, M. J., Salerno, J. A., et al. (1994). Age-related changes in cortical blood flow activation during visual processing of faces and location. *The Journal of Neuroscience, 14*(3 Pt 2), 1450-1462.

Greicius, M. D., Srivastava, G., Reiss, A. L., & Menon, V. (2004). Default-mode network activity distinguishes Alzheimer's disease from healthy aging: Evidence from functional MRI. *Proceedings of the National Academy of Sciences of the United States of America, 101*(13), 4637-4642.

Griffanti, L., Salimi-Khorshidi, G., Beckmann, C. F., Auerbach, E. J., Douaud, G., Sexton, C. E., et al. (2014). ICA-based artefact removal and accelerated fMRI acquisition for improved resting state network imaging. *NeuroImage, 95*, 232-247.

Guttman, L. (1954). Some necessary conditions for common-factor analysis. *Psychometrika, 19*(2), 149-161.

Hafkemeijer, A., van der Grond, J., & Rombouts, S. A. (2012a). Imaging the default mode network in aging and dementia. *Biochimica et Biophysica Acta, 1822*(3), 431-441.

Hafkemeijer, A., van der Grond, J., & Rombouts, S. A. R. B. (2012b). Imaging the default mode network in aging and dementia. *Biochimica et Biophysica Acta, 1822*(3), 431-441.

Hampel, H., Prvulovic, D., Teipel, S., Jessen, F., Luckhaus, C., Frölich, L., et al. (2011). The future of Alzheimer's disease: the next 10 years. *Progress in Neurobiology, 95*(4), 718-728.

Hedden, T., & Gabrieli, J. D. (2004). Insights into the ageing mind: a view from cognitive neuroscience. *Nature Reviews Neuroscience, 5*(2), 87-96.

Hedman, A. M., van Haren, N. E., Schnack, H. G., Kahn, R. S., & Hulshoff Pol, H. E. (2012). Human brain changes across the life span: a review of 56

longitudinal magnetic resonance imaging studies. *Human Brain Mapping, 33*(8), 1987-2002.

Hjelmervik, H., Hausmann, M., Osnes, B., Westerhausen, R., & Specht, K. (2014). Resting states are resting traits--an FMRI study of sex differences and menstrual cycle effects in resting state cognitive control networks. *PloS One, 9*(7), e103492.

Hogstrom, L. J., Westlye, L. T., Walhovd, K. B., & Fjell, A. M. (2013). The structure of the cerebral cortex across adult life: age-related patterns of surface area, thickness, and gyrification. *Cerebral Cortex, 23*(11), 2521-2530.

Hu, S., Chao, H. H., Zhang, S., Ide, J. S., & Li, C. S. (2014). Changes in cerebral morphometry and amplitude of low-frequency fluctuations of BOLD signals during healthy aging: correlation with inhibitory control. *Brain structure & function, 219*(3), 983-994.

Hultsch, D. F., MacDonald, S. W., & Dixon, R. A. (2002). Variability in reaction time performance of younger and older adults. *The Journal of Gerontology, 57*(2), P101-115.

Ikram, M. A., Vrooman, H. A., Vernooij, M. W., den Heijer, T., Hofman, A., Niessen, W. J., et al. (2010). Brain tissue volumes in relation to cognitive function and risk of dementia. *Neurobiology of Aging, 31*(3), 378-386.

Jenkinson, M., Bannister, P., Brady, M., & Smith, S. (2002). Improved optimization for the robust and accurate linear registration and motion correction of brain images. *NeuroImage, 17*(2), 825-841.

Jenkinson, M., Beckmann, C. F., Behrens, T. E., Woolrich, M. W., & Smith, S. M. (2012). Fsl. *NeuroImage, 62*(2), 782-790.

Jenkinson, M., & Smith, S. (2001). A global optimisation method for robust affine registration of brain images. *Medical Image Analysis, 5*(2), 143-156.

Jones, D. T., Machulda, M. M., Vemuri, P., McDade, E. M., Zeng, G., Senjem, M. L., et al. (2011). Age-related changes in the default mode network are more advanced in Alzheimer disease. *Neurology, 77*(16), 1524-1531.

Katzman, R. (1993). Education and the prevalence of dementia and Alzheimer's disease. *Neurology, 43*(1), 13-20.

Klostermann, E. C., Braskie, M. N., Landau, S. M., O'Neil, J. P., & Jagust, W. J. (2012). Dopamine and frontostriatal networks in cognitive aging. *Neurobiology of Aging, 33*(3), 623. e615-623. e624.

Koch, W., Teipel, S., Mueller, S., Buerger, K., Bokde, A. L. W., Hampel, H., et al. (2010). Effects of aging on default mode network activity in resting state fMRI: does the method of analysis matter? *NeuroImage, 51*(1), 280-287.

Kochunov, P., Mangin, J. F., Coyle, T., Lancaster, J., Thompson, P., Riviere, D., et al. (2005). Age-related morphology trends of cortical sulci. *Human Brain Mapping, 26*(3), 210-220.

Kochunov, P., Thompson, P. M., Coyle, T. R., Lancaster, J. L., Kochunov, V., Royall, D., et al. (2008). Relationship among neuroimaging indices of cerebral health during normal aging. [Research Support, N.I.H., Extramural]. *Human brain mapping, 29*(1), 36-45.

Koshino, H., Minamoto, T., Yaoi, K., Osaka, M., & Osaka, N. (2014). Coactivation of the Default Mode Network regions and Working Memory Network regions during task preparation. *Sci. Rep., 4*.

Kovalev, V. A., Kruggel, F., & von Cramon, D. Y. (2003). Gender and age effects in structural brain asymmetry as measured by MRI texture analysis. *NeuroImage, 19*(3), 895-905.

Kriegstein, A., Noctor, S., & Martinez-Cerdeno, V. (2006). Patterns of neural stem and progenitor cell division may underlie evolutionary cortical expansion. *Nature Reviews Neuroscience, 7*(11), 883-890.

Kujovic, M., Zilles, K., Malikovic, A., Schleicher, A., Mohlberg, H., Rottschy, C., et al. (2013). Cytoarchitectonic mapping of the human dorsal extrastriate cortex. *Brain structure & function, 218*(1), 157-172.

Laird, A. R., Fox, P. M., Eickhoff, S. B., Turner, J. A., Ray, K. L., McKay, D. R., et al. (2011). Behavioral interpretations of intrinsic connectivity networks. *Journal of Cognitive Neuroscience, 23*(12), 4022-4037.

Landau, S. M., Lal, R., O'Neil, J. P., Baker, S., & Jagust, W. J. (2009). Striatal dopamine and working memory. *Cerebral Cortex, 19*(2), 445-454.

Lemaitre, H., Goldman, A. L., Sambataro, F., Verchinski, B. A., Meyer-Lindenberg, A., Weinberger, D. R., et al. (2012). Normal age-related brain morphometric changes: nonuniformity across cortical thickness, surface area and gray matter volume? *Neurobiology of Aging, 33*(3), 617 e611-619.

Liu, T., Wen, W., Zhu, W., Kochan, N. A., Trollor, J. N., Reppermund, S., et al. (2011). The relationship between cortical sulcal variability and cognitive performance in the elderly. *NeuroImage, 56*(3), 865-873.

Liu, T., Wen, W., Zhu, W., Trollor, J., Reppermund, S., Crawford, J., et al. (2010). The effects of age and sex on cortical sulci in the elderly. *NeuroImage, 51*(1), 19-27.

Lu, H., Xu, F., Rodrigue, K. M., Kennedy, K. M., Cheng, Y., Flicker, B., et al. (2010). Alterations in cerebral metabolic rate and blood supply across the adult lifespan. *Cerebral Cortex*, bhq224.

Lux, S., Hartje, W., Reich, C., & Nagel, C. (2012). *VGT: Verbaler Gedächtnistest: Bielefelder Kategorielle Wortlisten.* : Göttingen: Hogrefe

Magnotta, V. A., Andreasen, N. C., Schultz, S. K., Harris, G., Cizadlo, T., Heckel, D., et al. (1999). Quantitative in vivo measurement of gyrification in the human brain: changes associated with aging. *Cerebral Cortex, 9*(2), 151-160.

Malikovic, A., Amunts, K., Schleicher, A., Mohlberg, H., Eickhoff, S. B., Wilms, M., et al. (2007). Cytoarchitectonic analysis of the human extrastriate cortex in the region of V5/MT+: a probabilistic, stereotaxic map of area hOc5. *Cerebral cortex, 17*(3), 562-574.

Malikovic, A., Amunts, K., Schleicher, A., Mohlberg, H., Kujovic, M., Palomero-Gallagher, N., et al. (2015). Cytoarchitecture of the human lateral occipital cortex: mapping of two extrastriate areas hOc4la and hOc4lp. *Brain Structure & Function*.

Mann, S. L., Hazlett, E. A., Byne, W., Hof, P. R., Buchsbaum, M. S., Cohen, B. H., et al. (2011). Anterior and posterior cingulate cortex volume in healthy adults: effects of aging and gender differences. *Brain Research, 1401*, 18-29.

Mevel, K., Chetelat, G., Eustache, F., & Desgranges, B. (2011). The default mode network in healthy aging and Alzheimer's disease. *International Journal of Alzheimer's Disease, 2011*, 535816.

Middleton, F. A., & Strick, P. L. (2000a). Basal ganglia and cerebellar loops: motor and cognitive circuits. *Brain Research Reviews, 31*(2-3), 236-250.

Middleton, F. A., & Strick, P. L. (2000b). Basal ganglia output and cognition: evidence from anatomical, behavioral, and clinical studies. *Brain and Cognition, 42*(2), 183-200.

Miller, D. I., & Halpern, D. F. (2014). The new science of cognitive sex differences. *Trends in Cognitive Sciences, 18*(1), 37-45.

Morris, J. C., Heyman, A., Mohs, R. C., Hughes, J. P., Van Belle, G., Fillenbaum, G., et al. (1989). The CERAD investigators (1989) The Consortium to Establish a Registry for Alzheimer’s Disease (CERAD). Part I. Clinical and neuropsychological assessment of Alzheimer’s disease. *Neurology, 39*(9), 1159-1165.

Mowinckel, A. M., Espeseth, T., & Westlye, L. T. (2012). Network-specific effects of age and in-scanner subject motion: a resting-state fMRI study of 238 healthy adults. *NeuroImage, 63*(3), 1364-1373.

Mueller, S. G., Weiner, M. W., Thal, L. J., Petersen, R. C., Jack, C. R., Jagust, W., et al. (2005). Ways toward an early diagnosis in Alzheimer's disease: the Alzheimer's Disease Neuroimaging Initiative (ADNI). *Alzheimer's & dementia : the journal of the Alzheimer's Association, 1*(1), 55-66.

Muhammad, R., Wallis, J. D., & Miller, E. K. (2006). A Comparison of Abstract Rules in the Prefrontal Cortex, Premotor Cortex, Inferior Temporal Cortex, and Striatum. *Journal of Cognitive Neuroscience, 18*(6), 974-989.

Nachev, P., Kennard, C., & Husain, M. (2008). Functional role of the supplementary and pre-supplementary motor areas. *Nature reviews. Neuroscience, 9*(11), 856-869.

Nobre, A. C., Sebestyen, G. N., Gitelman, D. R., Mesulam, M. M., Frackowiak, R. S., & Frith, C. D. (1997). Functional localization of the system for visuospatial attention using positron emission tomography. *Brain, 120*(3), 515-533.

O'Sullivan, M., Jones, D. K., Summers, P. E., Morris, R. G., Williams, S. C., & Markus, H. S. (2001). Evidence for cortical "disconnection" as a mechanism of age-related cognitive decline. *Neurology, 57*(4), 632-638.

Olesen, P. J., Westerberg, H., & Klingberg, T. (2004). Increased prefrontal and parietal activity after training of working memory. *Nature Neuroscience, 7*(1), 75-79.

Oswald, W. D., & Fleischmann, U. M. (1997). Das Nürnberger-Alters-Inventar (NAI) Hogrefe: Göttingen.

Owen, A. M., McMillan, K. M., Laird, A. R., & Bullmore, E. (2005). N-back working memory paradigm: A meta-analysis of normative functional neuroimaging studies. *Human Brain Mapping, 25*(1), 46-59.

Palomero-Gallagher, N., Eickhoff, S. B., Hoffstaedter, F., Schleicher, A., Mohlberg, H., Vogt, B. A., et al. (2015). Functional organization of human subgenual cortical areas: Relationship between architectonical segregation and connectional heterogeneity. *NeuroImage*.

Palomero-Gallagher, N., Mohlberg, H., Zilles, K., & Vogt, B. (2008). Cytology and receptor architecture of human anterior cingulate cortex. *The Journal of Comparative Neurology, 508*(6), 906-926.

Palomero-Gallagher, N., Vogt, B. A., Schleicher, A., Mayberg, H. S., & Zilles, K. (2009). Receptor architecture of human cingulate cortex: evaluation of the four-region neurobiological model. *Human Brain Mapping, 30*(8), 2336-2355.

Pardo, J. V., Lee, J. T., Sheikh, S. A., Surerus-Johnson, C., Shah, H., Munch, K. R., et al. (2007). Where the brain grows old: decline in anterior cingulate and medial prefrontal function with normal aging. *NeuroImage, 35*(3), 1231-1237.

Park, D. C., Lautenschlager, G., Hedden, T., Davidson, N. S., Smith, A. D., & Smith, P. K. (2002). Models of visuospatial and verbal memory across the adult life span. *Psychology and aging, 17*(2), 299.

Park, D. C., & Reuter-Lorenz, P. (2009). The adaptive brain: aging and neurocognitive scaffolding. *Annual Review of Psychology, 60*, 173-196.

Pinal, D., Zurron, M., Diaz, F., & Sauseng, P. (2015). Stuck in default mode: inefficient cross-frequency synchronization may lead to age-related short-term memory decline. *Neurobiology of Aging*.

Prince, M., Bryce, R., Albanese, E., Wimo, A., Ribeiro, W., & Ferri, C. P. (2013). The global prevalence of dementia: a systematic review and metaanalysis. *Alzheimer's & Dementia, 9*(1), 63-75. e62.

Pugh, K. G., & Lipsitz, L. A. (2002). The microvascular frontal-subcortical syndrome of aging. *Neurobiology of Aging, 23*(3), 421-431.

Raichle, M. E., MacLeod, A. M., Snyder, A. Z., Powers, W. J., Gusnard, D. A., & Shulman, G. L. (2001). A default mode of brain function. *Proceedings of the National Academy of Sciences of the United States of America, 98*(2), 676-682.

Raina, P. S., Wolfson, C., Kirkland, S. A., Griffith, L. E., Oremus, M., Patterson, C., et al. (2009). The Canadian longitudinal study on aging (CLSA). *Canadian journal on aging = La revue canadienne du vieillissement, 28*(3), 221-229.

Ravizza, S. M., Delgado, M. R., Chein, J. M., Becker, J. T., & Fiez, J. A. (2004). Functional dissociations within the inferior parietal cortex in verbal working memory. *NeuroImage, 22*(2), 562-573.

Raz, N., & Rodrigue, K. M. (2006). Differential aging of the brain: patterns, cognitive correlates and modifiers. *Neuroscience and Biobehavioral Reviews, 30*(6), 730-748.

Regard, M., Strauss, E., & Knapp, P. (1982). Children's production on verbal and non-verbal fluency tasks. *Perceptual and Motor Skills, 55*(3 Pt 1), 839-844.

Reitz, C., Brayne, C., & Mayeux, R. (2011). Epidemiology of Alzheimer disease. *Nature Reviews Neurology, 7*(3), 137-152.

Rettmann, M. E., Kraut, M. A., Prince, J. L., & Resnick, S. M. (2006). Cross-sectional and longitudinal analyses of anatomical sulcal changes associated with aging. *Cerebral Cortex, 16*(11), 1584-1594.

Reuter-Lorenz, P. A., & Cappell, K. A. (2008). Neurocognitive aging and the compensation hypothesis. *Current Directions in Psychological Science, 17*(3), 177-182.

Reuter-Lorenz, P. A., Jonides, J., Smith, E. E., Hartley, A., Miller, A., Marshuetz, C., et al. (2000). Age differences in the frontal lateralization of verbal and spatial working memory revealed by PET. *Journal of Cognitive Neuroscience, 12*(1), 174-187.

Reuter-Lorenz, P. A., & Lustig, C. (2005). Brain aging: reorganizing discoveries about the aging mind. *Current Opinion in Neurobiology, 15*(2), 245-251.

Reuter-Lorenz, P. A., & Park, D. C. (2014). How does it STAC up? Revisiting the scaffolding theory of aging and cognition. *Neuropsychology Review, 24*(3), 355-370.

Richman, D. P., Stewart, R. M., Hutchinson, J. W., & Cavincss Jr, V. S. (1975). Mechanical mode of brain convolutional deve lopment. *Science, 189*, 18-21.

Rombouts, S. A., Barkhof, F., Goekoop, R., Stam, C. J., & Scheltens, P. (2005). Altered resting state networks in mild cognitive impairment and mild Alzheimer's disease: an fMRI study. *Human Brain Mapping, 26*(4), 231-239.

Roski, C., Caspers, S., Langner, R., Laird, A. R., Fox, P. T., Zilles, K., et al. (2013). Adult age-dependent differences in resting-state connectivity within and between visual-attention and sensorimotor networks. *Frontiers in Aging Neuroscience, 5*.

Rottschy, C., Langner, R., Dogan, I., Reetz, K., Laird, A. R., Schulz, J. B., et al. (2012). Modelling neural correlates of working memory: A coordinate-based meta-analysis. *NeuroImage, 60*(1), 830-846.

Rowe, J. W., & Kahn, R. L. (1997). Successful aging. *The Gerontologist, 37*(4), 433-440.

Rushworth, M. F., Hadland, K. A., Paus, T., & Sipila, P. K. (2002). Role of the human medial frontal cortex in task switching: a combined fMRI and TMS study. *Journal of neurophysiology, 87*(5), 2577-2592.

Rypma, B., & D'Esposito, M. (2000). Isolating the neural mechanisms of age-related changes in human working memory. *Nature Neuroscience, 3*(5), 509-515.

Salat, D. H., Tuch, D. S., Hevelone, N. D., Fischl, B., Corkin, S., Rosas, H. D., et al. (2005). Age-related changes in prefrontal white matter measured by diffusion tensor imaging. *Annals of the New York Academy of Sciences, 1064*, 37-49.

Salimi-Khorshidi, G., Douaud, G., Beckmann, C. F., Glasser, M. F., Griffanti, L., & Smith, S. M. (2014). Automatic denoising of functional MRI data: combining independent component analysis and hierarchical fusion of classifiers. *NeuroImage, 90*, 449-468.

Salthouse, T. A. (2004). What and when of cognitive aging. *Current Directions in Psychological Science, 13*(4), 140-144.

Salthouse, T. A. (2010). Selective review of cognitive aging. *Journal of the International Neuropsychological Society, 16*(5), 754-760.

Sambataro, F., Murty, V. P., Callicott, J. H., Tan, H. Y., Das, S., Weinberger, D. R., et al. (2010). Age-related alterations in default mode network: impact on working memory performance. *Neurobiology of Aging, 31*(5), 839-852.

Satz, P. (1993). Brain reserve capacity on symptom onset after brain injury: a formulation and review of evidence for threshold theory. *Neuropsychology, 7*(3), 273.

Scahill, R. I., Frost, C., Jenkins, R., Whitwell, J. L., Rossor, M. N., & Fox, N. C. (2003). A longitudinal study of brain volume changes in normal aging using

serial registered magnetic resonance imaging. *Archives of Neurology, 60*(7), 989-994.

Schaer, M., Cuadra, M. B., Schmansky, N., Fischl, B., Thiran, J. P., & Eliez, S. (2012). How to measure cortical folding from MR images: a step-by-step tutorial to compute local gyrification index. *Journal of Visualized Experiments*(59), e3417.

Schaer, M., Cuadra, M. B., Tamarit, L., Lazeyras, F., Eliez, S., & Thiran, J. P. (2008). A surface-based approach to quantify local cortical gyrification. *IEEE Transactions on Medical Imaging, 27*(2), 161-170.

Schaie, K. W. (1993). The Seattle Longitudinal Study: a thirty-five-year inquiry of adult intellectual development. *Zeitschrift fur Gerontologie, 26*(3), 129-137.

Schaie, K. W., & Willis, S. L. (2010). The Seattle Longitudinal Study of Adult Cognitive Development. *ISSBD Bulletin, 57*(1), 24-29.

Schaie, K. W., Willis, S. L., & Caskie, G. I. (2004). The Seattle longitudinal study: relationship between personality and cognition. *Neuropsychology, development, and cognition. Section B, Aging, neuropsychology and cognition, 11*(2-3), 304-324.

Schelling, D. (1997). Block-Tapping-Test. *Frankfurt: Swets Test Service GmbH*.

Scheperjans, F., Hermann, K., Eickhoff, S. B., Amunts, K., Schleicher, A., & Zilles, K. (2008). Observer-independent cytoarchitectonic mapping of the human superior parietal cortex. *Cerebral Cortex, 18*(4), 846-867.

Schlee, W., Leirer, V., Kolassa, I. T., Weisz, N., & Elbert, T. (2012). Age-related changes in neural functional connectivity and its behavioral relevance. *BMC Neuroscience, 13*, 16.

Schmermund, A., Möhlenkamp, S., Stang, A., Gronemeyer, D., Seibel, R., Hirche, H., et al. (2002). Assessment of clinically silent atherosclerotic disease and established and novel risk factors for predicting myocardial infarction and

cardiac death in healthy middle-aged subjects: Rationale and design of the Heinz Nixdorf RECALL Study. *American Heart Journal, 144*(2), 212-218.

Schmidt, K.-H., & Metzler, P. (1992). *Wortschatztest: WST*: Beltz.

Seghier, M. L. (2013). The angular gyrus: multiple functions and multiple subdivisions. *The Neuroscientist, 19*(1), 43-61.

Shalom, D. B., & Poeppel, D. (2008). Functional anatomic models of language: assembling the pieces. *The Neuroscientist, 14*(1), 119-127.

Silk, T. J., Bellgrove, M. A., Wrafter, P., Mattingley, J. B., & Cunnington, R. (2010). Spatial working memory and spatial attention rely on common neural processes in the intraparietal sulcus. *NeuroImage, 53*(2), 718-724.

Simmonds, D. J., Pekar, J. J., & Mostofsky, S. H. (2008). Meta-analysis of Go/No-go tasks demonstrating that fMRI activation associated with response inhibition is task-dependent. *Neuropsychologia, 46*(1), 224-232.

Smith, S. M. (2002). Fast robust automated brain extraction. *Human Brain Mapping, 17*(3), 143-155.

Smith, S. M., Fox, P. T., Miller, K. L., Glahn, D. C., Fox, P. M., Mackay, C. E., et al. (2009). Correspondence of the brain's functional architecture during activation and rest. *Proceedings of the National Academy of Sciences of the United States of America, 106*(31), 13040-13045.

Smith, S. M., Jenkinson, M., Woolrich, M. W., Beckmann, C. F., Behrens, T. E., Johansen-Berg, H., et al. (2004). Advances in functional and structural MR image analysis and implementation as FSL. *NeuroImage, 23 Suppl 1*, S208-219.

Sowell, E. R., Peterson, B. S., Thompson, P. M., Welcome, S. E., Henkenius, A. L., & Toga, A. W. (2003). Mapping cortical change across the human life span. *Nature Neuroscience, 6*(3), 309-315.

Speck, O., Ernst, T., Braun, J., Koch, C., Miller, E., & Chang, L. (2000). Gender differences in the functional organization of the brain for working memory. *Neuroreport, 11*(11), 2581-2585.

Stern, Y. (2002). What is cognitive reserve? Theory and research application of the reserve concept. *Journal of the International Neuropsychological Society, 8*(03), 448-460.

Stern, Y. (2009). Cognitive reserve. *Neuropsychologia, 47*(10), 2015-2028.

Stocco, A., & Prat, C. S. (2014). Bilingualism trains specific brain circuits involved in flexible rule selection and application. *Brain and language, 137*(0), 50-61.

Stroop, J. R. (1935). Studies of interference in serial verbal reactions. *Journal of Experimental Psychology, 18*, 643-662.

Sturm, W., Willmes, K., & Horn, W. (1993). Leistungsprüfungssystem für 50–90jährige. *Handanweisung, 2nd Edn. Göttingen: Hogrefe*.

Szewczyk-Krolikowski, K., Menke, R. A., Rolinski, M., Duff, E., Salimi-Khorshidi, G., Filippini, N., et al. (2014). Functional connectivity in the basal ganglia network differentiates PD patients from controls. *Neurology, 83*(3), 208-214.

Teichmann, M., Dupoux, E., Kouider, S., & Bachoud-Lévi, A.-C. (2006). The Role of the Striatum in Processing Language Rules: Evidence from Word Perception in Huntington's Disease. *Journal of Cognitive Neuroscience, 18*(9), 1555-1569.

Tomasi, D., & Volkow, N. D. (2012). Gender differences in brain functional connectivity density. *Human Brain Mapping, 33*(4), 849-860.

Van den Heuvel, M. P., Mandl, R. C., Kahn, R. S., & Hulshoff Pol, H. E. (2009). Functionally linked resting-state networks reflect the underlying structural connectivity architecture of the human brain. *Human Brain Mapping, 30*(10), 3127-3141.

Van Essen, D. C. (1997). A tension-based theory of morphogenesis and compact wiring in the central nervous system. *Nature, 385*(6614), 313-318.

Wagner, S., Sebastian, A., Lieb, K., Tuscher, O., & Tadic, A. (2014). A coordinate-based ALE functional MRI meta-analysis of brain activation during verbal fluency tasks in healthy control subjects. *BMC Neuroscience, 15*, 19.

Welker, W. (1990). Why Does Cerebral Cortex Fissure and Fold? In E. Jones & A. Peters (Eds.), *Cerebral Cortex* (Vol. 8B, pp. 3-136): Springer US.

Westlye, E. T., Lundervold, A., Rootwelt, H., Lundervold, A. J., & Westlye, L. T. (2011). Increased hippocampal default mode synchronization during rest in middle-aged and elderly APOE epsilon4 carriers: relationships with memory performance. *The Journal of Neuroscience, 31*(21), 7775-7783.

Wu, J. T., Wu, H. Z., Yan, C. G., Chen, W. X., Zhang, H. Y., He, Y., et al. (2011). Aging-related changes in the default mode network and its anti-correlated networks: a resting-state fMRI study. *Neuroscience Letters, 504*(1), 62-67.

Xu, C., Li, C., Wu, H., Wu, Y., Hu, S., Zhu, Y., et al. (2015). Gender Differences in Cerebral Regional Homogeneity of Adult Healthy Volunteers: A Resting-State fMRI Study. *BioMed Research International, 2015*.

Ylikoski, R., Ylikoski, A., Keskivaara, P., Tilvis, R., Sulkava, R., & Erkinjuntti, T. (1999). Heterogeneity of congnitive profiles in aging: successful aging, normal aging, and individuals at risks for cognitive decline. *European Journal of Neurology, 6*(6), 645-652.

Yuan, Y., Chen, Y. P., Boyd-Kirkup, J., Khaitovich, P., & Somel, M. (2012). Accelerated aging-related transcriptome changes in the female prefrontal cortex. [Research Support, Non-U.S. Gov't]. *Aging cell, 11*(5), 894-901.

Zhang, S., & Li, C.-S. R. (2014). Functional Clustering of the Human Inferior Parietal Lobule by Whole-Brain Connectivity Mapping of Resting-State

Functional Magnetic Resonance Imaging Signals. *Brain Connectivity, 4*(1), 53-69.

Zilles, K., & Amunts, K. (2010). Centenary of Brodmann's map--conception and fate. *Nature Reviews Neuroscience, 11*(2), 139-145.

Zilles, K., Armstrong, E., Schleicher, A., & Kretschmann, H. J. (1988). The human pattern of gyrification in the cerebral cortex. *Anatomy and Embryology, 179*(2), 173-179.

Zilles, K., & Palomero-Gallagher, N. (2015). Gyrification in the human brain *Brain Mapping: An Encyclopedic Reference (Eds. Toga, A.W.). Section Anatomy & Physiology (Eds. Zilles, K., Amunts, K.)* (pp. 37-44). San Diego: Elsevier Academic Press.

Zilles, K., Palomero-Gallagher, N., & Amunts, K. (2013). Development of cortical folding during evolution and ontogeny. *Trends in Neurosciences, 36*(5), 275-284.

Auflistungen der eigenen Publikationen

Helmstaedter, C., Jockwitz, C., & Witt, J. A. (2015). Menstrual cycle corrupts reliable and valid assessment of language dominance: Consequences for presurgical evaluation of patients with epilepsy. *Seizure*, *28*, 26-31.

Caspers, S., Axer, M., Caspers, J., Jockwitz, C., Jütten, K., Reckfort, J., et al. (2015). Target sites for transcallosal fibers in human visual cortex – A combined diffusion and polarized light imaging study. *Cortex, 72*, 40-53.

Danksagung

Zuvorderst bedanke ich mich bei meinem Doktorvater Herrn Prof. Dr. Dr. Karl Zilles für das spannende Promotionsthema. Seine vielfältige Unterstützung, seine konstruktiven und wegweisenden Anmerkungen und Denkanstöße waren sowohl von essentiellem Wert für die Verwirklichung der beiden Studien als auch dieser Arbeit. Ich bedanke mich ebenfalls für die kritischen sowie inspirierenden wissenschaftlichen Diskussionen und die insgesamt in aller Hinsicht lehrreiche Zeit als Doktorandin.

Ebenfalls ganz herzlich bedanken möchte ich mich bei meiner direkten Betreuerin Frau Prof. Dr. Dr. Svenja Caspers für die tatkräftige und ausgezeichnete Betreuung und ihre Geduld während meiner gesamten Promotionsphase. Die vielen hilfreichen und unterstützenden Gespräche, für die sie sich immer wieder Zeit nahm, haben wesentlich zum Gelingen dieser Arbeit beigetragen.

Des Weiteren bedanke ich mich bei Frau Prof. Dr. Katrin Amunts für die mannigfaltige fachliche Beratung, wie auch für die Unterstützung, an diversen Fortbildungen und Konferenzen teilnehmen zu dürfen, um meine neurowissenschaftlichen und vor allem neuroanatomischen Kenntnisse zu verbessern.

Die vorliegende Arbeit wäre ohne die eingehenden wissenschaftlichen und technischen Hilfestellungen nicht möglich gewesen, für die ich mich im Folgenden ganz herzlich bedanken möchte.

Herrn Prof. Dr. Dr. Karl Zilles, Frau Prof. Dr. Katrin Amunts und Frau Prof. Dr. Dr. Svenja Caspers danke ich für die Erstellung und Überwachung des Studiendesigns.

Bei Frau Prof. Dr. Silke Lux und Frau Prof. Dr. Dr. Svenja Caspers bedanke ich mich für die Hilfestellung hinsichtlich der Auswahl und statistischen Auswertung der neuropsychologischen Variablen.

Frau Prof. Dr. Dr. Svenja Caspers, Herrn Prof. Dr. Simon Eickhoff, Herrn Dr. Andrew Reid und Herrn Dr. Felix Hoffstaedter danke ich für die Hilfestellung bei der statistischen Auswertung der Resting State Daten.

Des Weiteren bedanke ich mich bei Frau Prof. Dr. Dr. Svenja Caspers, Herrn Prof. Dr. Dr. Karl Zilles, Herrn Prof. Dr. Simon Eickhoff, sowie Herrn Dr. Axel Schleicher für die Unterstützung in statistischen Fragen zur Auswertung der Gyrifizierungsdaten.

Für die hilfreichen Diskussionen, Anregungen und kritischen Anmerkungen zur Interpretation der Resting State- und Gyrifizierungsdaten bin ich Frau Prof. Dr. Dr. Svenja Caspers, Herrn Prof. Dr. Dr. Karl Zilles und Frau Prof. Dr. Katrin Amunts zu großem Dank verpflichtet.

Zudem bin ich Herrn Prof. Dr. Dr. Karl Zilles und Frau Prof. Dr. Dr. Svenja Caspers für die Korrektur dieser Arbeit sehr verbunden.

Ich bedanke mich bei den Kollegen der Heinz-Nixdorf Recall Studie, Frau Prof. Dr. Susanne Moebus, Herrn Prof. Dr. Karl-Heinz Jöckel, und Herrn Prof. Dr. Raimund Erbel, sowie Herrn Prof. Dr. Markus M. Nöthen und Herrn Prof. Dr. Sven Cichon für die Studienkonzeption in epidemiologischen Großstudien.

Frau Prof. Dr. Susanne Moebus, Herrn Prof. Dr. Karl-Heinz Jöckel, und Herrn Prof. Dr. Raimund Erbel danke ich zudem für die Interpretation der Studiendaten aus epidemiologischer Sicht.

Herrn Prof. Markus M. Nöthen gilt mein zusätzlicher Dank für die kritische Edition des Manuskripts zur Resting State Analyse.

Herrn Prof. Dr. N. Jon Shah danke ich für das Studiendesign der MR Bildgebung.

Zudem möchte ich mich bei Kerstin Jütten und Stefan Lenzen für die Unterstützung bei der Datenerhebung bedanken. Meiner Mitstreiterin und Bürokollegin Kerstin Jütten danke ich außerdem für die vielen (Fach-) Gespräche

und die wunderbare Arbeitsatmosphäre, die die Doktorandenphase zu einer unvergesslichen Zeit gemacht hat.

Weiterhin möchte ich mich bei Frau Dr. Noreen Pundt für die Erhebung der epidemiologischen Daten, Frau Heidi Mellenthin für die technische Unterstützung bei der Erhebung der neuropsychologischen Daten, sowie Frau Barbara Elghawaghi, Frau Dorothe Krug, Frau Andrea Muren, und Frau Anita Köth für die technische Unterstützung bei der Erhebung der bildgebenden Daten bedanken.

Vor allem möchte ich mich auch bei allen Probanden der 1000BRAINS-Studie bedanken, die diese wissenschaftliche Arbeit erst möglich gemacht haben.

Ein großer Dank gilt meinen Freunden und meiner Familie. Ich danke meiner Schwester Stefanie Jockwitz, sowie meinen Großeltern, für ihre stetige Unterstützung und Zuversicht. Mein größter Dank gilt meinen Eltern, Volker und Petra Jockwitz für ihre fortwährende und liebevolle Unterstützung sowie die unerschütterliche Zuversicht, die sie mir allzeit entgegen gebracht haben. Ihnen ist diese Arbeit gewidmet.

Erklärung § 5 Abs. 1 zur Datenaufbewahrung

Hiermit erkläre ich, dass die dieser Dissertation zu Grunde liegenden Originaldaten

in dem **Institut für Neurowissenschaft und Medizin -1 des Forschungszentrum Jülich**

hinterlegt sind.

Eidesstattliche Erklärung gemäß § 5 Abs. (1) und § 11 Abs. (3) 12. der Promotionsordnung

Hiermit erkläre ich, **Christiane Jockwitz** an Eides statt, dass ich folgende in der von mir selbstständig erstellten Dissertation „**Structure-Function Relationships in elderly Resting-State-Networks: Influence of Age and Cognitive Performance**“ dargestellten Ergebnisse erhoben habe:

- Datenerhebung: 40%
- Auswahl und statistische Auswertung der neuropsychologischen Variablen: 60%
- Statistische Auswertung der Resting State Daten: 60%
- Statistische Auswertung der Gyrifizierungsdaten: 60%
- Interpretation der Resting State Daten: 60%
- Interpretation der Gyrifizierungsdaten: 60%
- Interpretation und Zusammenbringung der beiden Studien im gesamtheitlichen Kontext: 100%

Bei der Durchführung der Arbeit hatte ich folgende Hilfestellungen, die in der Danksagung angegeben sind:

Prof. Dr. Dr. Karl Zilles:
- Studiendesign und Studienüberwachung (40%)
- Statistische Auswertung der Gyrifizierungsdaten (10%)
- Interpretation der Gyrifizierungsdaten (10%)
- Interpretation der Resting State Daten (10%)
- Korrektur der Dissertation

Prof. Dr. Dr. Svenja Caspers:
- Studiendesign und Studienüberwachung (30%)
- Statistische Auswertung der Resting State Daten (20%)
- Statistische Auswertung der Gyrifizierungsdaten (20%)
- Auswahl und statistische Auswertung der neuropsychologischen Variablen (10%)
- Interpretation der Resting State Daten 20%)
- Interpretation der Gyrifizierungsdaten (20%)
- Korrektur der Dissertation

Prof. Dr. Katrin Amunts:
- Studiendesign und Studienüberwachung (30%)
- Interpretation der Resting State Daten (10%)
- Interpretation der Gyrifizierungsdaten (10%)

Prof. Dr. Silke Lux:

- Auswahl und statistische Auswertung der neuropsychologischen Variablen (30%)

Prof. Dr. Simon B. Eickhoff:
- Statistische Auswertung der Resting State Daten (10%)
- Statistische Auswertung der Gyrifizierungsdaten (5%)

Dr. Axel Schleicher:
- Statistische Auswertung der Gyrifizierungsdaten (5%)

Dr. Andrew Reid
- Statistische Auswertung der Resting State Daten (5%)

Dr. Felix Hoffstaedter:
- Statistische Auswertung der Resting State Daten (5%)

Prof. Dr. Susanne Moebus
- Interpretation aus epidemiologischer Sicht (33%)
- Studienkonzeption in epidemiologischen Großstudien (20%)

Prof. Dr. Karl-Heinz Jöckel
- Interpretation aus epidemiologischer Sicht (33%)
- Studienkonzeption in epidemiologischen Großstudien (20%)

Prof. Dr. Raimund Erbel
- Interpretation aus epidemiologischer Sicht (33%)
- Studienkonzeption in epidemiologischen Großstudien (20%)

Prof. Dr. Markus M. Nöthen
- Kritische Edition des Manuskripts zur Resting State Analyse
- Studienkonzeption in epidemiologischen Großstudien (20%)

Prof. Dr. Sven Cichon
- Studienkonzeption in epidemiologischen Großstudien (20%)

Prof. Dr. N. Jon Shah
- Studiendesign MR Bildgebung

Kerstin Jütten:
- Datenerhebung (40%)

Stefan Lenzen:
- Datenerhebung (20%)

Dr. Noreen Pundt

- Erhebung der epidemiologischen Daten

Heidi Mellenthin:
- Technische Unterstützung bei der Erhebung der neuropsychologischen Daten

Barbara Elghawaghi
- Technische Unterstützung bei der Erhebung der bildgebenden Daten (25%)

Dorothe Krug
- Technische Unterstützung bei der Erhebung der bildgebenden Daten (25%)

Andrea Muren
- Technische Unterstützung bei der Erhebung der bildgebenden Daten (25%)

Anita Köth:
- Technische Unterstützung bei der Erhebung der bildgebenden Daten (25%)

_____
Unterschrift der Doktorandin/ des Doktoranden

Als Betreuer der obigen Dissertation bestätige ich die Angaben von Christiane Jockwitz

_____
Unterschrift des Doktorvaters

LEBENSLAUF

Christiane Jockwitz

Josef-Metternich-Straße 13
50354 Hürth
Deutschland
Tel.: +49 2233 - 4053338
c.jockwitz@fz-juelich.de

Persönliches

Geburtsdatum:	21. Juli 1986
Geburtsort:	Köln
Nationalität:	Deutsch

Beruflicher Werdegang

Juli 2015 - heute	Wissenschaftliche Mitarbeiterin, C. und O. Vogt Institut für Hirnforschung, Universitätsklinikum Düsseldorf
Oktober 2011 - Juni 2015:	Wissenschaftliche Mitarbeiterin, Forschungszentrum Jülich, Institut für Neurowissenschaften und Medizin

Lehr- und Reviewer-Tätigkeiten

Mai 2015 - Juli 2015	Dozent: „Einführung in die Anatomie des menschlichen Gehirns“, Masterstudiengang: Psychologie, Heinrich-Heine Universität Düsseldorf
Mai 2015	Reviewer: Brain Structure and Function (BSAF)
Februar 2008 - Oktober 2010:	Tutor: „Statistics I“, „Memory“, „Sensation and Perception“, „Communication skills“, „Research methods“, Bachelorstudiengang: Psychologie, Universität Maastricht

Studium

August 2011:	(Research) Master of Science in Cognitive and Clinical Neuroscience (Fachrichtung Neuropsychologie) an der Universität Maastricht; Thema: Sex-dependent dynamics in Language Dominance: Reliability and Stability of the functional Transcranial Doppler Sonography using the Animation Description Paradigm
August 2009:	Bachelor of Science in Psychologie (Biologische Psychologie) an der Universität Maastricht; Thema: Ecstasy and its influence on memory function
Januar - April 2009:	Auslandssemester an der Brock University (St. Catherines, Ontario, Kanada)
September 2006:	Beginn des Studiums der Psychologie an der Universität Maastricht

Schulische Ausbildung

2005:	Abitur
1996-2005:	Ernst Mach Gymnasium, Hürth
1992-1996:	Deutschherrenschule, Hürth

Publikationen

Helmstaedter, C., Jockwitz, C., & Witt, J. A. (2015). Menstrual cycle corrupts reliable and valid assessment of language dominance: Consequences for presurgical evaluation of patients with epilepsy. *Seizure*, *28*, 26-31.

Caspers, S., Axer, M., Caspers, J., Jockwitz, C., Jütten, K., Reckfort, J., et al. (2015). Target sites for transcallosal fibers in human visual cortex – A combined diffusion and polarized light imaging study. *Cortex, 72*, 40-53.

Abstracts

Caspers, C., Moebus, S., Lux, S., Jockwitz, C., Jütten, K., Lenzen, S., Schütz, H., Gras, V., Mühleisen, T., Roski, C., Hoffstädter, F., Jöckel, K.-H., Mödder, U., Cichon, S., Bauer, A., Sturma, D., Shah, N.J., Zilles, K., Amunts, K. (2012).

1000BRAINS: Assessing normal ageing of the human brain in a population-based German cohort. Neurovisionen 8, Aachen.

Jockwitz, C., Caspers, S., Lux, S., Jütten, K., Lenzen, S., Moebus, S., Pundt, N., Schütz, H., Gras, V., Jöckel, K.-H., Erbel, R., Mödder, U., Cichon, S., Bauer, A., Sturma, D., Shah, N. J., Zilles, K., Amunts, K. (2013). Altersabhängige Veränderungen der Ruheaktivität des Gehirns bei Exekutivfunktionen. 39. Tagung Psychologie und Gehirn, Würzburg.

Jockwitz, C., Caspers, S., Lux, S., Jütten, K., Lenzen, S., Moebus, S., Schütz, H., Gras, V., Jöckel, K.-H., Erbel, R., Mödder, U., Cichon, S., Bauer, A., Sturma, D., Shah, N. J., Zilles, K., Amunts, K. (2013). Age-related dynamics of executive functions in resting state networks. 19th Annual meeting of the OHBM, Seattle.

Jockwitz, C., Caspers, S., Lux, S., Jütten, K., Lenzen, S., Moebus, S., Pundt, N., Schütz, H., Gras, V., Jöckel, K.-H., Erbel, R., Mödder, U., Cichon, S., Bauer, A., Sturma, D., Shah, N. J., Zilles, K., Amunts, K. (2013). Influence of age and cognitive performance on resting state functional connectivity in an elderly population-based cohort. Neurovisionen 9, Köln.

Pflanz, C.P., Caspers, S. ,Lux, S., Jütten, K., Lenzen, S., Jockwitz, C., Amunts, K. (2013). Age-related changes in brain networks involved in action observation, execution, and imagination. Neurovisionen 9, Köln.

Jockwitz, C., Caspers, S., Lux, S., Jütten, K., Lenzen, S., Moebus, S., Muehleisen, T., Pundt, N., Schütz, H., Gras, V., Jöckel, K.-H., Erbel, R., Mödder, U., Cichon, S., Bauer, A., Sturma, D., Shah, N. J., Amunts, K., Zilles, K. (2014). Gyrification changes in Default Mode Network as correlate of its functional reorganization with age. 20th Annual meeting of the OHBM, Hamburg.

Caspers, S., Axer, M., Jockwitz, C., Jütten, K., Lenzen, S., Reckfort, J., Grässel, D., Amunts, K., Zilles, K. (2014). Target sites of callosal fibres in human visual cortex: a combined diffusion and PLI study. 20th Annual meeting of the OHBM, Hamburg.

Jütten, K., Lux, S., Caspers, S., Jockwitz, C., Lenzen, S., Mühleisen, T., Moebus, S., Pundt, N., Schütz, H., Gras, V., Jöckel, K. H., Erbel, R., Mödder, U., Cichon, S., Bauer, Andreas, Sturma, D., Shah, N. J., Zilles, K., Amunts, K. (2014). Common neural activations of action observation, execution, an imagination in elderly. 20th Annual meeting of the OHBM, Hamburg.

Lux, S., Lenzen, S., Caspers, S., Jütten, K., Jockwitz, C., Schleicher, A., Muehleisen, T., Moebus, S., Pundt, N., Schütz, H., Gras, V., Jöckel, K.-H., Erbel, R., Mödder, U., Cichon, S., Bauer, A., Sturma, D., Shah, N. J., Zilles, K., Amunts,

K. (2014). Relating neuropsychological performance profiles to cognitive resting state networks in elderly. 20th Annual meeting of the OHBM, Hamburg.

Muehleisen, T., Lux, S., Lenzen, S., Vaitsiakhovich, T., Caspers, S., Schleicher, A., Jockwitz, C., Jütten, K., Hoffmann, P., Moebus, S., Pundt, N., Schütz, H., Gras, V., Jöckel, K.-H., Erbel, R., Mödder, U., Bauer, A., Sturma, D., Shah, N. J., Zilles, K., Becker, T., Amunts, K., Cichon, S. (2014). Genome-wide analysis implicates variation at a potassium channel gene (KCNH8) in cognitive aging. 20th Annual meeting of the OHBM, Hamburg.

Jockwitz, C., Caspers, S., Lux, S., Jütten, K., Lenzen, S., Moebus, S., Pundt, N., Schütz, H., Gras, V., Jöckel, K.-H., Erbel, R., Mödder, U., Cichon, S., Bauer, A., Sturma, D., Shah, N. J., Zilles, K., Amunts, K. (2014). Alters- und Leistungsabhängige Veränderungen der Ruheaktivität des alternden Gehirns in einer populationsbasierten Kohorte. 9. Jahrestagung der Deutschen Gesellschaft für Epidemiologie, Ulm.

Jockwitz, C., Caspers, S., Lux, S., Jütten, K., Lenzen, S., Moebus, S., Muehleisen, T., Pundt, N., Schütz, H., Gras, V., Jöckel, K.-H., Erbel, R., Mödder, U., Cichon, S., Bauer, A., Sturma, D., Shah, N. J., Amunts, K., Zilles, K. (2014). Gyrification changes in Default Mode Network as correlate of its functional reorganization with age. Neurovisionen 10, Jülich.

Müehleisen, T., Teumer, A., Wittfeld, K., Jockwitz, C., Herms, S., Hoffmann, P., Nöthen., M.M., Caspers, S., Homuth, G., Hegenscheid, K., Zilles, K., Amunts, K., Cichon, S., Grabe, H.-J. (2015). Identification of Common and Low-frequency Genetic Variants Associated with Gyrification in Humans. 21th Annual meeting of the OHBM, Hawaii.

Vorträge

Jockwitz, C., Caspers, S., Lux, S., Jütten, K., Eickhoff, S.B., Amunts, K., Zilles, K. (2015). Gyrification changes in Default Mode Network as correlate of its functional reorganization with age. Active Healthy Aging, Magdeburg.

Hürth, den 09.11.2015

Christiane Jockwitz